INTERIM REPORT

9-17-79

Accession No. ______________

____

Contract Program or Project Title: LOFT Experimental Program Division

Subject of this Document: RELAP4/MOD6 Prediction Comparisons with LOFT LOCE L2-3 Data

Type of Document: LOFT Technical Report

Author(s): C. D. Keeler, J. R. White

Date of Document: August 1979

Responsible NRC Individual and NRC Office or Division: G. D. McPherson

This document was prepared primarily for preliminary or internal use. It has not received full review and approval. Since there may be substantive changes, this document should not be considered final.

Kay Rose for
H. P. Pearson, Supervisor
Information Processing
EG&G Idaho

Prepared for
U.S. Nuclear Regulatory Commission
Washington, D.C. 20555

NRC Fin #A6048

INTERIM REPORT

POOR ORIGINAL

NRC Research and Technical Assistance Report

995 294

7909260245

EG&G Idaho

FORM EG&G-954
(Rev. 9-76)

INTEROFFICE CORRESPONDENCE

NO. R-4935

date AUG 29 1979

to DISTRIBUTION

from LOFT CDCS, TAN 602, Ext. 6177 S K Hathaway

subject DOCUMENT TRANSMITTAL

The following documents released by LOFT CDCS, are hereby transmitted for your use and information:

DOCUMENT NO.	REV.	CHG.	DATE
LTR 20-104	Ø		8-16-79
"RELAP 4/MOD6 Prediction Comparisons with LOFT LOCE L2-3 Data"			
C. D. Keeler, J. R. White			

REMARKS: This LTR documents comparisons between experimental data and computer code analysis. There are no recommendations specific to LOFT plant configuration. Future analysis will be done to gain better understanding of modeling heat transfer processes.

Distribution:

M. Akimoto - 2
W. Amidei w/o Att.
B. O. Anderson
E. C. Anderson w/o Att.
J. G. Arendts
G. A. Dinneen
D. B. Engelman
B. L. Freed - orig + 7
R. T. French
R. C. Gottula
R. C. Guenzler
J. C. Haire
G. L. Hunt
F. K. Hyer w/o Att.
N. C. Kaufman w/o Att.
S. T. Kelppe
J. L. Liebenthal
A. S. Lockhart
D. W. Marshall
S. Matovich
M. I. McKnight
G. D. McPherson
O. R. Meyer w/o Att.
M. J. Johnson
J. Morrow
N. E. Pace w/o Att.
T. F. Pointer
G. Rieger
P. Schally
D. G. Satterwhite w/o Att.
W. A. Spencer
J. C. Stachew w/o Att.
K. C. Sumpter
R. E. Tiller
G. Weimann
L. Winters
S. R. Behling
V. T. Berta
T. R. Charlton
J. A. Dearien
L. D. Goodrich
W. H. Grush
D. J. Hanson
H. Henze
G. W. Johnson
E. J. Kee
C. D. Keeler - 2
T. K. Larson
G. D. Lassahn
L. P. Leach
J. C. Lin
P. E. McDonald
S. A. Naff San by SkH per telecon
R. A. Nelson
P. North
D. J. Olson
A. C. Peterson
V. H. Ransom
S. Z. Rouhani
M. L. Russell
T. K. Samuels
M. S. Shinko
T. Sudoh
E. L. Tolman
L. L. Wheat
J. R. White - 2

995 295

LTR 20-104
Proj. No. P 394
for U.S. Nuclear Regulatory Commission

RELAP4/MOD6 PREDICTION COMPARISONS WITH LOFT LOCE L2-3 DATA

C.D. KEELER J.R. WHITE

August 1979

EG&G Idaho, Inc.
IDAHO NATIONAL ENGINEERING LABORATORY
DEPARTMENT OF ENERGY
IDAHO OPERATIONS OFFICE UNDER CONTRACT DE-AC07-76IDO1570

995 296

EG&G Idaho, Inc.

FORM EG&G-229
(Rev. 12-76)

LOFT TECHNICAL REPORT
LOFT PROGRAM

TITLE RELAP4/MOD6 PREDICTION COMPARISONS WITH LOFT LOCE L2-3 DATA	REPORT NO LTR 20-104
AUTHOR C. D. Keeler and J. R. White	GWA NO.
PERFORMING ORGANIZATION LOFT Experimental Program Division	DATE August 16, 1979
LOFT APPROVAL LEPD Mgr	

RESOLUTION OF RECOMMENDATIONS

This LTR documents comparisons between experimental data and computer code analysis. There are no recommendations specific to LOFT plant configuration. Future analysis will be done to gain better understanding of modeling heat transfer processes.

995 297

EG&G Idaho, Inc.

FORM EG&G-398
(Rev 12-78)

INTERIM REPORT

Accession No. ______

Report No. LTR 20-104

Proj. No. P 394

Contract Program or Project Title:

LOFT Experimental Program Division

Subject of this Document:

RELAP4/MOD6 Prediction Comparisons with LOFT LOCE L2-3 Data

Type of Document:

LOFT Technical Report

Author(s):

C. D. Keeler and J. R. White

Date of Document:

August 1979

Responsible NRC Individual and NRC Office or Division:

G. D. McPherson, Acting Chief, LOFT Research Branch, Division of Reactor Safety Research, USNRC

This document was prepared primarily for preliminary or internal use. It has not received full review and approval. Since there may be substantive changes, this document should not be considered final.

EG&G Idaho, Inc.
Idaho Falls, Idaho 83401

Prepared for the
U.S. Nuclear Regulatory Commission
and the U.S. Department of Energy
Idaho Operations Office
Under contract No. DE-AC07-76ID01570
NRC FIN No. A6048

995 298

INTERIM REPORT

SUMMARY

This document contains comparison between RELAP4/MOD6 predicted and experimental measured quantities for Loss-of-Coolant Experiment (LOCE) L2-3 performed in the Loss-of-Fluid Test (LOFT) facility. These data comparisons provide a detailed record for subsequent analysis.

Comparisons indicate that the trends in the system hydraulic response were generally well predicted. The core thermal response, in general, was not well predicted due to the code failing to predict the early rewet. It is recommended that future LOCE L2-3 posttest analysis efforts be centered on gaining a better understanding of modeling rewet phenomena with the RELAP4/MOD6 heat transfer surface. Better modeling of the performance of the steam generator secondary side is also needed before modeling small break LOCEs.

995 299

CONTENTS

SUMMARY ii

1. INTRODUCTION 1

2. DATA COMPARISONS 2

2.1 Experimental Data Classifications 2
2.2 Experimental Parameters Compared 4

3. CONCLUSIONS AND RECOMMENDATIONS 60

4. REFERENCES 60

APPENDIX A - EXPERIMENTAL MEASUREMENT LOCATIONS IN THE LOFT SYSTEM 61

FIGURES

1. Comparison of predicted and measured average density in broken loop cold leg (DE-BL-1) 7

2. Comparison of predicted and measured average density in broken loop hot leg (DE-BL-2) 7

3. Comparison of predicted and measured average density in intact loop cold leg (DE-PC-1) 8

4. Comparison of predicted and measured average density in intact loop hot leg (DE-PC-2) 8

5. Comparison of predicted and measured differential pressure across 14- to 5-in. reducer (PdE-BL-1) 9

6. Comparison of predicted and measured differential pressure across pump simulator (PdE-BL-5) 9

7. Comparison of predicted and measured differential pressure across steam generator simulator (PdE-BL-7) 10

8. Comparison of predicted and measured differential pressure across pumps (PdE-PC-1) 10

9. Comparison of predicted and measured differential pressure across intact loop steam generator (PdE-PC-2) 11

10. Comparison of predicted and measured differential pressure across Pump 1 (PdE-PC-9) 11

995 300

11. Comparison of predicted and measured differential pressure across Pump 2 (PdE-PC-10) 12

12. Comparison of predicted and measured flow rate from accumulator (FT-P120-36-1) 12

13. Comparison of predicted and measured flow rate from low-pressure injection system pump (FT-P120-85) 13

14. Comparison of predicted and measured flow rate from high-pressure injection system pump (FT-P128-104) 13

15. Comparison of predicted and measured liquid level in accumulator (LIT-P120-44) 14

16. Comparison of predicted and measured liquid level in steam generator secondary side (LT-P004-8B) 14

17. Comparison of predicted and measured liquid level in pressurizer Channel B (LT-P139-7) 15

18. Comparison of predicted and measured mass flow in broken loop cold leg (FR-BL-1) 15

19. Comparison of predicted and measured mass flow in broken loop hot leg (FR-BL-2) 16

20. Comparison of predicted and measured mass flow in intact loop cold leg (FR-PC-1) 16

21. Comparison of predicted and measured mass flow in intact loop hot leg (FR-PC-2) 17

22. Comparison of predicted and measured total ECC flow rate (FR-ECC-1) 17

23. Comparison of predicted and measured integral of ECC flow (MS-RV-001) 18

24. Comparison of predicted and measured momentum flux in broken loop cold leg (ME-BL-1) 18

25. Comparison of predicted and measured momentum flux in broken loop hot leg (ME-BL-2) 19

26. Comparison of predicted and measured momentum flux in intact loop cold leg (ME-PC-1) 19

27. Comparison of predicted and measured momentum flux in intact loop hot leg (ME-PC-2) 20

28. Comparison of predicted and measured momentum flux at instrument Stalk 1 (ME-1ST-1) 20

29. Comparison of predicted and measured momentum flux in upper end box (ME-1UP-1) 21

30. Comparison of predicted and measured momentum flux in upper end box (ME-3UP-1) 21

31. Comparison of predicted and measured momentum flux at instrument Stalk 2 (ME-2ST-1) 22

32. Comparison of predicted and measured pressure in broken loop cold leg (PE-BL-1) 22

33. Comparison of predicted and measured pressure in broken loop hot leg (PE-BL-2) 23

34. Comparison of predicted and measured pressure in broken loop hot leg pump simulator outlet (PE-BL-3) 23

35. Comparison of measured and predicted pressure at steam generator simulator outlet (PE-BL-6) 24

36. Comparison of predicted and measured pressure in broken loop cold leg spool piece midpoint (PE-BL-8) 24

37. Comparison of predicted and measured pressure in intact loop cold leg (PE-PC-1) 25

38. Comparison of predicted and measured pressure in intact loop hot leg (PE-PC-2) 25

39. Comparison of predicted and measured pressure in intact loop pressurizer (PE-PC-4) 26

40. Comparison of measured and predicted pressure at instrument Stalk 1 (PE-1ST-1A) 26

41. Comparison of predicted and measured pressure at instrument Stalk 1 (PE-1ST-3A) 27

42. Comparison of predicted and measured pressure in upper end box (PE-1UP-1A) 27

43. Comparison of predicted and measured pressure at instrument Stalk 2 (PE-2ST-1A) 28

44. Comparison of predicted and measured pressure in blowdown suppression tank (PE-SV-17) 28

45. Comparison of predicted and measured pressure in steam generator secondary side (PT-P004-10A) 29

46. Comparison of predicted and measured pressure in accumulator (PT-P120-43) 29

995 302

47. Comparison of predicted and measured pressure at ECC cold leg injection point (PT-P120-61) 30

48. Comparison of predicted and measured pump speed for Pump 1 (RPE-PC-1) 30

49. Comparison of predicted and measured average velocity in broken loop cold leg (FE-BL-1) 31

50. Comparison of predicted and measured average velocity in broken loop hot leg (FE-BL-2) 31

51. Comparison of predicted and measured average velocity in intact loop cold leg (FE-PC-1) 32

52. Comparison of predicted and measured average velocity in intact loop hot leg (FE-PC-2) 32

53. Comparison of predicted and measured average coolant temperature in broken loop cold leg (TE-BL-1). 33

54. Comparison of predicted and measured average coolant temperature in broken loop hot leg (TE-BL-2) 33

55. Comparison of predicted and measured average coolant temperature in intact loop cold leg (TE-PC-1). 34

56. Comparison of predicted and measured average coolant temperature in intact loop hot leg (TE-PC-2) 34

57. Comparison of predicted and measured coolant temperature on instrument Stalk 1 (TE-1ST-1) 35

58. Comparison of predicted and measured coolant temperature on instrument Stalk 1 (TE-1ST-2) 35

59. Comparison of predicted and measured coolant temperature on instrument Stalk 1 (TE-1ST-3) 36

60. Comparison of predicted and measured coolant temperature on instrument Stalk 1 (TE-1ST-4) 36

61. Comparison of predicted and measured coolant temperature on instrument Stalk 1 (TE-1ST-5) 37

62. Comparison of predicted and measured coolant temperature on instrument Stalk 1 (TE-1ST-6) 37

63. Comparison of predicted and measured coolant temperature on instrument Stalk 1 (TE-1ST-8) 38

64. Comparison of predicted and measured coolant temperature on instrument Stalk 1 (TE-1ST-9) 38

995 303

65. Comparison of predicted and measured coolant temperature on instrument Stalk 1 (TE-1ST-11) 39

66. Comparison of predicted and measured coolant temperature on instrument Stalk 1 (TE-1ST-12) 39

67. Comparison of predicted and measured coolant temperature on instrument Stalk 1 (TE-1ST-13) 40

68. Comparison of predicted and measured coolant temperature on instrument Stalk 1 (TE-1ST-14) 40

69. Comparison of predicted and measured coolant temperature on instrument Stalk 2 (TE-2ST-1) 41

70. Comparison of predicted and measured coolant temperature on instrument Stalk 2 (TE-2ST-2) 41

71. Comparison of predicted and measured coolant temperature on instrument Stalk 2 (TE-2ST-3) 42

72. Comparison of predicted and measured coolant temperature on instrument Stalk 2 (TE-2ST-5) 42

73. Comparison of predicted and measured coolant temperature on instrument Stalk 2 (TE-2ST-7) 43

74. Comparison of predicted and measured coolant temperature on instrument Stalk 2 (TE-2ST-9) 43

75. Comparison of predicted and measured coolant temperature on instrument Stalk 2 (TE-2ST-10) 44

76. Comparison of predicted and measured coolant temperature on instrument Stalk 2 (TE-2ST-13) 44

77. Comparison of predicted and measured coolant temperature on instrument Stalk 2 (TE-2ST-14) 45

78. Comparison of predicted and measured coolant temperature in lower end box (TE-1LP-1) 45

79. Comparison of predicted and measured coolant temperature in lower end box (TE-2LP-1) 46

80. Comparison of predicted and measured coolant temperature in lower end box (TE-3LP-1) 46

81. Comparison of predicted and measured coolant temperature in upper end box (TE-1UP-1) 47

82. Comparison of predicted and measured coolant temperature on drag disc-turbine transducer FE-1UP-1 (TE-1UP-5) 47

995 304

83. Comparison of predicted and measured coolant temperature in upper end box (TE-2UP-1) 48

84. Comparison of predicted and measured coolant temperature in upper end box (TE-3UP-1) 48

85. Comparison of predicted and measured coolant temperature on drag disc-turbine transducer FE-3UP-1 (TE-3UP-5) 49

86. Comparison of predicted and measured coolant temperature in upper end box (TE-4UP-1) 49

87. Comparison of predicted and measured coolant temperature in upper end box (TE-5UP-1) 50

88. Comparison of predicted and measured coolant temperature on drag disc-turbine transducer FE-5UP-1 (TE-5UP-9) 50

89. Comparison of predicted and measured coolant temperature in upper end box (TE-6UP-1) 51

90. Comparison of predicted and measured cladding temperature in fuel Assembly 5 (TE-5F4-15) 51

91. Comparison of predicted and measured cladding temperature in fuel Assembly 5 (TE-5J4-15) 52

92. Comparison of predicted and measured cladding temperature in fuel Assembly 5 (TE-5F4-21) 52

93. Comparison of predicted and measured cladding temperature in fuel Assembly 5 (TE-5J4-21) 53

94. Comparison of predicted and measured cladding temperature in fuel Assembly 5 (TE-5F4-26) 53

95. Comparison of predicted and measured cladding temperature in fuel Assembly 5 (TE-5J4-26) 54

96. Comparison of predicted and measured cladding temperature in fuel Assembly 5 (TE-5D6-30) 54

97. Comparison of predicted and measured cladding temperature in fuel Assembly 5 (TE-5F4-30) 55

98. Comparison of predicted and measured cladding temperature in fuel Assembly 5 (TE-5J4-30) 55

99. Comparison of predicted and measured cladding temperature in fuel Assembly 5 (TE-5L6-30) 56

100. Comparison of predicted and measured cladding temperature in fuel Assembly 5 (TE-5D6-32) 56

101. Comparison of predicted and measured cladding temperature in fuel Assembly 5 (TE-5L6-32) 57

102. Comparison of predicted and measured cladding temperature in fuel Assembly 5 (TE-5D6-37) 57

103. Comparison of predicted and measured cladding temperature in fuel Assembly 5 (TE-5L6-37) 58

104. Comparison of predicted and measured cladding temperature in fuel Assembly 5 (TE-5D6-39) 58

105. Comparison of predicted and measured cladding temperature in fuel Assembly 5 (TE-5L6-39) 59

A-1. Intact loop measurement locations 65

A-2. Broken loop measurement locations 67

A-3. Reactor vessel measurement locations 69

A-4. Reactor vessel upper plenum measurement locations 71

A-5. Core map showing fuel rod position designations 73

RELAP4/MOD6 PREDICTION COMPARISONS WITH LOFT LOCE L2-3 DATA

1. INTRODUCTION

An extensive comparison has been made between the experimental data from Loss-of-Coolant Experiment (LOCE) L2-3[1], performed in the Loss-of-Fluid Test (LOFT) facility, and data from the experimental prediction for LOCE L2-3[2], performed using a modified version of RELAP4/MOD6. The objective of this report is to make these comparisons generally available, with only limited qualitative observations, and to define areas of future posttest analysis.

The LOFT facility[3] is a 50 MW(t) volumetrically scaled pressurized water reactor (PWR) system designed to study the response of the engineered safety features in commercial PWR systems during the postulated loss-of-coolant accident. The LOFT system contains major components representative of those in a typical four-loop PWR and can be operated at conditions typical of a PWR. The LOFT reactor vessel contains a downcomer, a lower plenum, a nuclear core, and an upper head. The LOFT piping system consists of an intact loop, which represents the three unbroken loops of a four-loop PWR, and a broken loop, which represents a broken loop of a PWR.

LOCE L2-3 was a nuclear experiment simulating a 200% (100% break area in each leg of the LOFT broken loop) double-ended offset shear in the cold leg of a four-loop PWR. At experiment initiation the LOFT system was operating at a power level of 36.7 MW, which yielded a maximum linear heat generation rate of 39.4 kW/m, the mass flow rate in the intact loop was 199.8 kg/s, and the temperature of the primary coolant ranged from 560.7 to 592.9 K. Emergency core coolant (ECC) injection into the intact loop cold leg was initiated automatically at 14 s after experiment initiation. The specific objectives for LOCE L2-3 are stated in Reference 4.

995 307

The experiment prediction for LOCE L2-3 is best-estimate calculations of thermal-hydraulic responses in the LOFT system and was performed prior to conducting the experiment using the RELAP4/MOD6 computer code[5]. RELAP4/MOD6 is designed to calculate thermal-hydraulic responses, including fuel rod cladding temperatures, in a PWR during the blowdown and reflood phases of a loss-of-coolant transient. The test parameters used in the calculations are specified in Reference 4.

The experiment prediction and experimental data for LOCE L2-3 are compared in Section 2 on data plots with data from both sources overlaid. The experimental data shown are classified as qualified engineering units data, restrained data, not reviewed data, or computed data. These data classifications and the parameters compared are discussed in Section 2. Conclusions from the data comparisons and recommendations for future LOCE L2-3 posttest analysis work are presented in Section 3. Locations of the experimental measurements in the LOFT system are shown in figures in Appendix A. These figures are on foldout sheets that, when unfolded, allow the figures to be viewed alongside the data plots for reader convenience.

2. DATA COMPARISONS

In the context of this report, the experimental and experiment prediction data are most easily compared on data plots showing corresponding data from both sources. (The reader is encouraged to consider the error bands listed in Reference 1 in relation to the experimental data.) The experimental data are classified on each plot as QEUD (qualified engineering units data), REST (restrained data), NORE (not reviewed data), or COPE (computed data). These classifications are defined in Section 2.1. The experimental parameters compared are discussed in Section 2.2

2.1 Experimental Data Classifications

Individual plots of experimental data discussed in this report are classified in one of the following four categories.

995 308

2.1.1 Qualified Engineering Units Data. Qualified engineering units data (QEUD) must meet the following criteria:

(1) Have had all calibration corrections applied

(2) Have been compared with independent data and found to agree during the period of interest within specified uncertainty limits

(3) Have been verified to represent the parameter being measured.

Analytical use of the data is unrestricted for th specified time periods and within the defined uncertainty bands.

2.1.2 Restrained Data. Restrained data (REST) appear reasonable but cannot be classified QEUD because they meet either one of the following criteria:

(1) They are outside uncertainty bands established by reference measurements or derived from redundant measurements when such are available

(2) There are no independent data available for applying required calibration corrections during particular time intervals, and there are either no redundant measurements with which to compare the data or the data are outside uncertainty bands derived by such comparison when redundant measurements are available.

Restricted data used in numerical analyses are constrained by their restrictive statements included on the data plots.

2.1.3 Not Reviewed Data. Not reviewed data (NORE) have not been reviewed by the Data Integrity Review Committee (DIRC) (this definition is for internal recordkeeping only).

2.1.4 Computed Data. Computed data (COPE) have been calculated from measured data using data processing subroutines. In the figures, the four letter acronym appears on the plot; the test data trace is indicated by open squares, while the experiment prediction trace is indicated by solid circles.

2.2 Experimental Parameters Compared

Many of the data plots for the parameters compared show a difference in initial conditions between the experiment prediction and experimental data. This difference is probably the result of one of two errors or a combination of both. The first probable error to be considered is that the initial test conditions were not exactly known prior to the experiment, and the second is that the physical system was not accurately described via input data to the RELAP4/MOD6 solution scheme. The figures showing data discussed in the following subsections are presented at the end of Section 2.

2.2.1 Fluid Density. Figures 1 through 4 show that the trends in the density behavior were well predicted. The intermittent slug flow past the densitometer in the intact loop cold leg upstream of the ECC injection point was not predicted, as can be seen in Figure 3.

2.2.2 Differential Pressure. Figures 5 through 11 show comparisons between predicted and measured differential pressures. In general, the trends of the experimental data were well predicted. The initial differential pressure across the pumps (see Figures 8, 10, and 11) and steam generator (see Figure 9) in the intact loop reflect an adjustment due to the elevation head between the taps. The experiment prediction data cannot be corrected for this transducer calibration effect, and consequently, do not agree with the data before the start of the transient.

2.2.3 ECC Flow Rate. Figures 12 through 14 show comparisons between predicted and measured ECC volumetric flow rates. The trends of the experimental data were well predicted.

2.2.4 Liquid Level. The liquid level comparisons are shown in Figures 15 through 17. The trends in the experimental data were well predicted with the exception of steam generator secondary level. This is probably due to a misstatement of either the steam generator secondary feed or steam flow boundary conditions.

2.2.5 Mass Flow Rates. Figures 18 through 23 show comparisons between predicted and measured mass flow rates. The predictions are within the error bands of the experimental data for the majority of the transient.

2.2.6 Momentum Flux. Figures 24 through 31 show comparisons between predicted and measured momentum fluxes. With the exception of the broken loop cold leg, the prediction is for the most part in good agreement with the trends of the experimental data.

2.2.7 Pressure. Figures 32 through 47 show comparisons between the predicted and measured pressures. The pressures in the primary system were well predicted. The pressure in the blowdown suppression tank (see Figure 44) and steam generator secondary side (see Figure 45) were not well predicted.

2.2.8 Pump Speed. Figure 48 shows a comparison between predicted and measured pump speeds. The agreement is satisfactory.

2.2.9 Fluid Velocity. Figures 49 through 52 show comparisons between predicted and measured fluid velocities. The velocity in the broken loop cold leg (see Figure 49) was not well predicted; however, the trend of the velocity in the broken loop hot leg was well predicted.

The velocity in the intact loop hot and cold legs are in good agreement with the predictions. Since the velocity measurement transducers are unidirectional, it is believed that the experimental data shown in Figure 52 should be inverted from 8 to 30 s which would be in agreement with the predictions. This is substantiated by the bidirectional momentum flux measurements shown in Figure 27.

2.2.10 Fluid Temperature. Figures 53 through 89 show comparisons between predicted and measured fluid temperatures. In general, the trends of the predictions and the experimental data are in good agreement.

2.2.11 Fuel Rod Cladding Temperature. Figures 90 through 105 show comparisons between predicted and measured fuel rod cladding temperatures. The prediction exhibits early departure from nucleate boiling relative to the experimental data, and the rewet, which occurs early in the transient, is not predicted by the code. Considering the general good agreement of other experimental measurements, it is surprising that the cladding temperatures are not in better agreement. This may be an indication of a heat transfer problem in the code.

995 312

POOR ORIGINAL

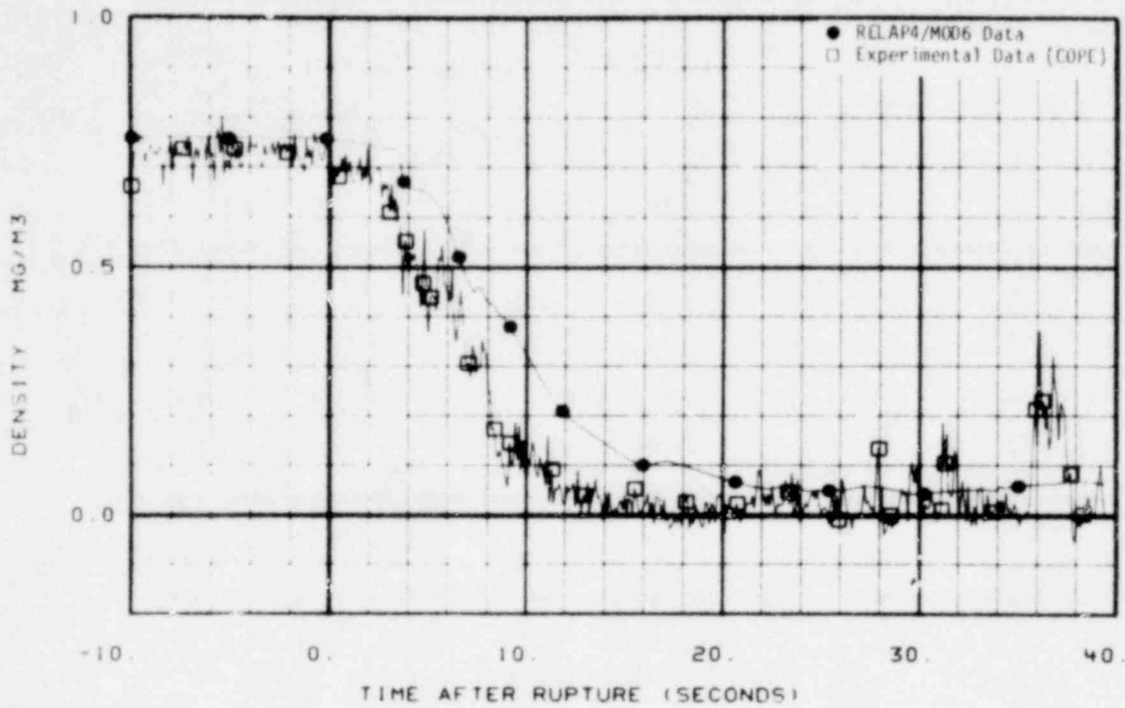

Fig. 1 Comparison of predicted and measured average density in broken loop cold leg (DE-BL-1).

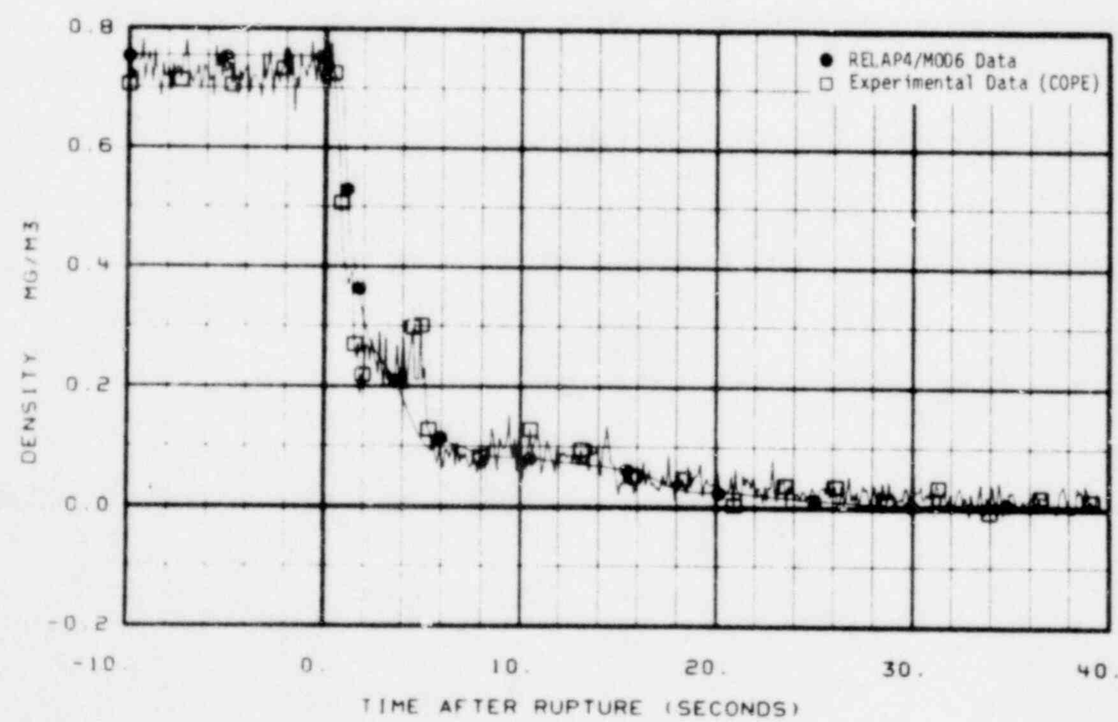

Fig. 2 Comparison of predicted and measured average density in broken loop hot leg (DE-BL-2).

995 313

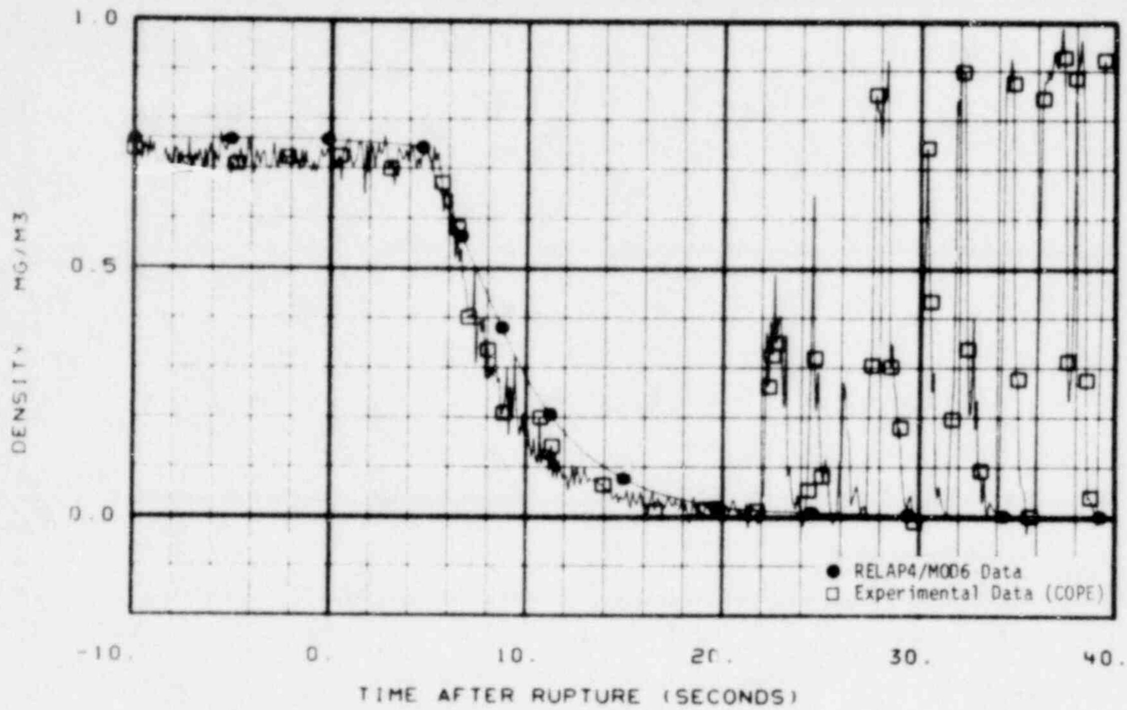

Fig. 3 Comparison of predicted and measured average density in intact loop cold leg (DE-PC-1).

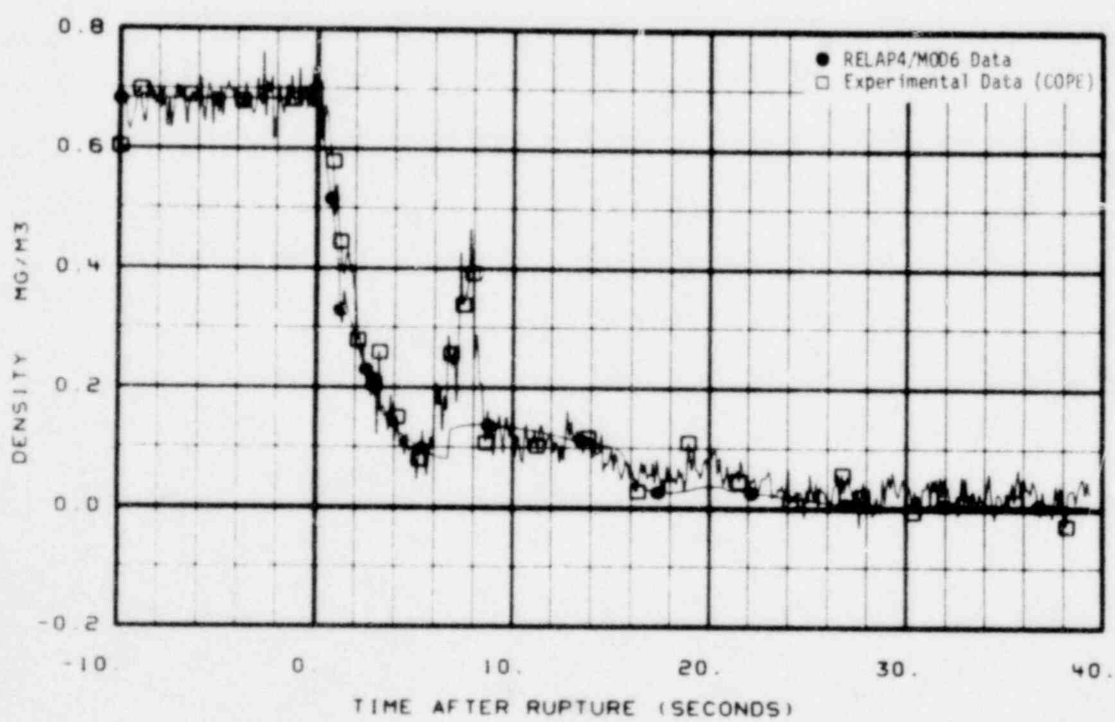

Fig. 4 Comparison of predicted and measured average density in intact loop hot leg (DE-PC-2).

995 314

POOR ORIGINAL

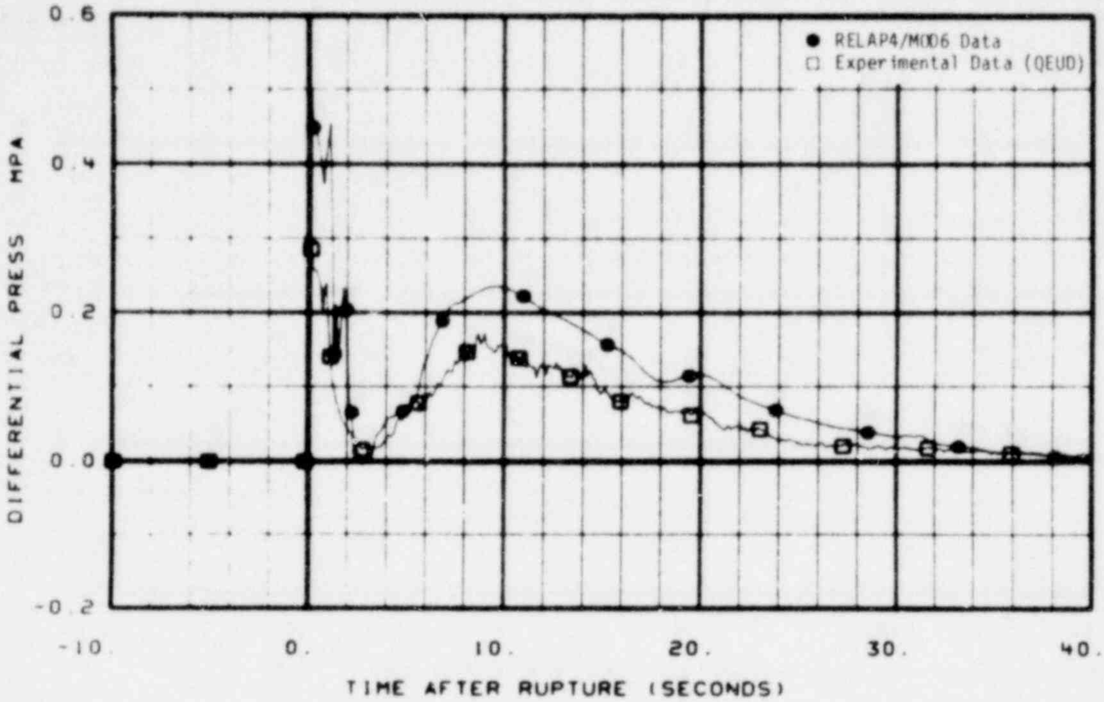

Fig. 5 Comparison of predicted and measured differential pressure across 14- to 5-in. reducer (PdE-BL-1).

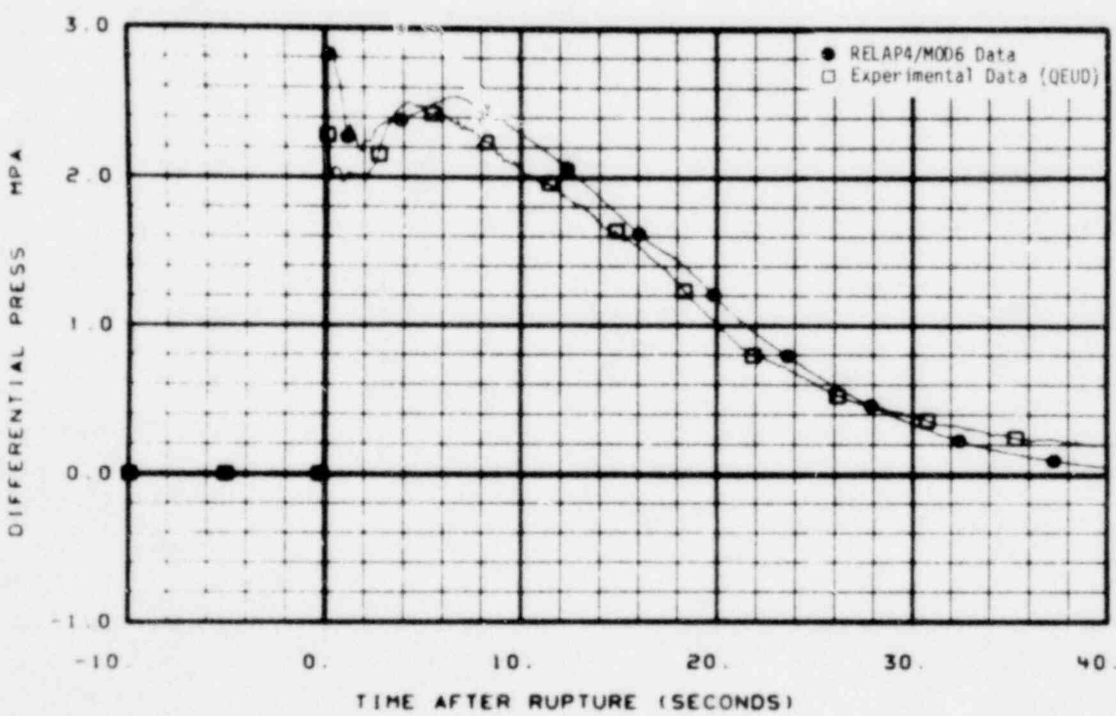

Fig. 6 Comparison of predicted and measured differential pressure across pump simulator (PdE-BL-5).

995 315

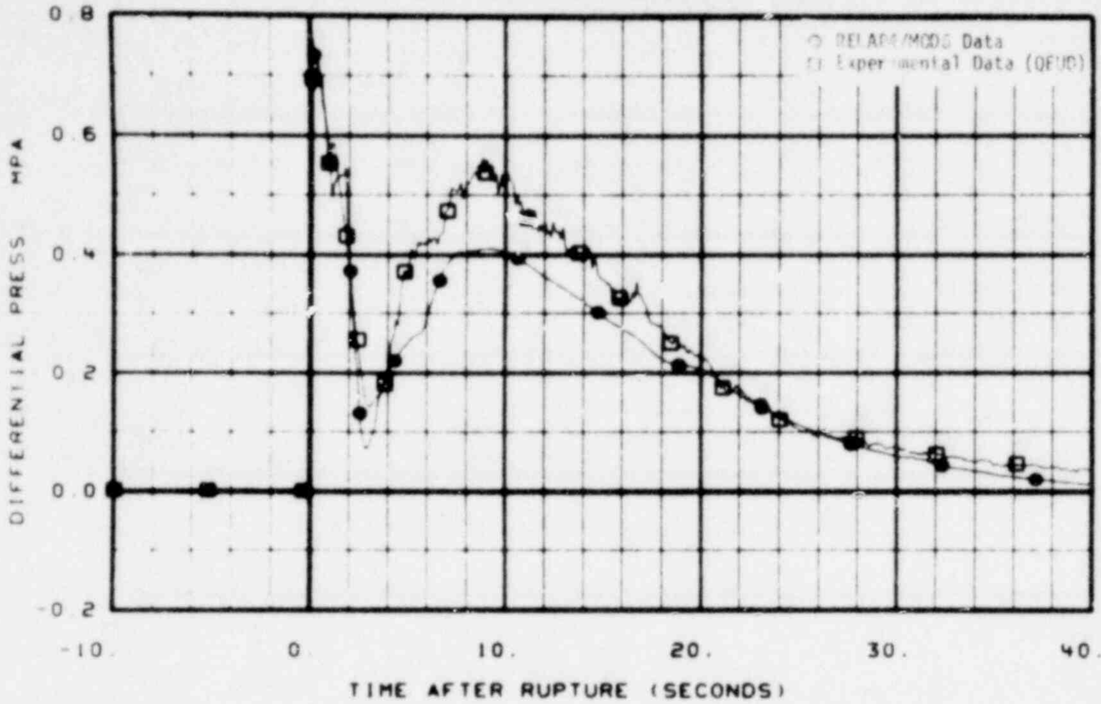

Fig. 7 Comparison of predicted and measured differential pressure across steam generator simulator (PdE-BL-7).

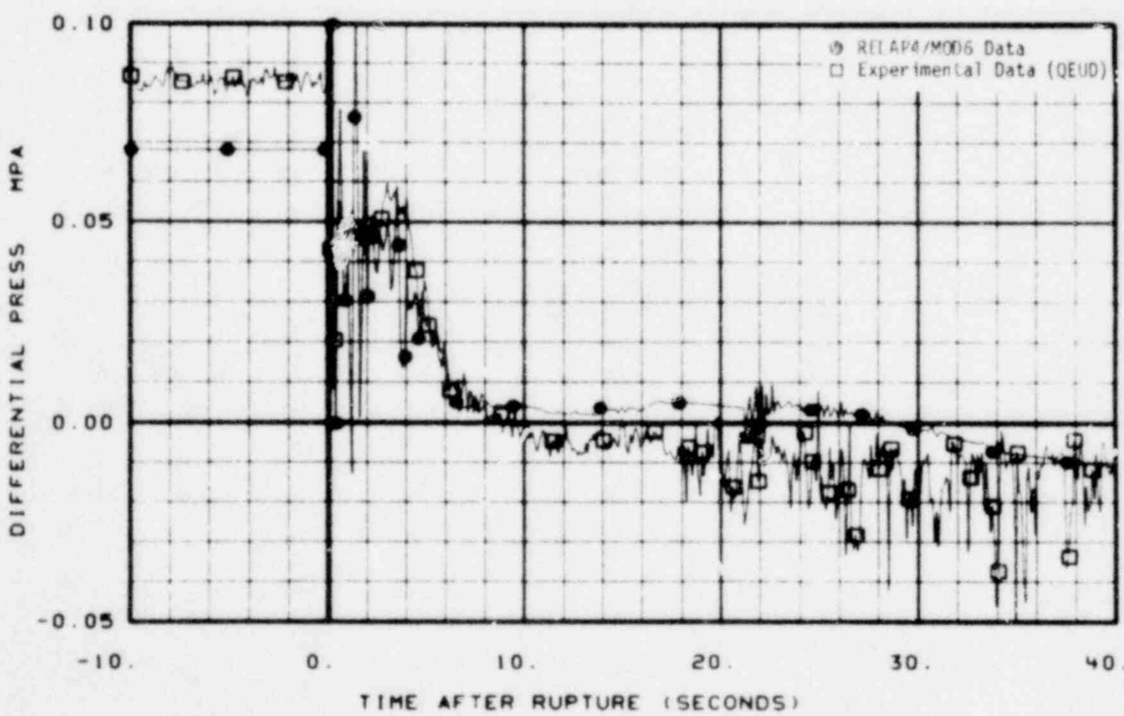

Fig. 8 Comparison of predicted and measured differential pressure across pumps (PdE-PC-1).

995 316

POOR ORIGINAL

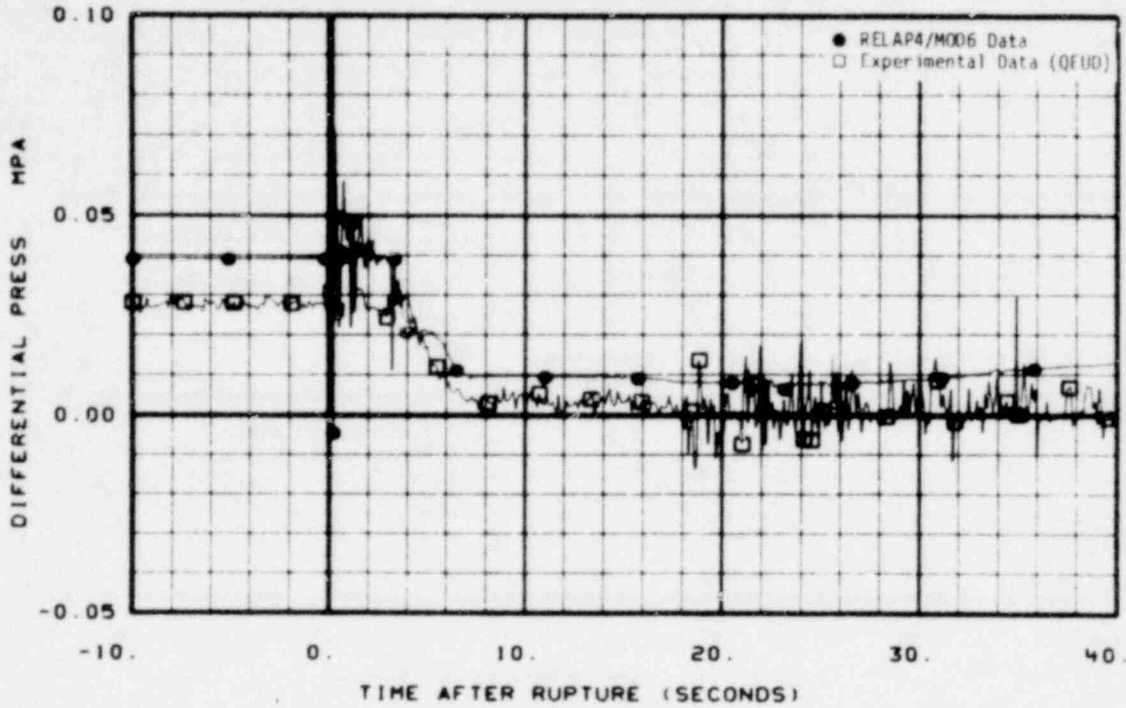

Fig. 9 Comparison of predicted and measured differential pressure across intact loop steam generator (PdE-PC-2).

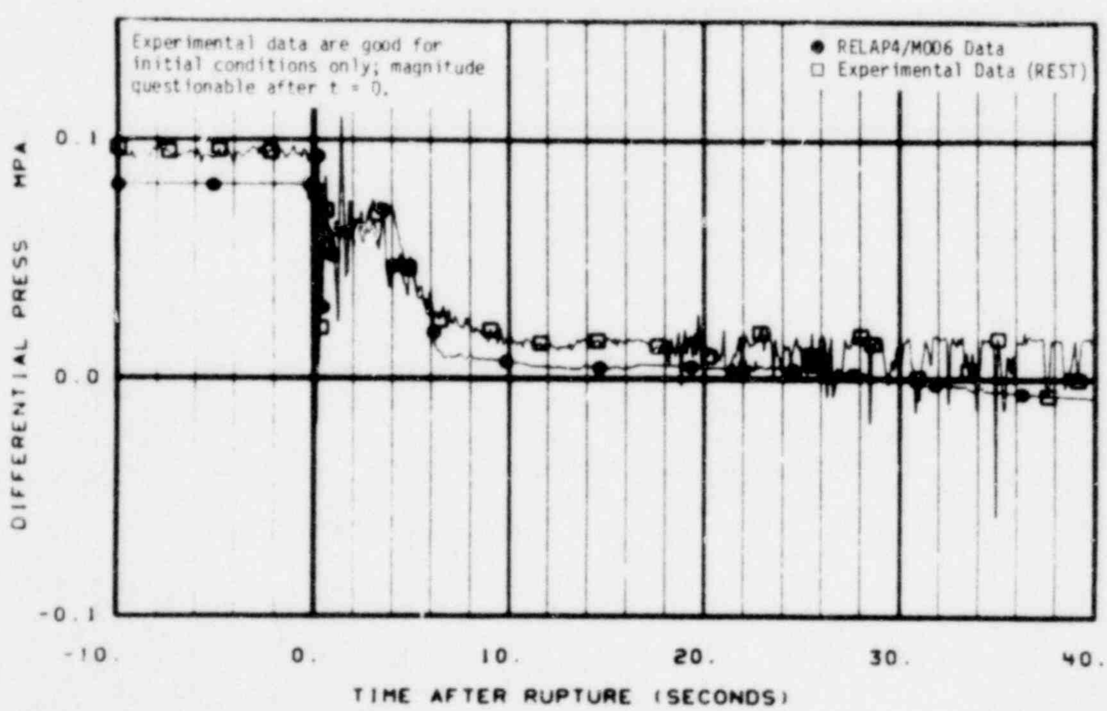

Fig. 10 Comparison of predicted and measured differential pressure across Pump 1 (PdE-PC-9).

995 317

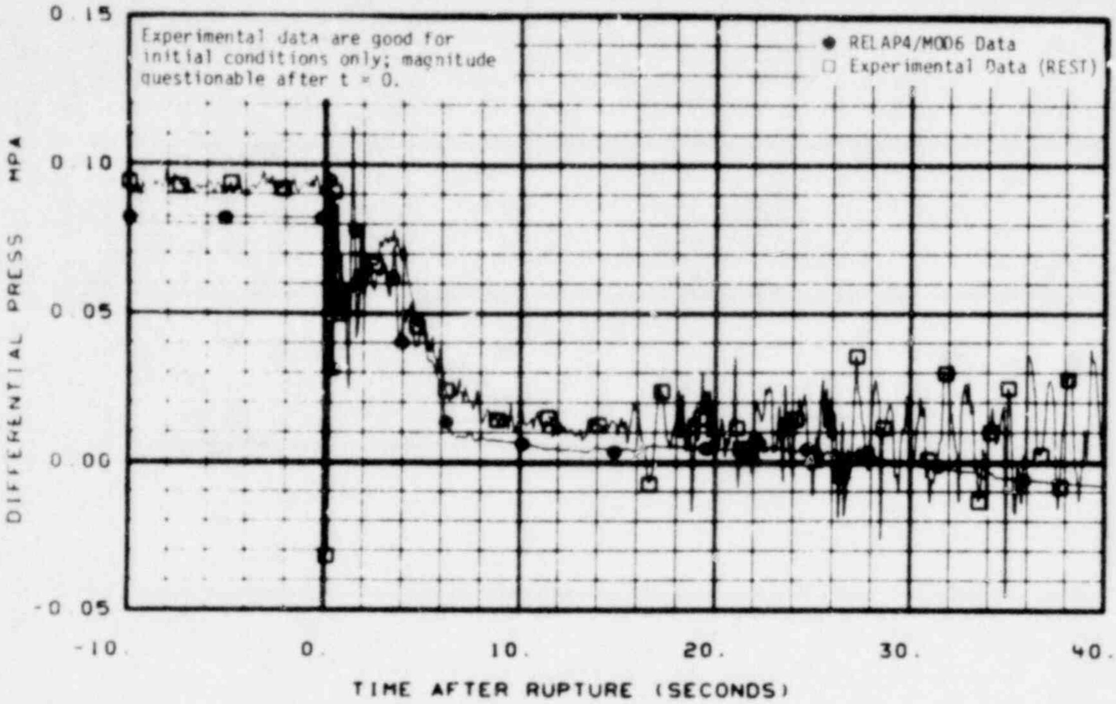

Fig. 11 Comparison of predicted and measured differential pressure across Pump 2 (PdE-PC-10).

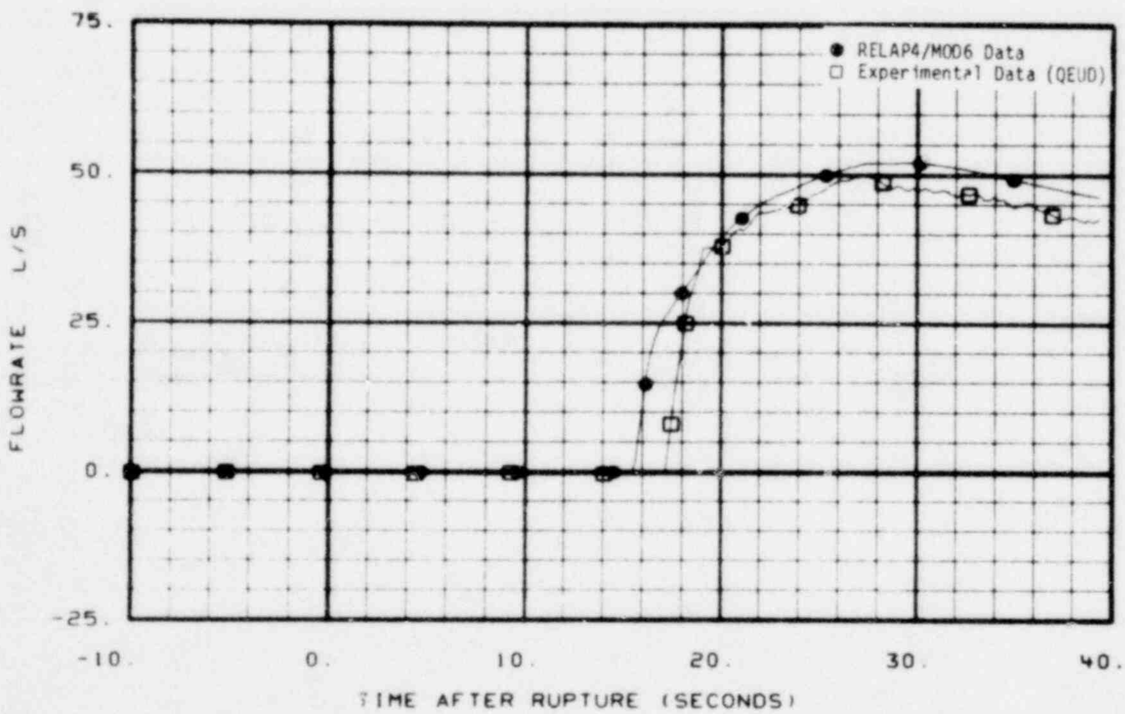

Fig. 12 Comparison of predicted and measured flow rate from accumulator (FT-P120-36-1).

995 318

POOR ORIGINAL

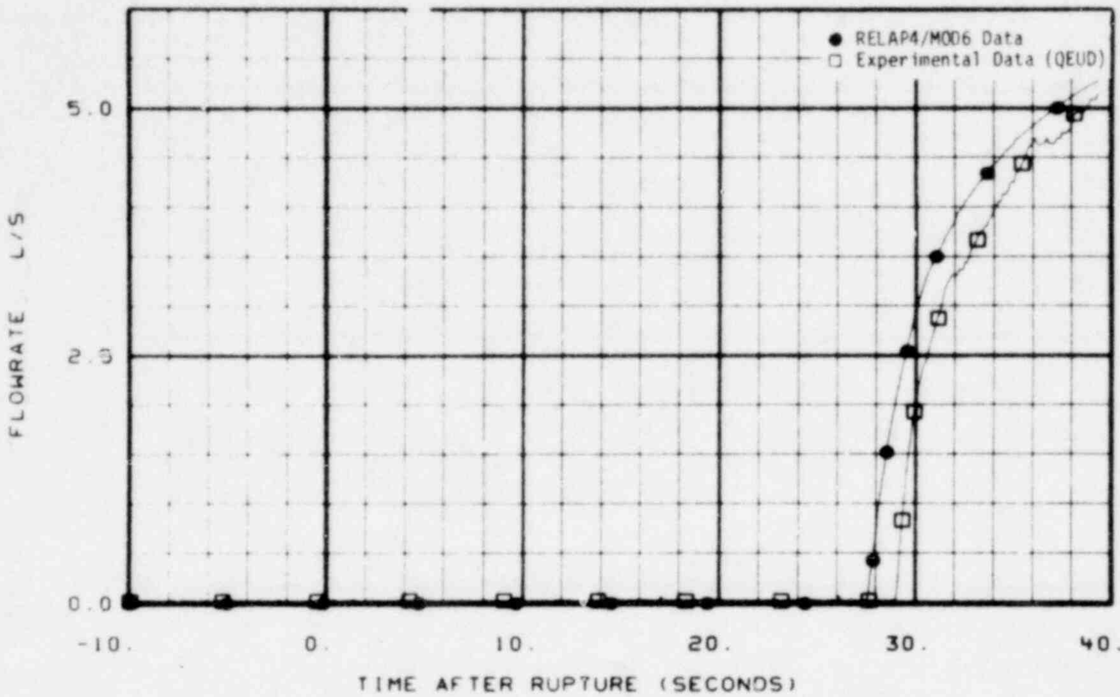

Fig. 13 Comparison of predicted and measured flow rate from low-pressure injection system pump (FT-P120-85).

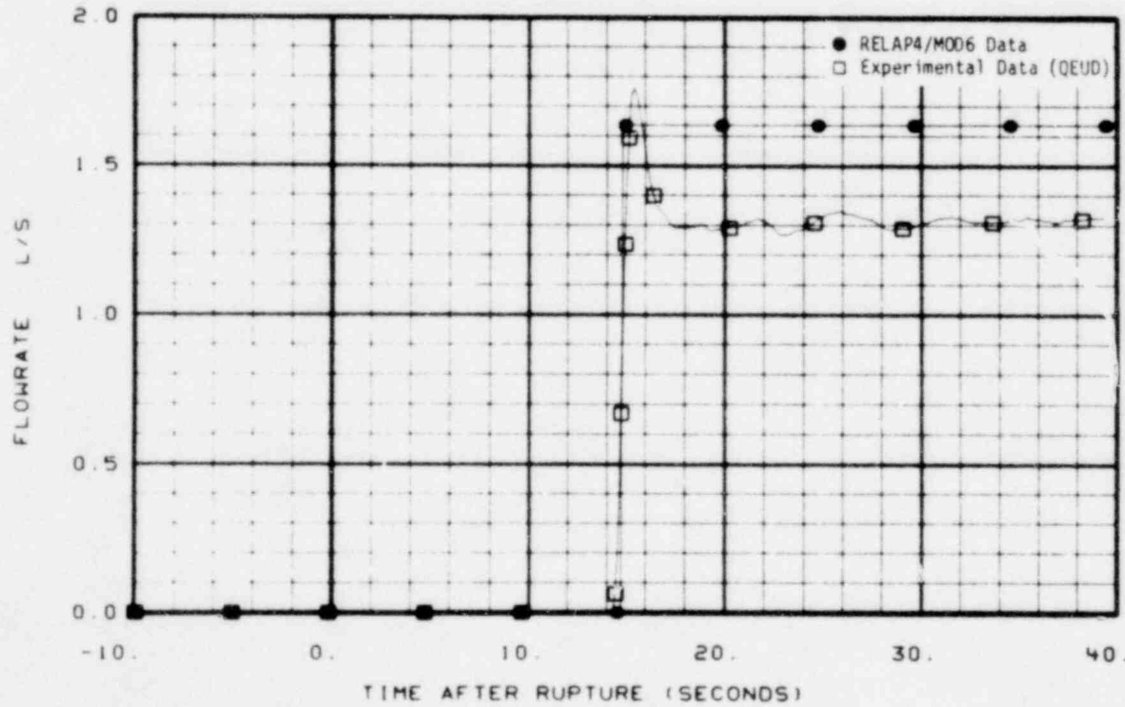

Fig. 14 Comparison of predicted and measured flow rate from high-pressure injection system pump (FT-P128-104).

995 319

POOR ORIGINAL

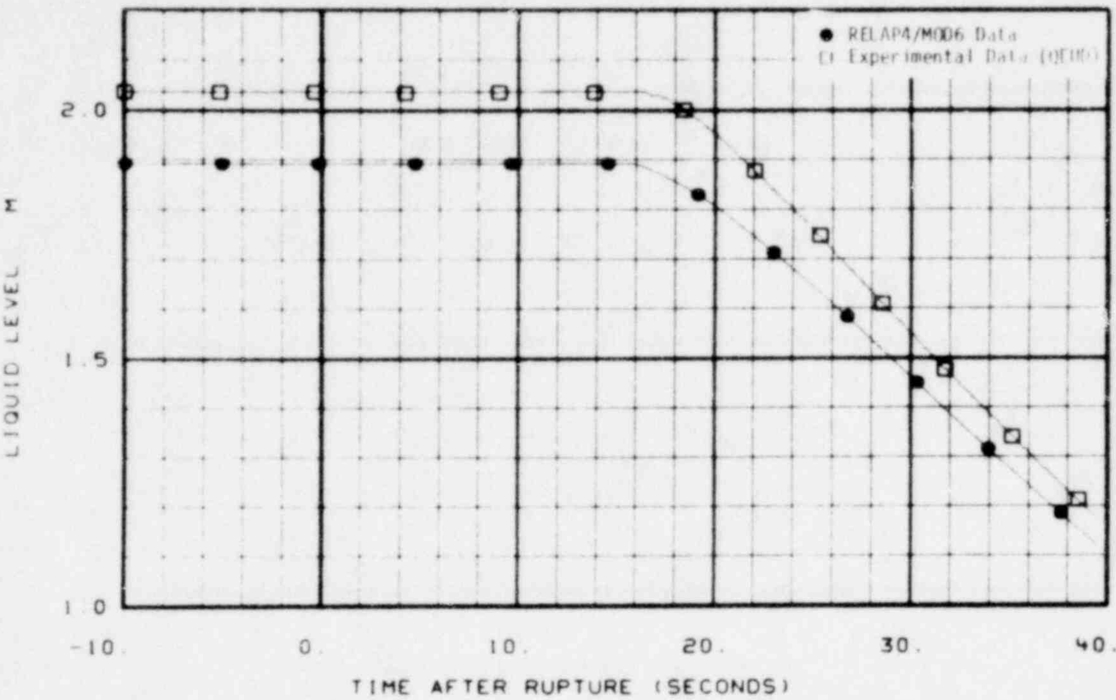

Fig. 15 Comparison of predicted and measured liquid level in accumulator (LIT-P120-44).

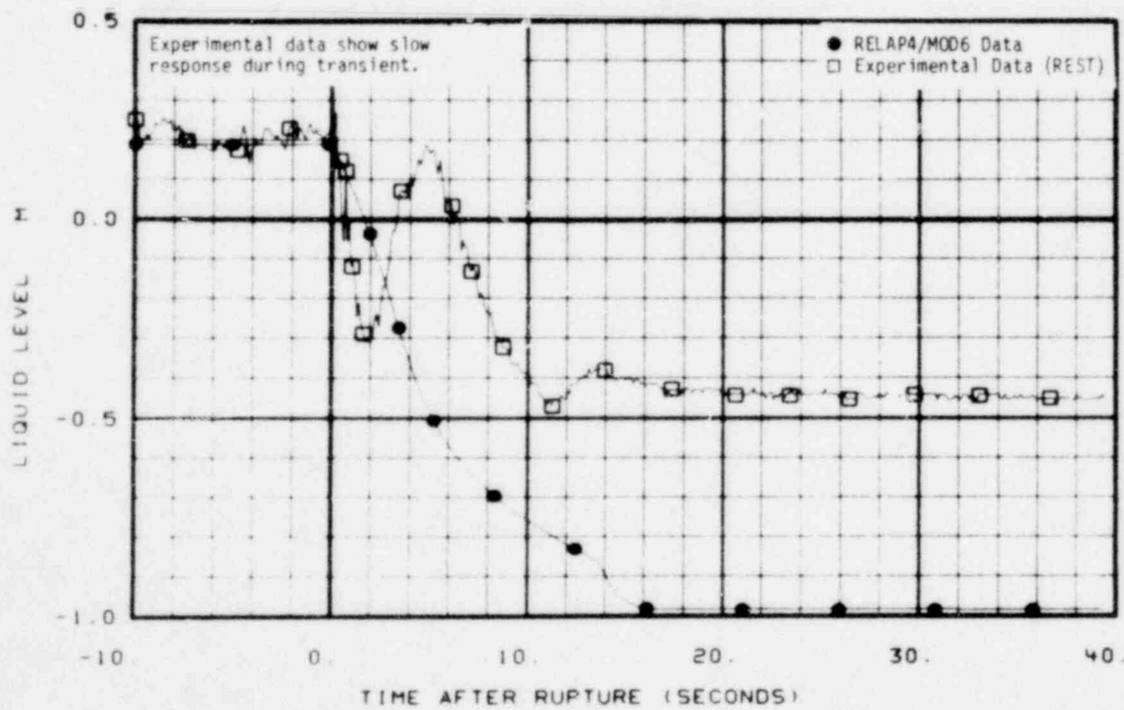

Fig. 16 Comparison of predicted and measured liquid level in steam generator secondary side (LT-P004-8B).

995 320

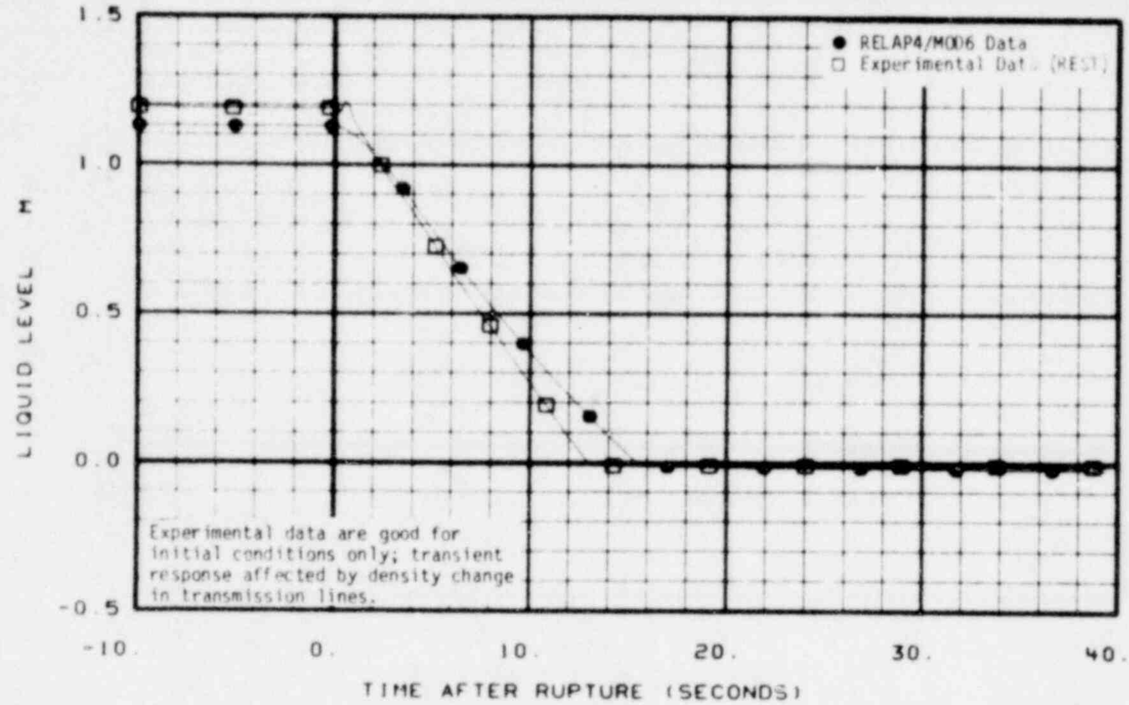

Fig. 17 Comparison of predicted and measured liquid level in pressurizer Channel B (LT-P139-7).

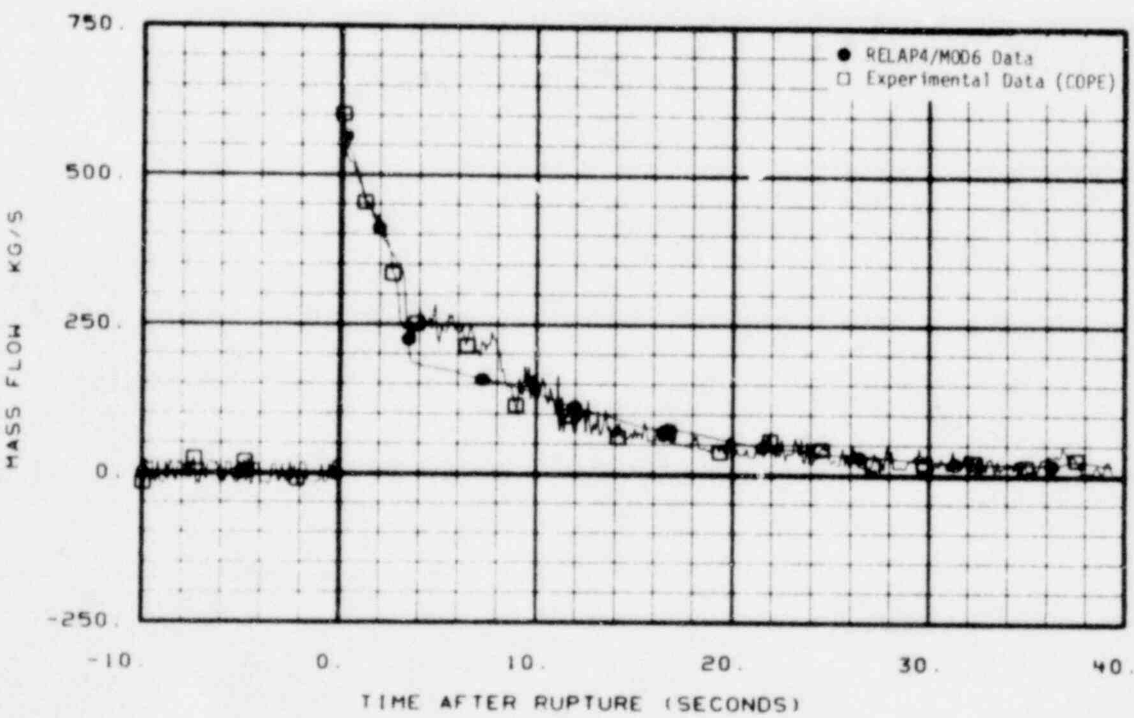

Fig. 18 Comparison of predicted and measured mass flow in broken loop cold leg (FR-BL-1).

995 321

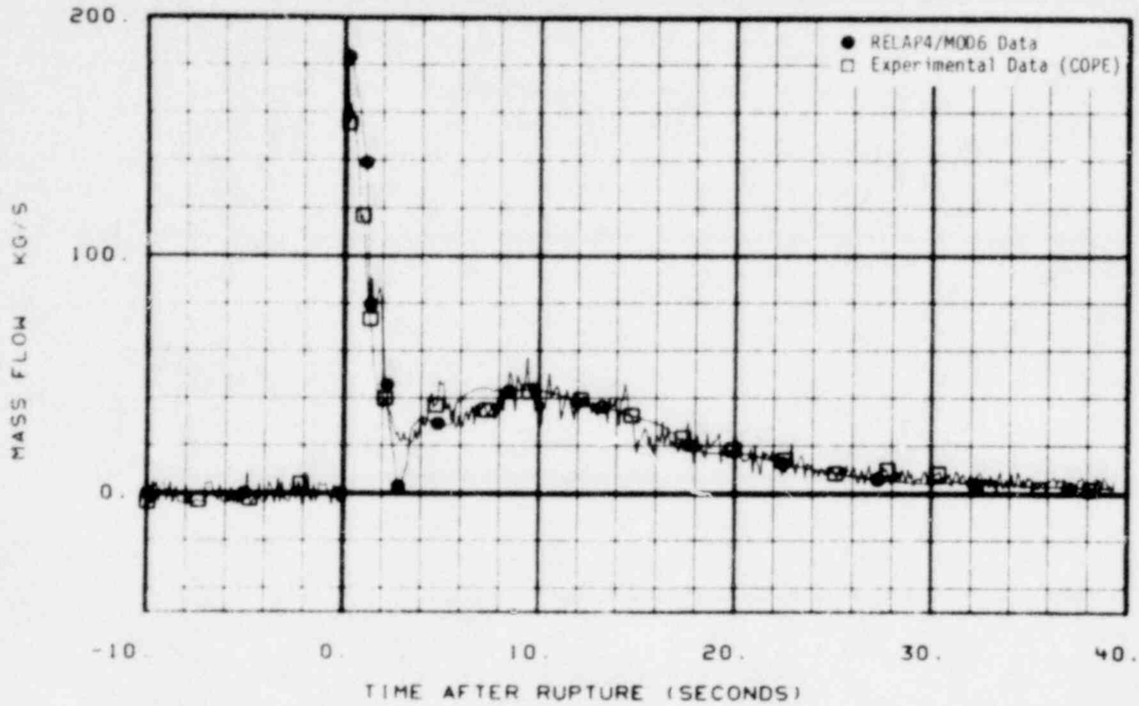

Fig. 19 Comparison of predicted and measured mass flow in broken loop hot leg (FR-BL-2).

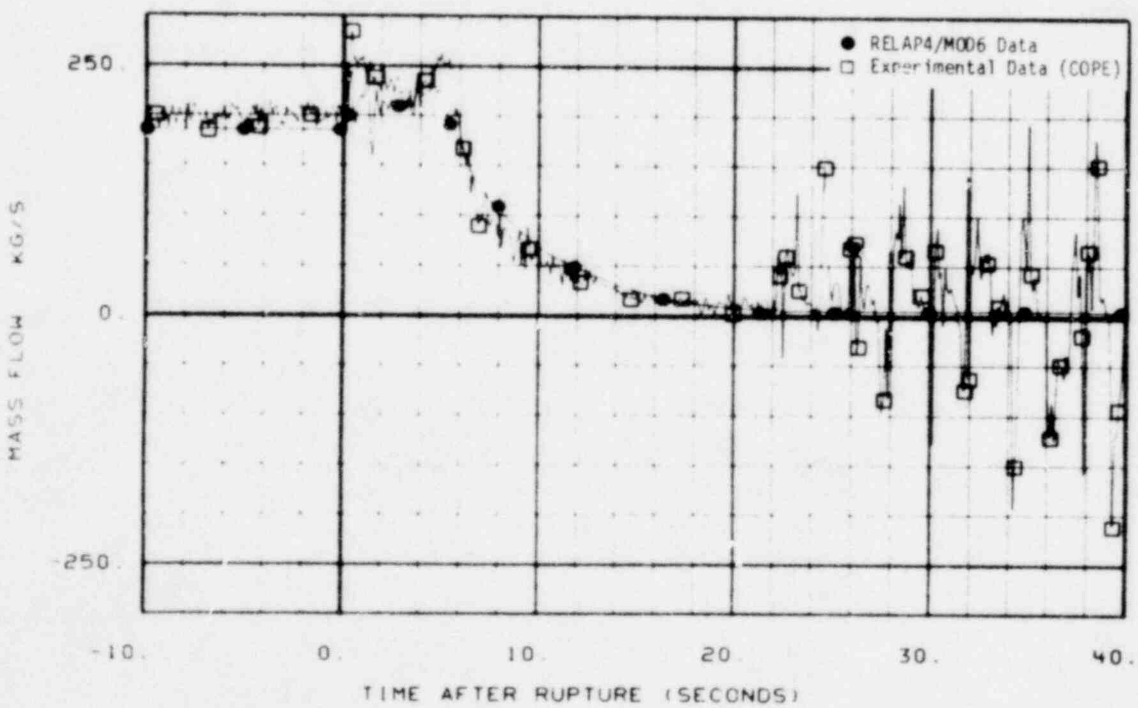

Fig. 20 Comparison of predicted and measured mass flow in intact loop cold leg (FR-PC-1).

995 322

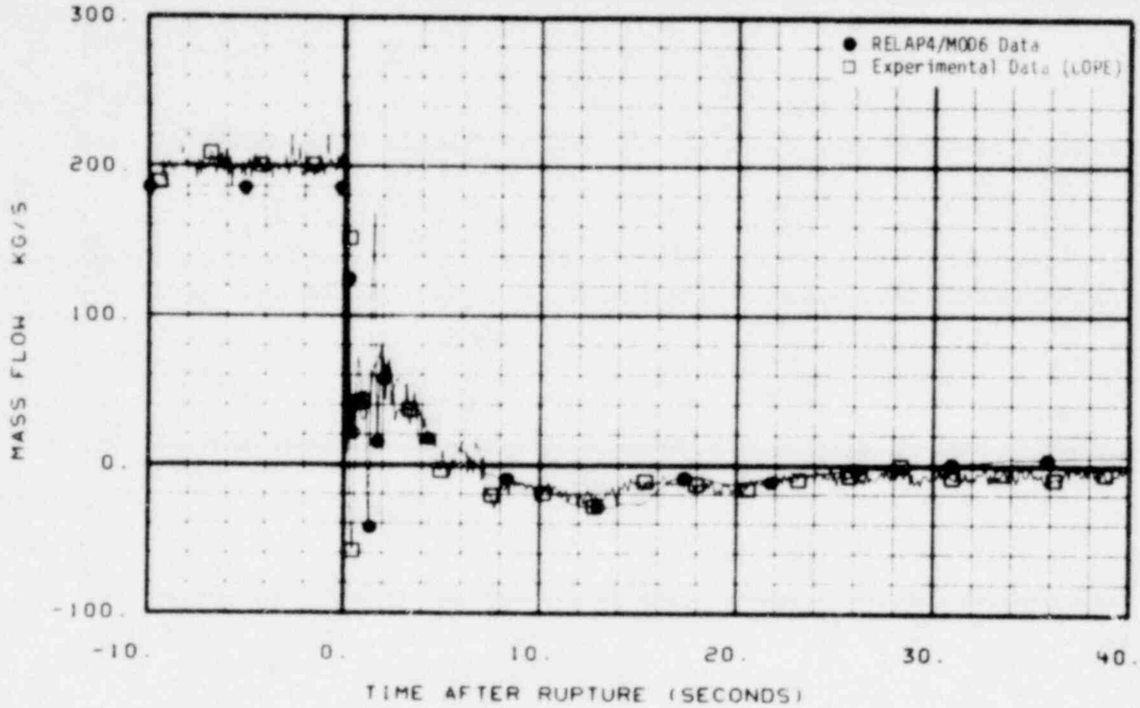

Fig. 21 Comparison of predicted and measured mass flow in intact loop hot leg (FR-PC-2).

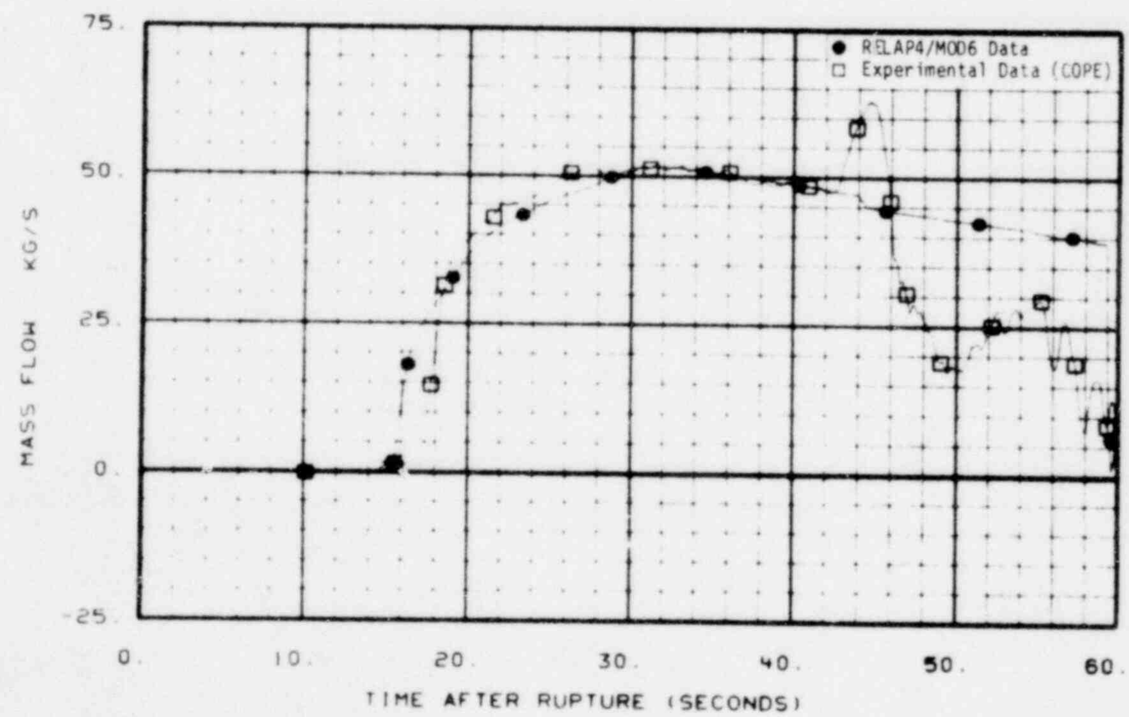

Fig. 22 Comparison of predicted and measured total ECC flow rate (FR-ECC-1).

995 325

POOR ORIGINAL

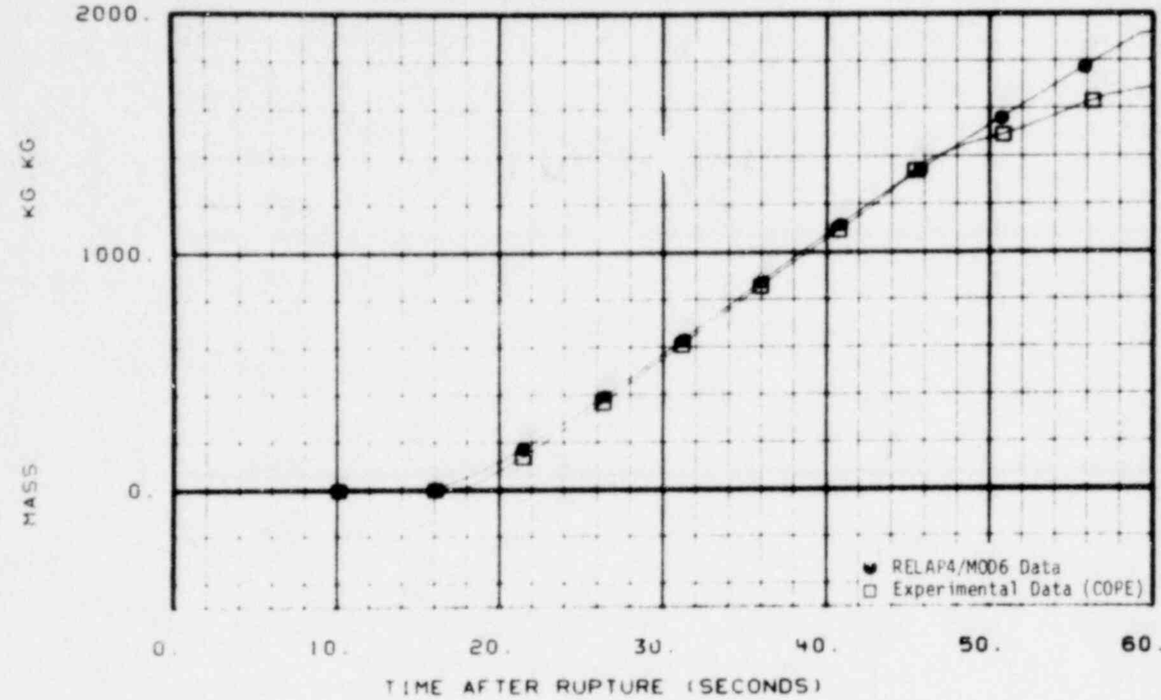

Fig. 23 Comparison of predicted and measured integral of ECC flow (MS-RV-001).

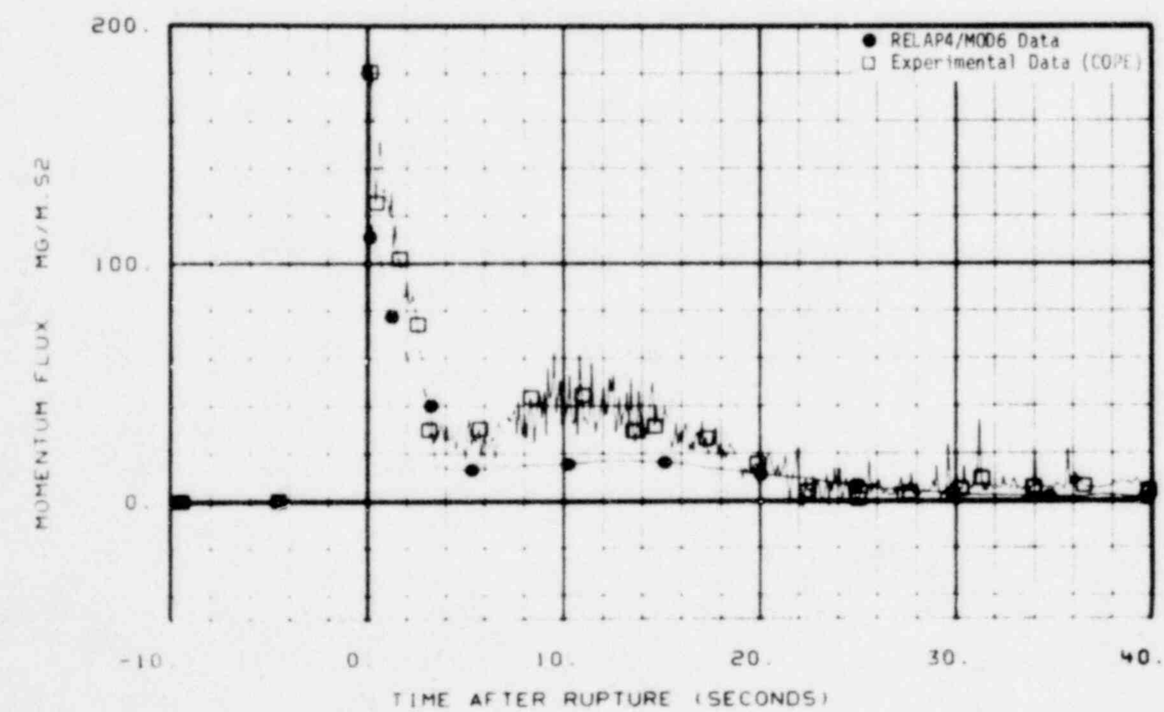

Fig. 24 Comparison of predicted and measured momentum flux in broken loop cold leg (ME-BL-1).

995 324

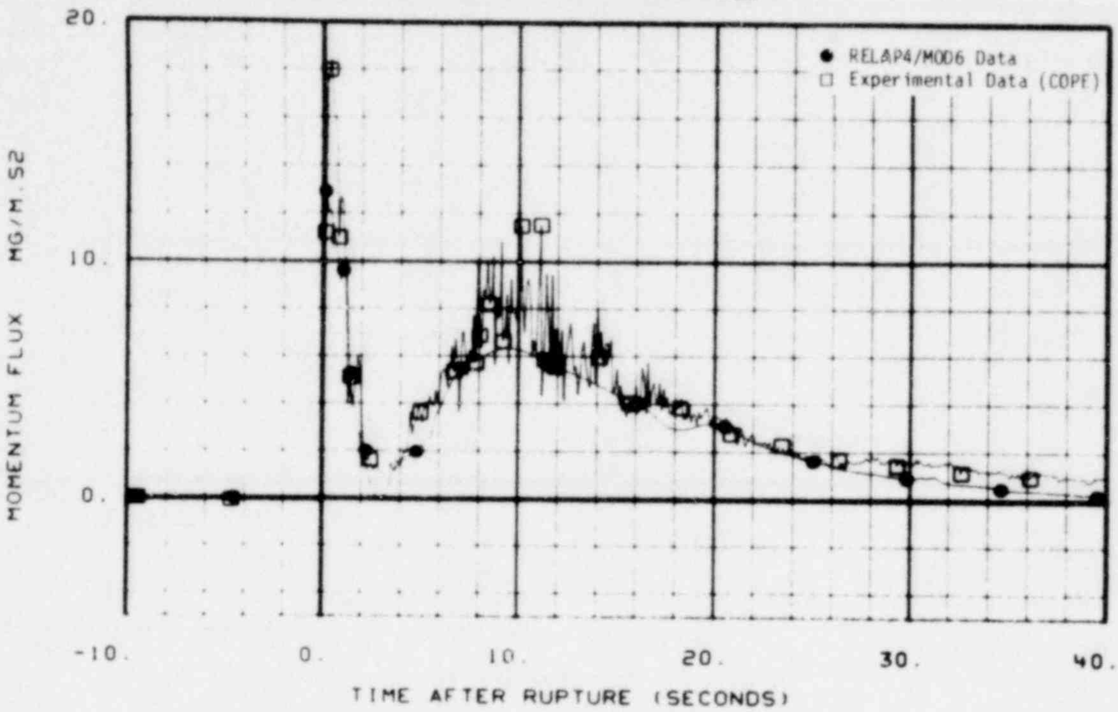

Fig. 25 Comparison of predicted and measured momentum flux in broken loop hot leg (ME-BL-2).

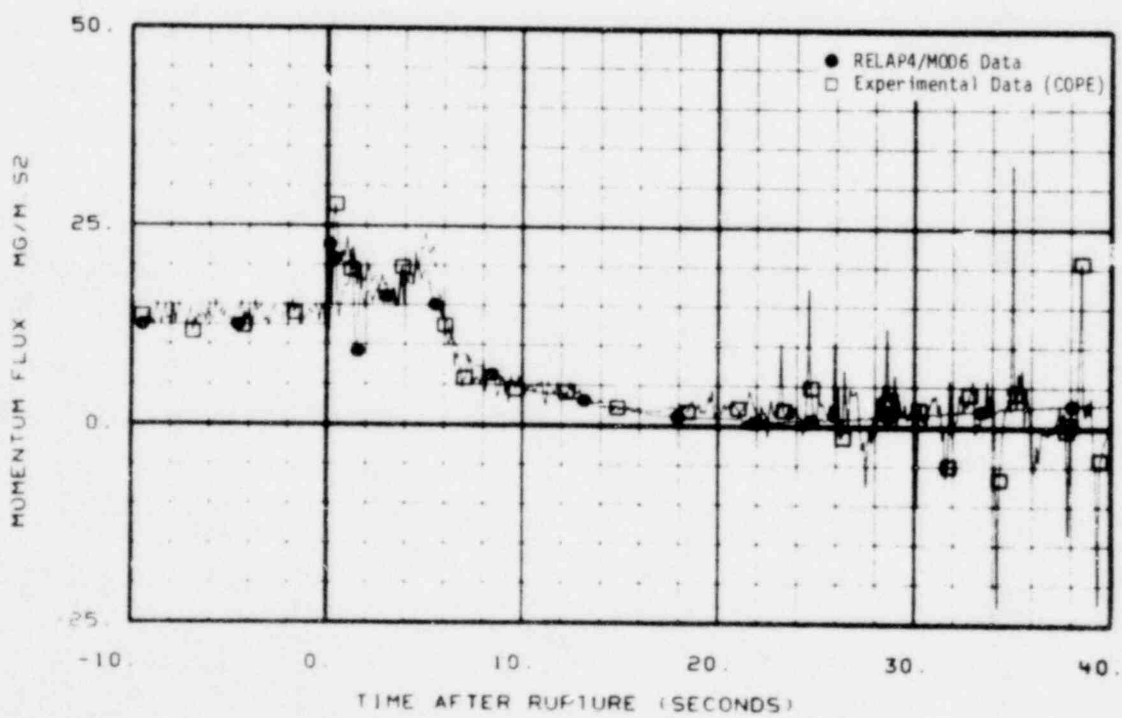

Fig. 26 Comparison of predicted and measured momentum flux in intact loop cold leg (ME-PC-1).

995 325

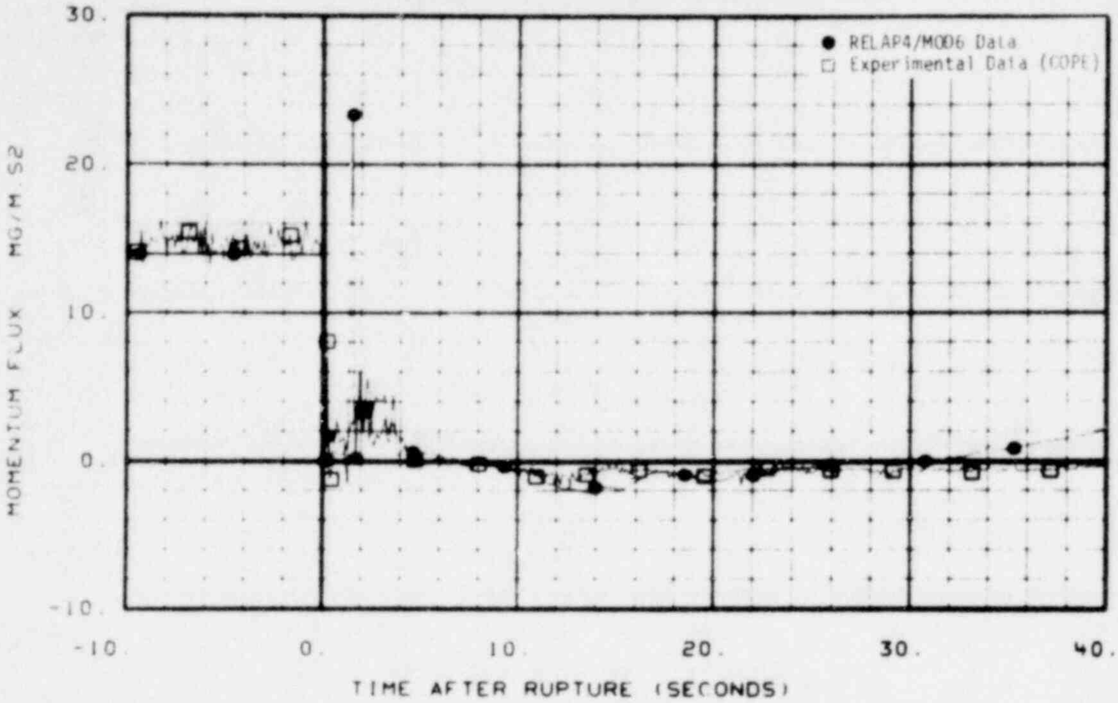

Fig. 27 Comparison of predicted and measured momentum flux in intact loop hot leg (ME-PC-2).

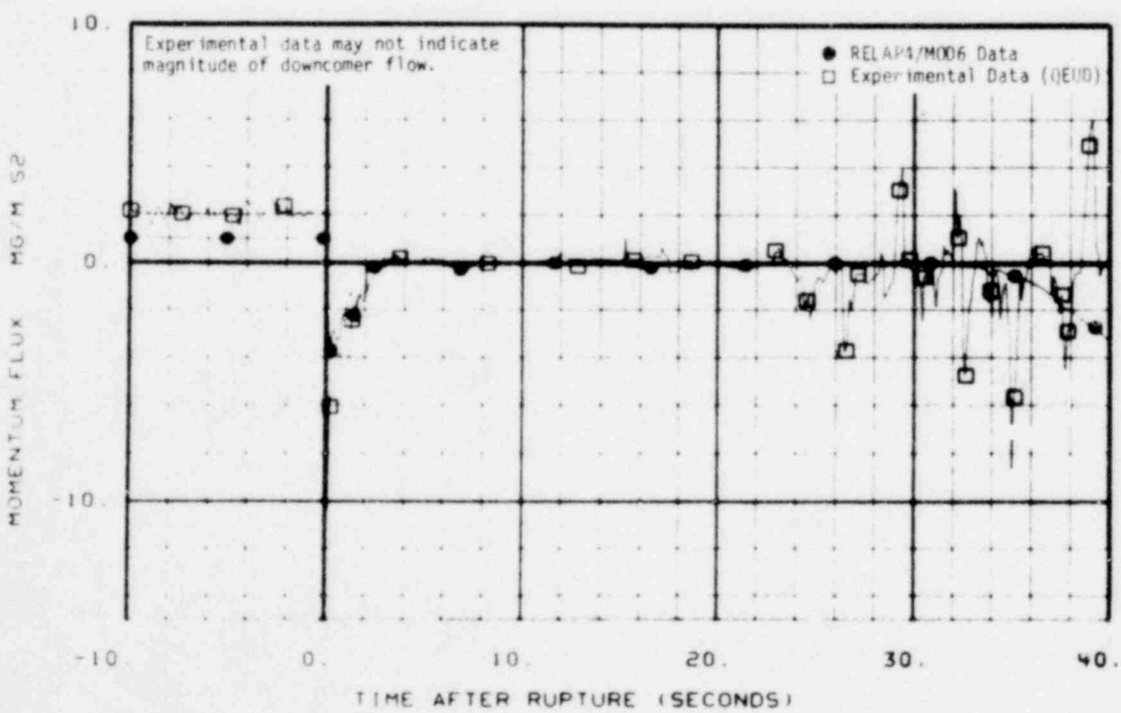

Fig. 28 Comparison of predicted and measured momentum flux at instrument Stalk 1 (ME-1ST-1).

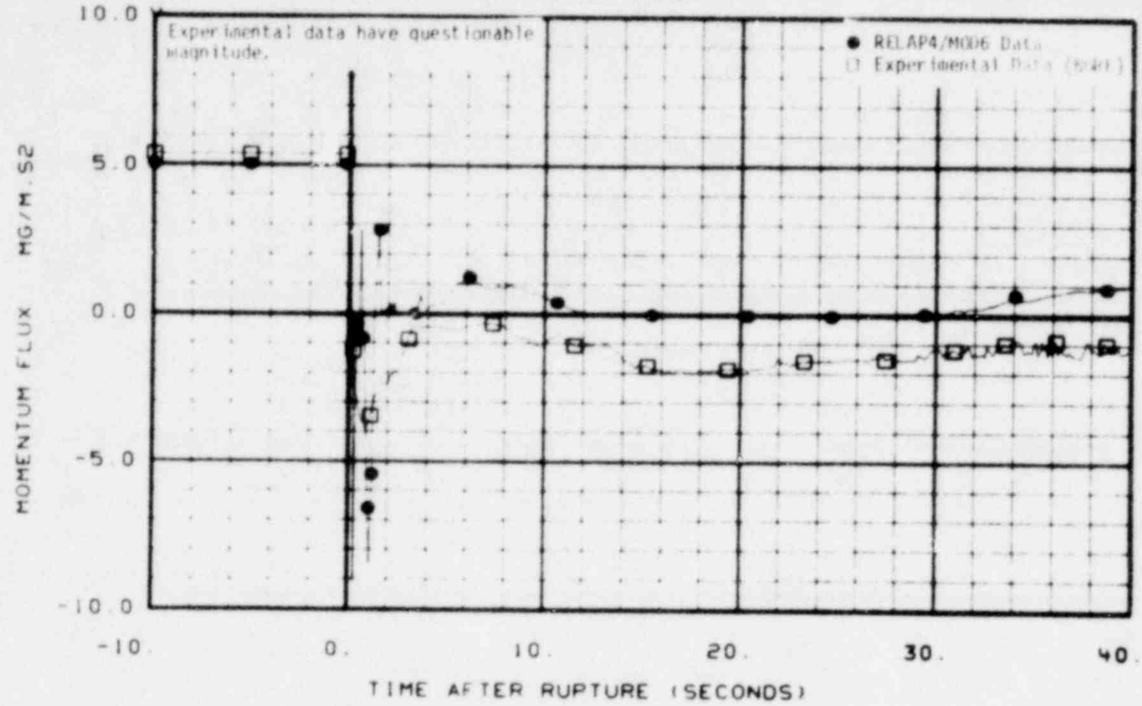

Fig. 29 Comparison of predicted and measured momentum flux in upper end box (ME-1UP-1).

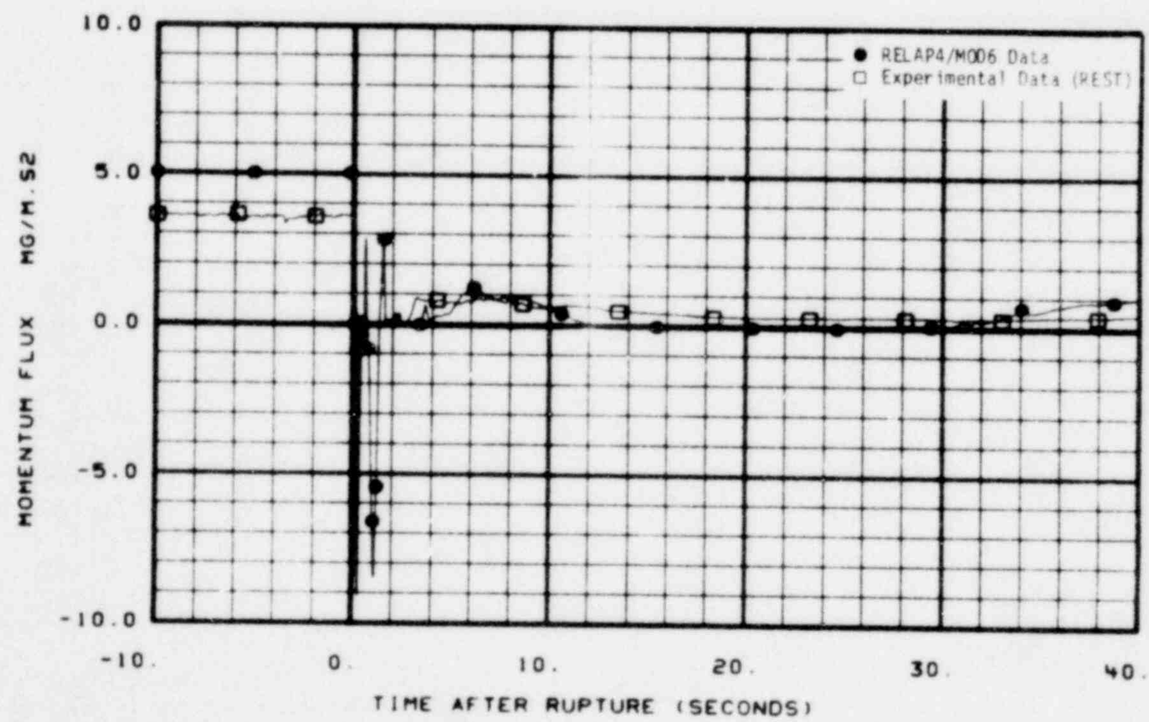

Fig. 30 Comparison of predicted and measured momentum flux in upper end box (ME-3UP-1)

995 327

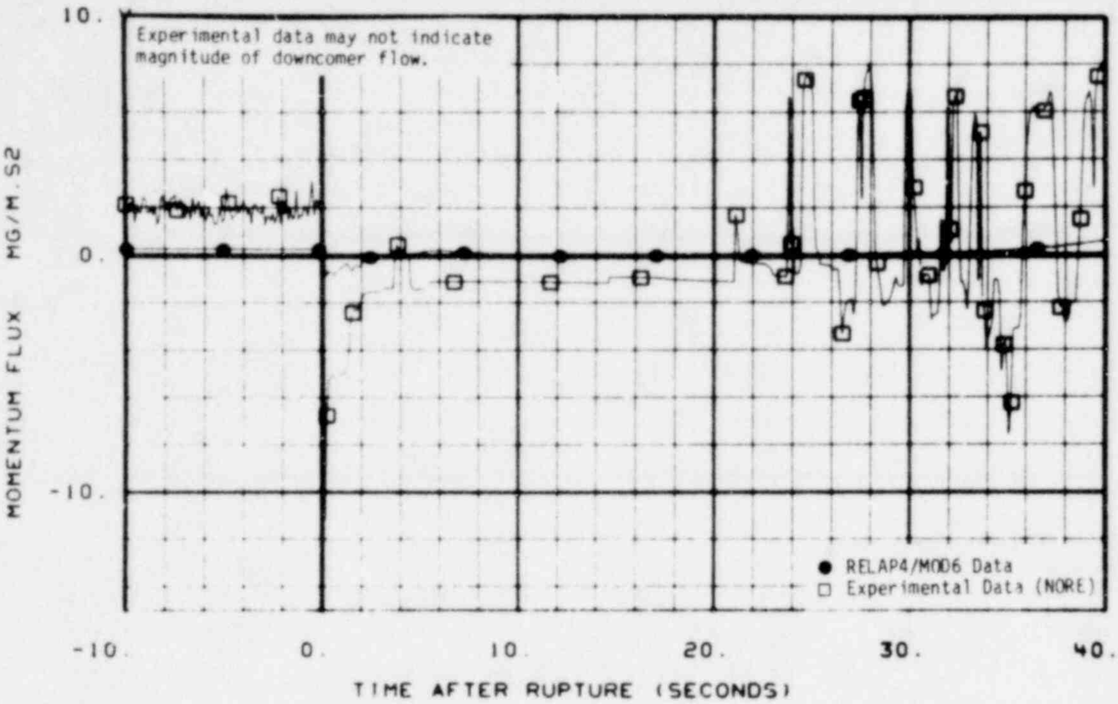

Fig. 31 Comparison of predicted and measured momentum flux at instrument Stalk 2 (ME-2ST-1).

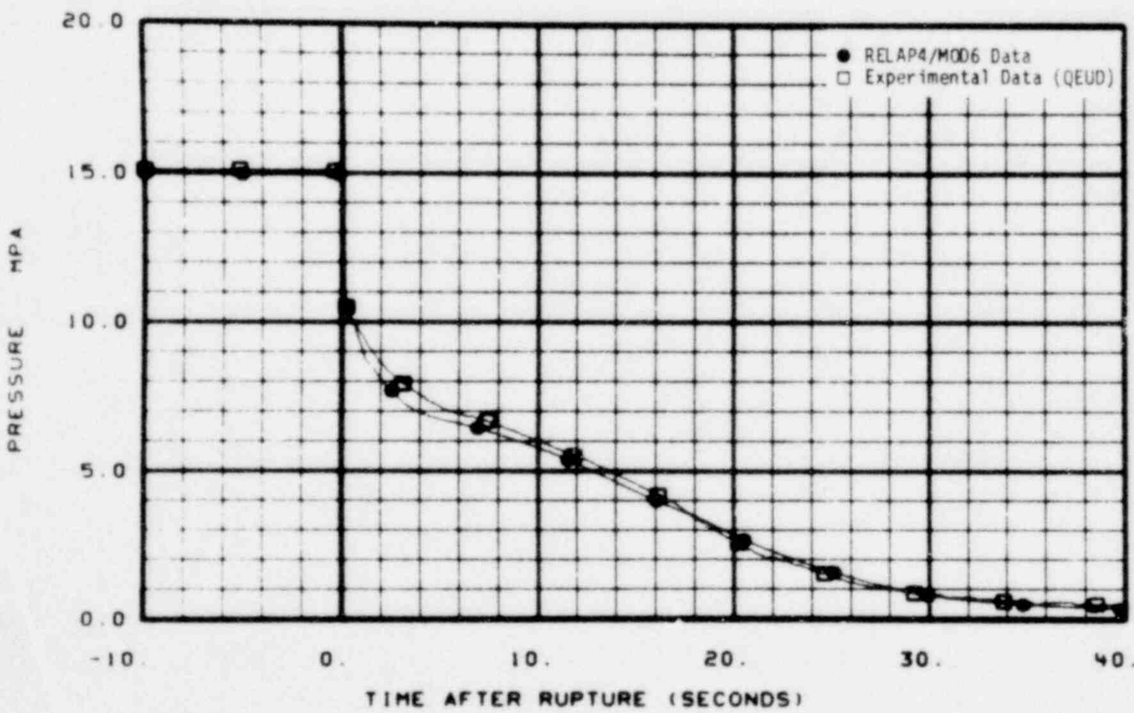

Fig. 32 Comparison of predicted and measured pressure in broken loop cold leg (PE-BL-1).

995 328

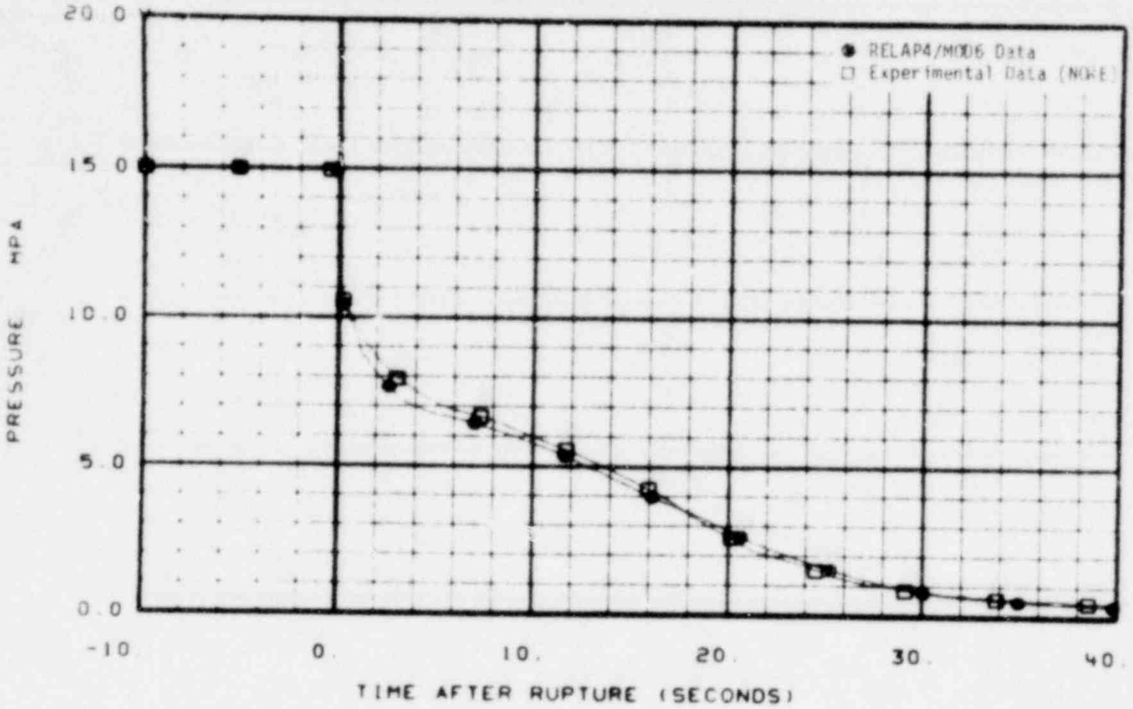

Fig. 33 Comparison of predicted and measured pressure in broken loop hot leg (PE-BL-2).

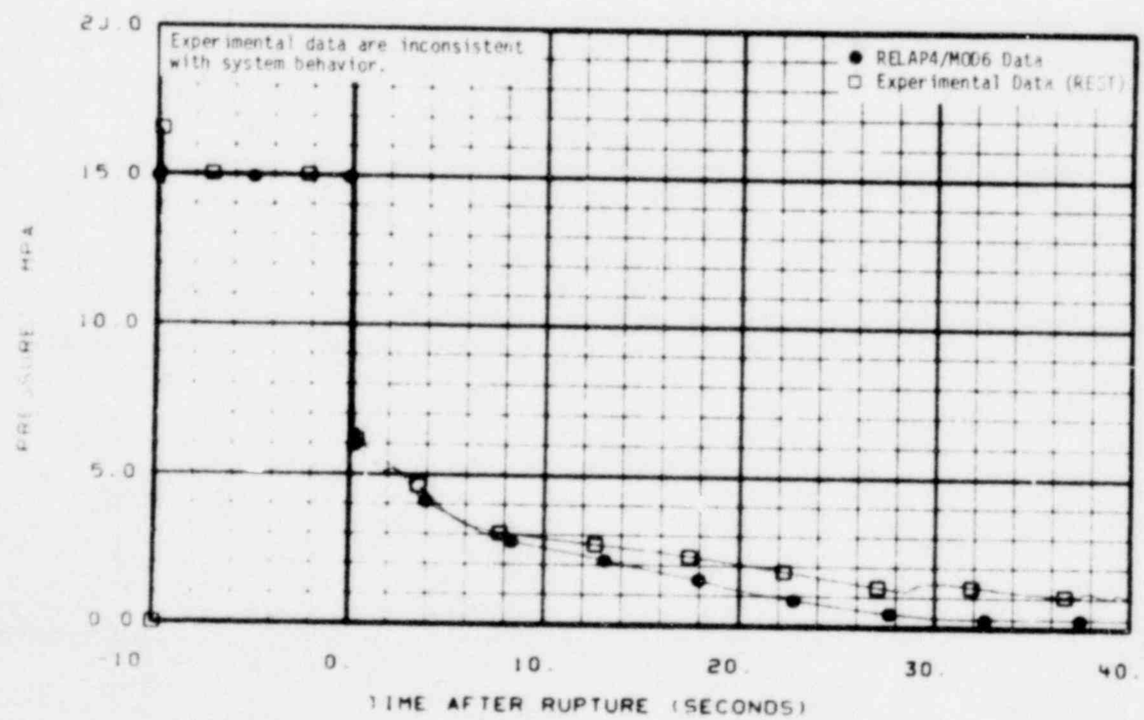

Fig. 34 Comparison of predicted and measured pressure in broken loop hot leg pump simulator outlet (PE-BL-3).

995 327

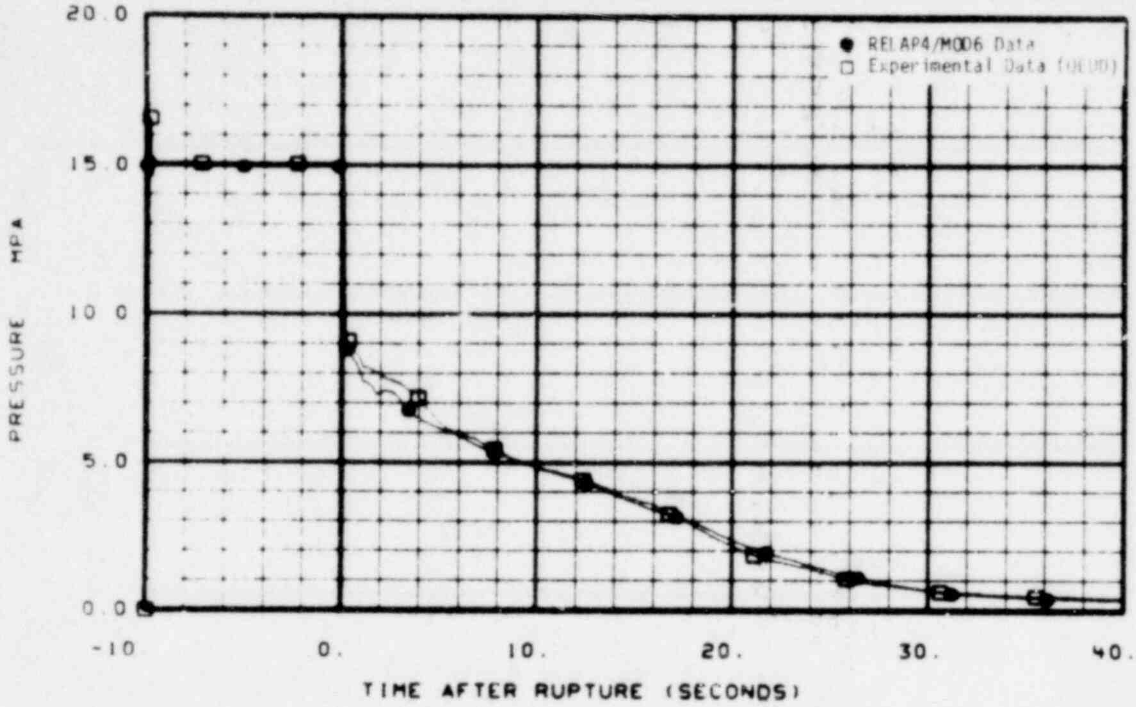

Fig. 35 Comparison of measured and predicted pressure at steam generator simulator outlet (PE-BL-6).

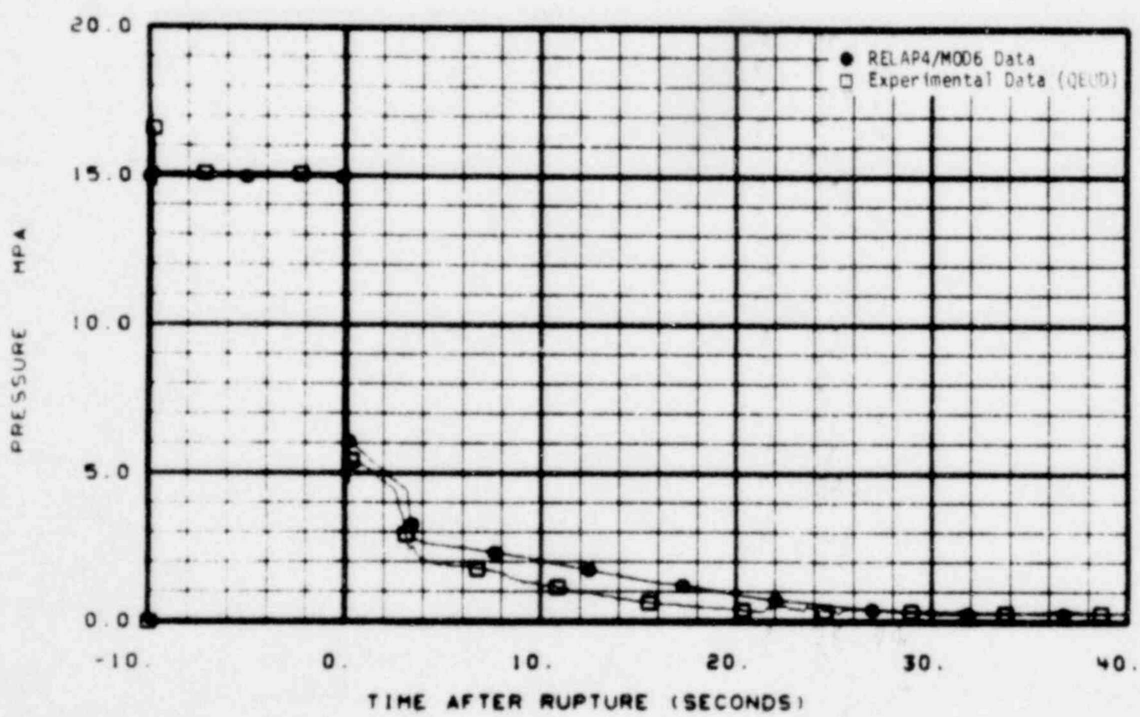

Fig. 36 Comparison of predicted and measured pressure in broken loop cold leg spool piece midpoint (PE-BL-8).

995 330

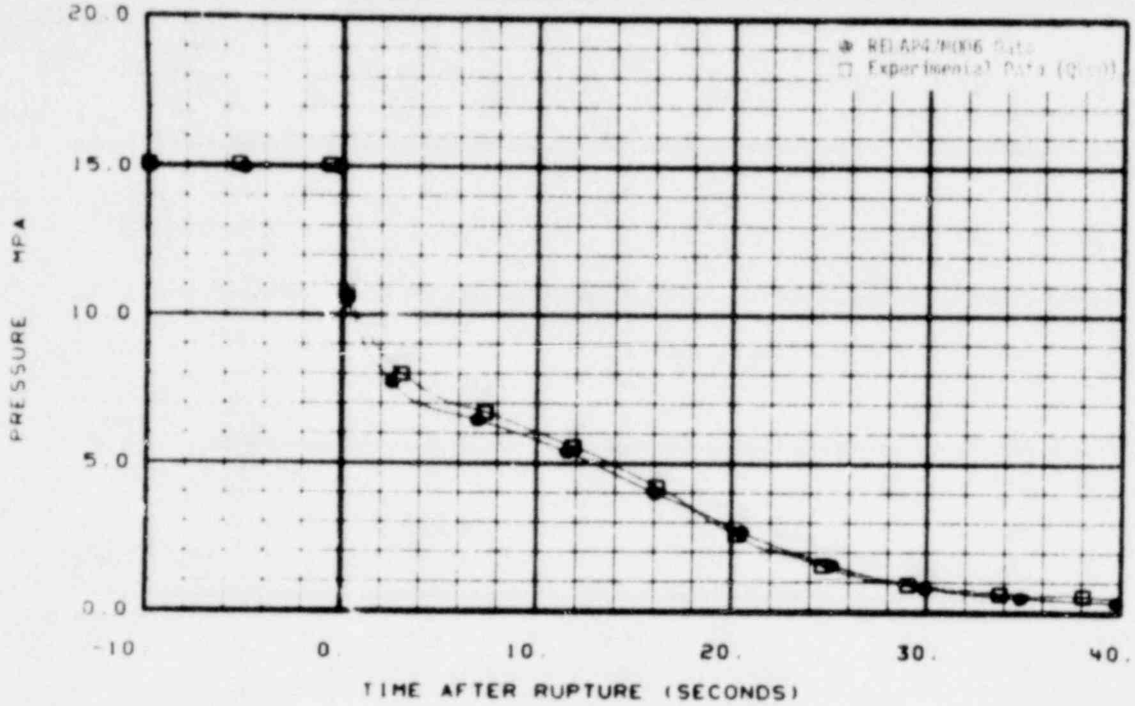

Fig. 37 Comparison of predicted and measured pressure in intact loop cold leg (PE-PC-1).

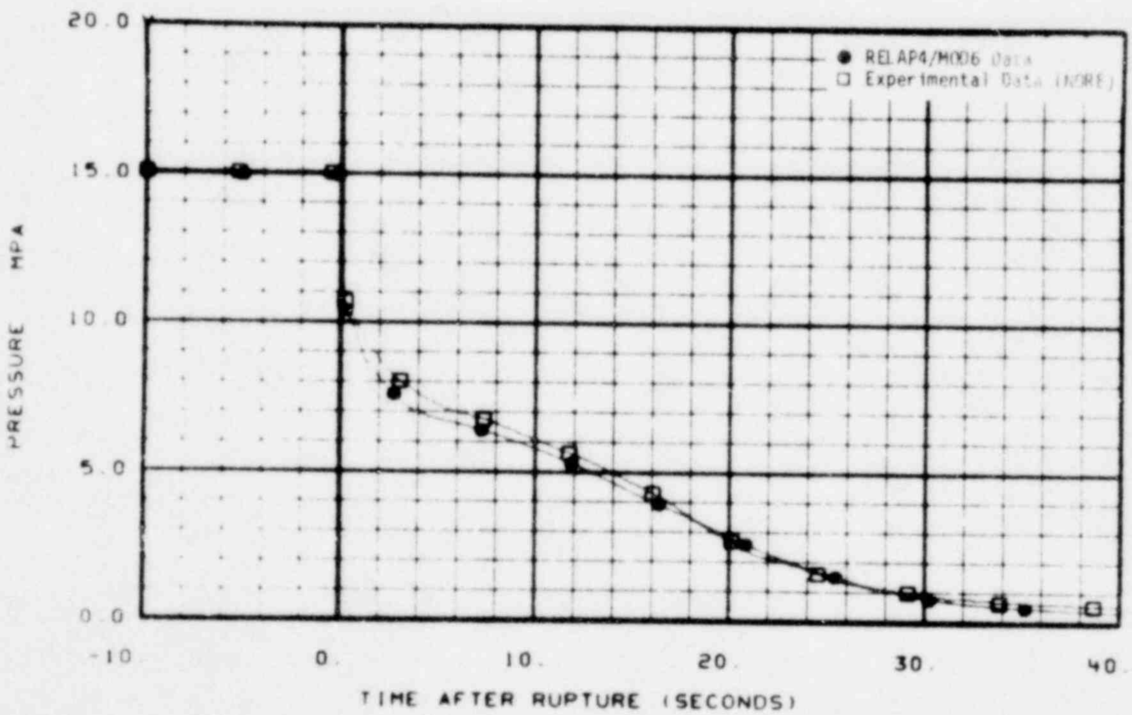

Fig. 38 Comparison of predicted and measured pressure in intact loop hot leg (PE-PC-2).

995 331

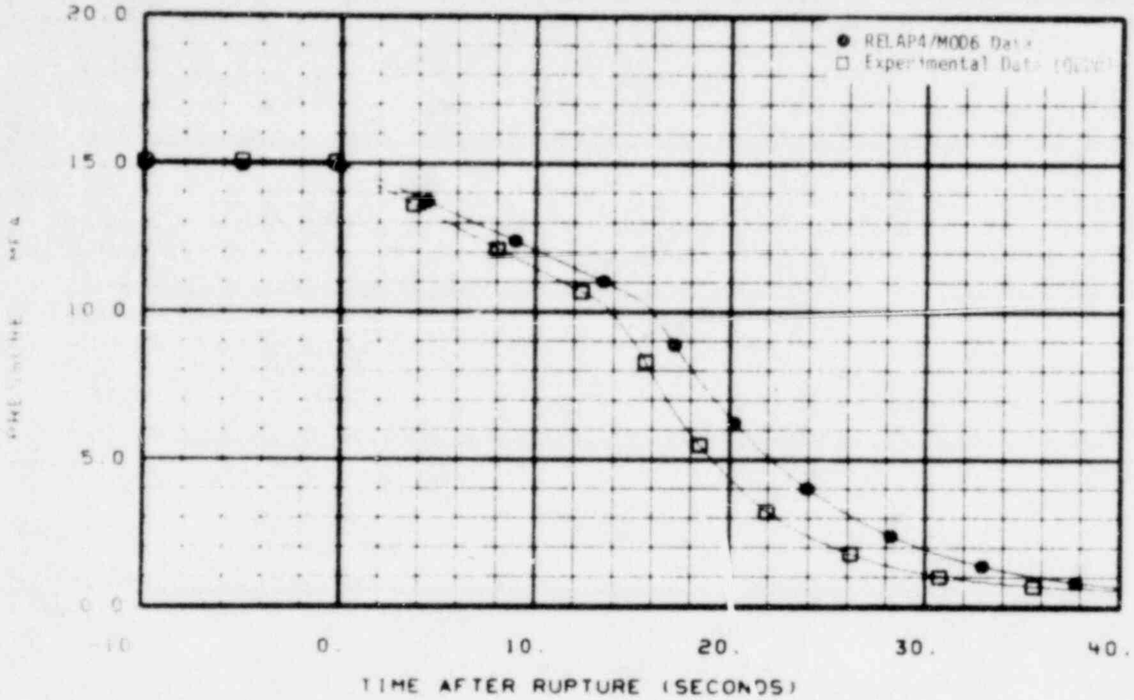

Fig. 39 Comparison of predicted and measured pressure in intact loop pressurizer (PE-PC-4).

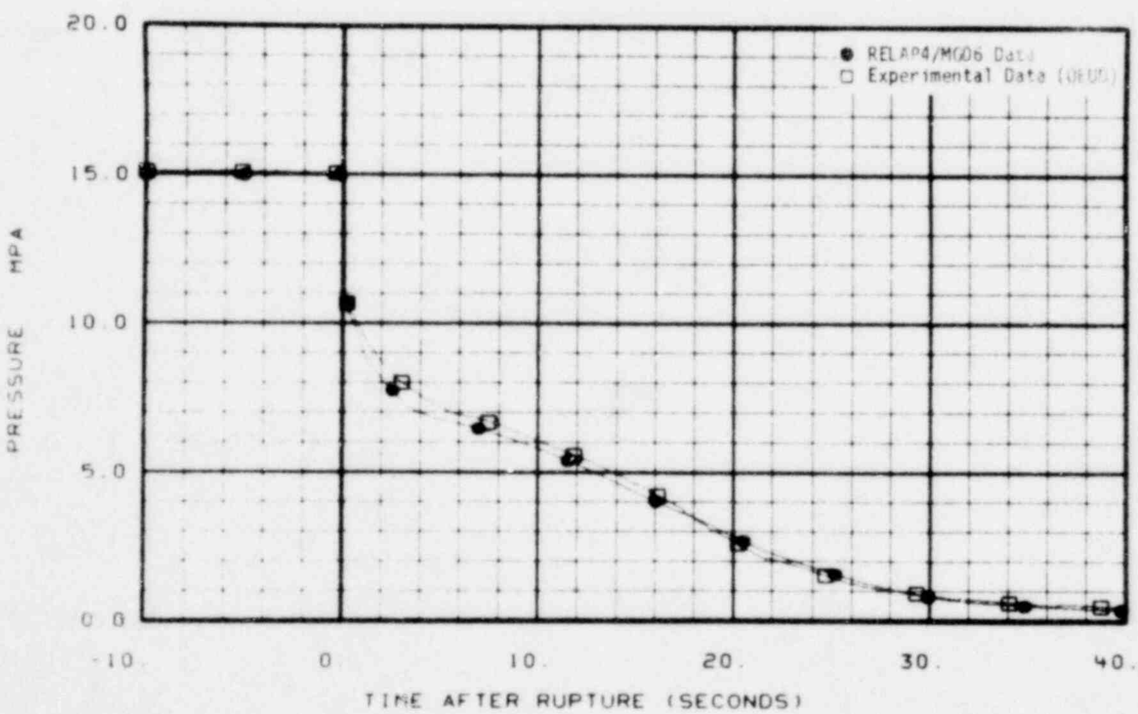

Fig. 40 Comparison of measured and predicted pressure at instrument Stalk 1 (PE-1ST-1A).

995 332

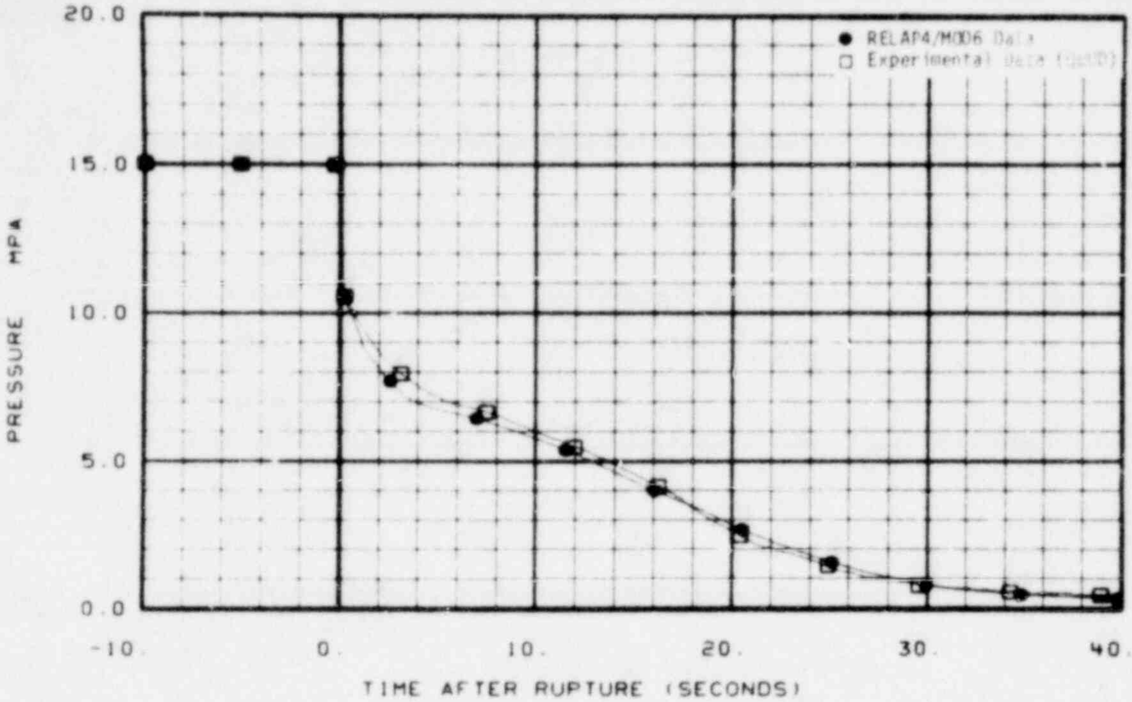

Fig. 41 Comparison of predicted and measured pressure at instrument Stalk 1 (PE-1ST-3A).

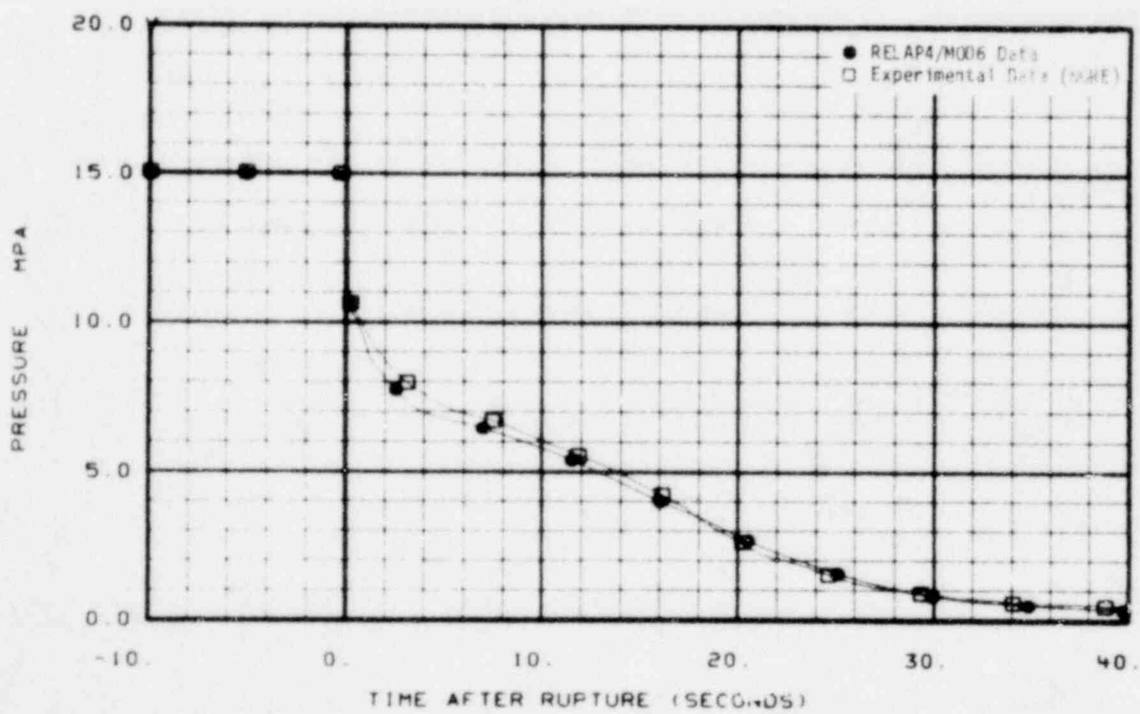

Fig. 42 Comparison of predicted and measured pressure in upper end box (PE-1UP-1A).

POOR ORIGINAL

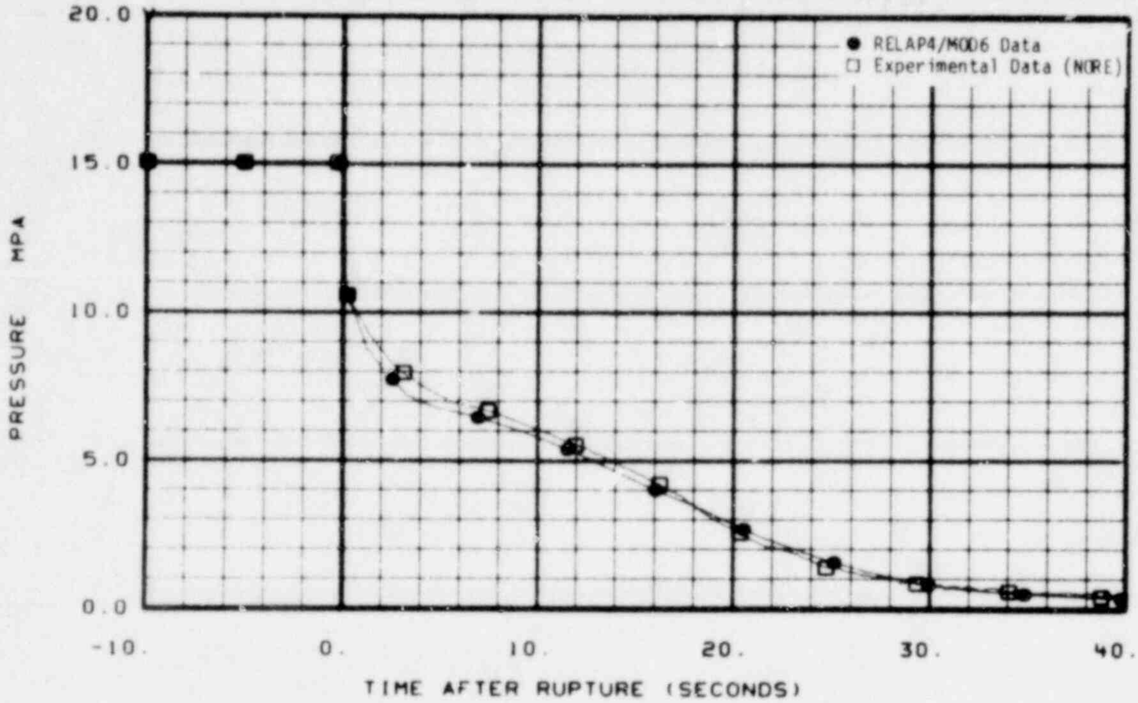

Fig. 43 Comparison of predicted and measured pressure at instrument Stalk 2 (PE-2ST-1A).

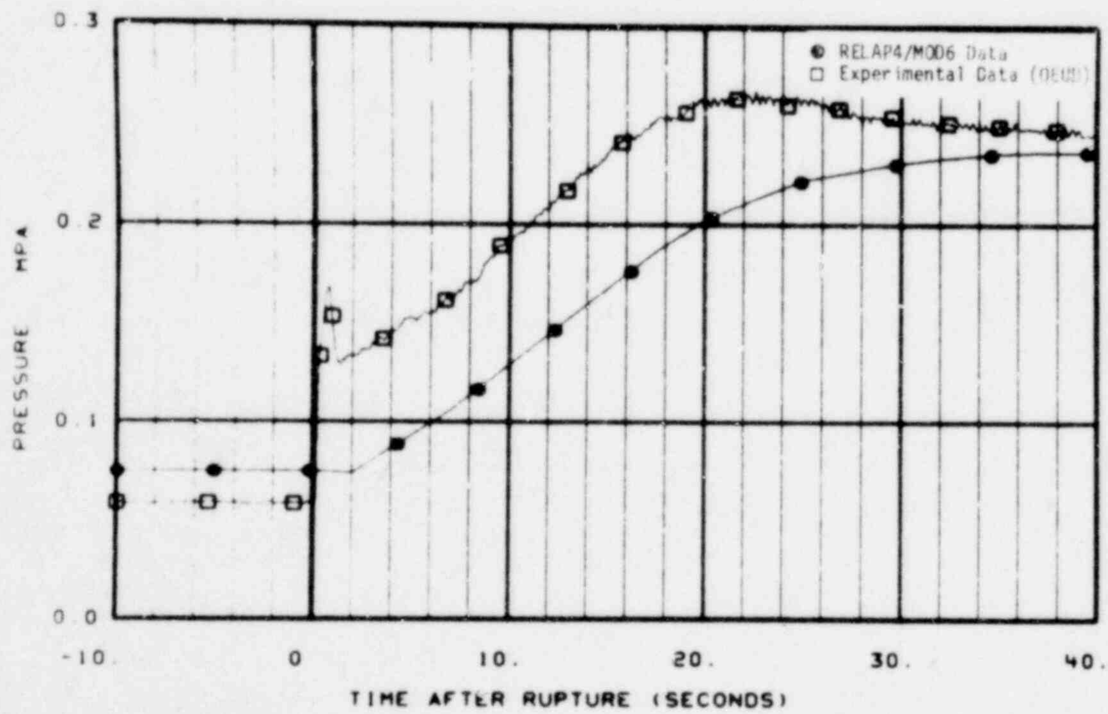

Fig. 44 Comparison of predicted and measured pressure in blowdown suppression tank (PE-SV-17).

995 334

POOR ORIGINAL

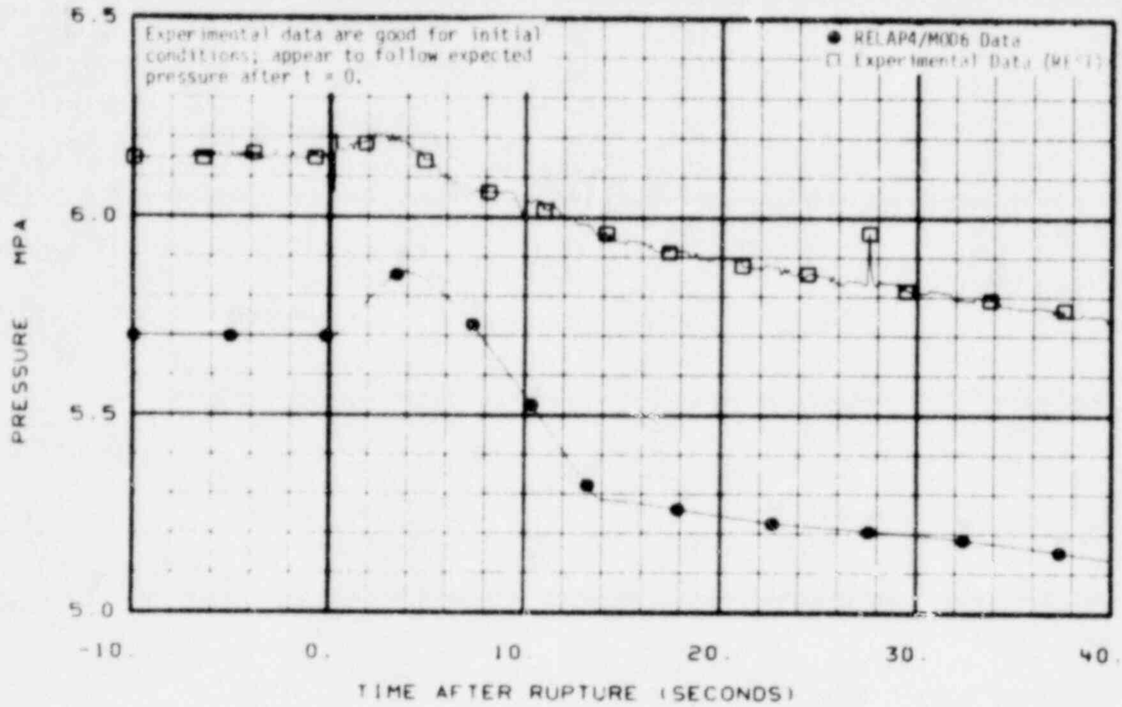

Fig. 45 Comparison of predicted and measured pressure in steam generator secondary side (PT-P004-10A).

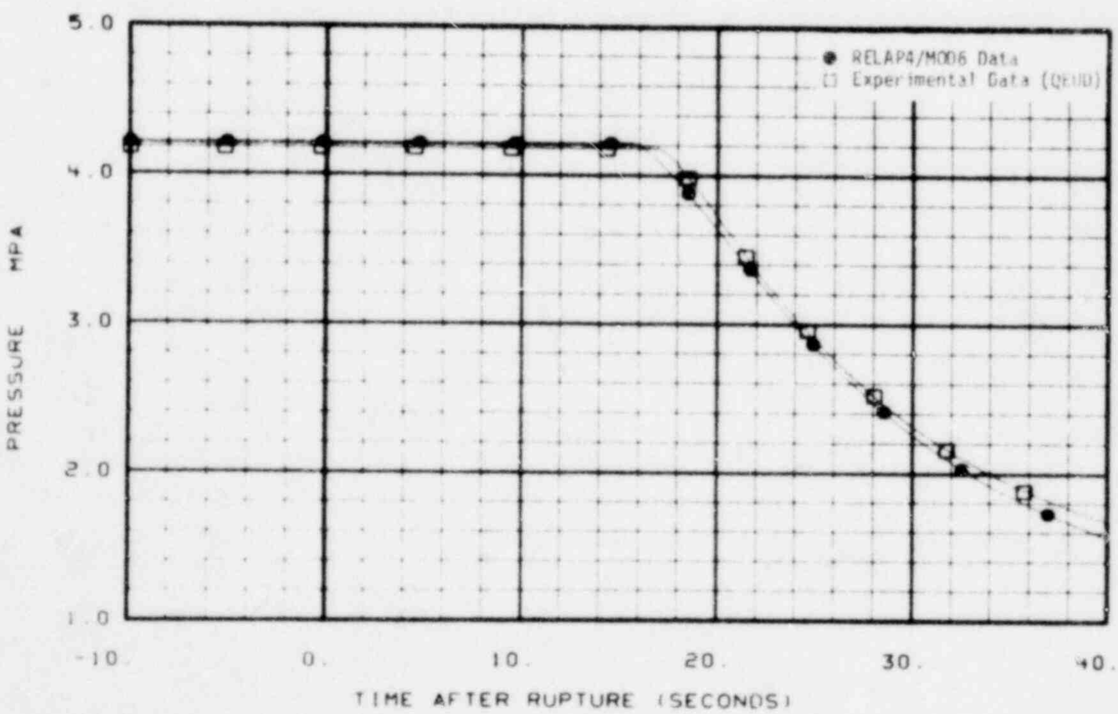

Fig. 46 Comparison of predicted and measured pressure in accumulator (PT-P120-43).

995 335

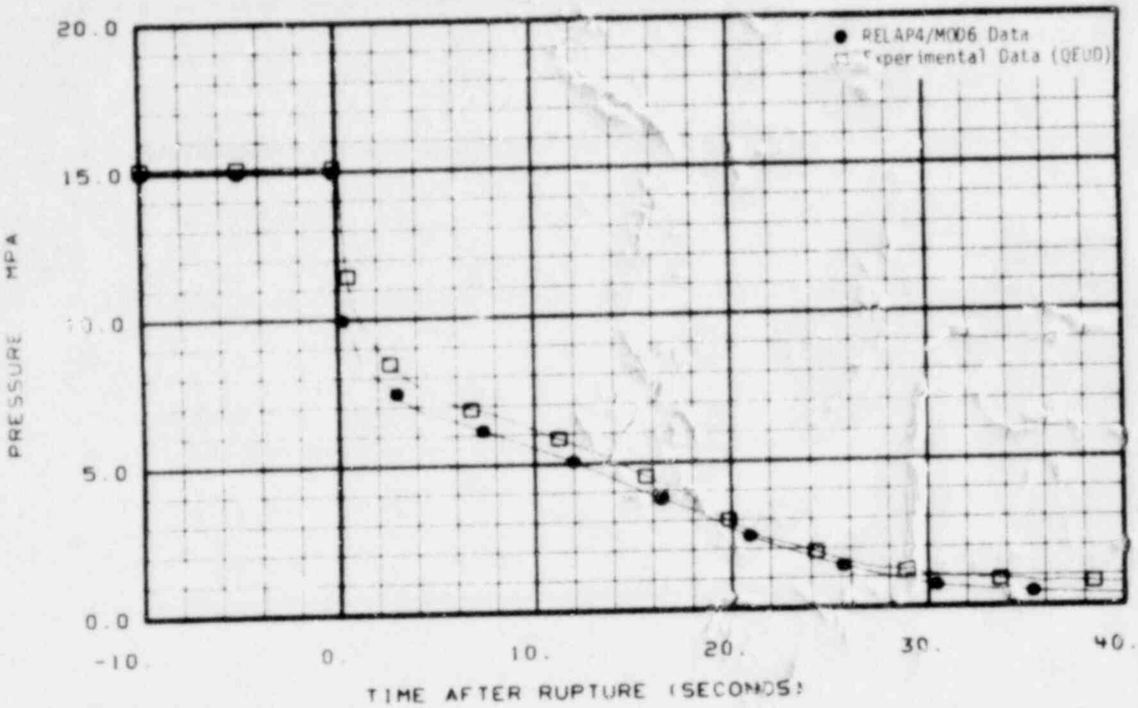

Fig. 47 Comparison of predicted and measured pressure at ECC cold leg injection point (PT-P120-61).

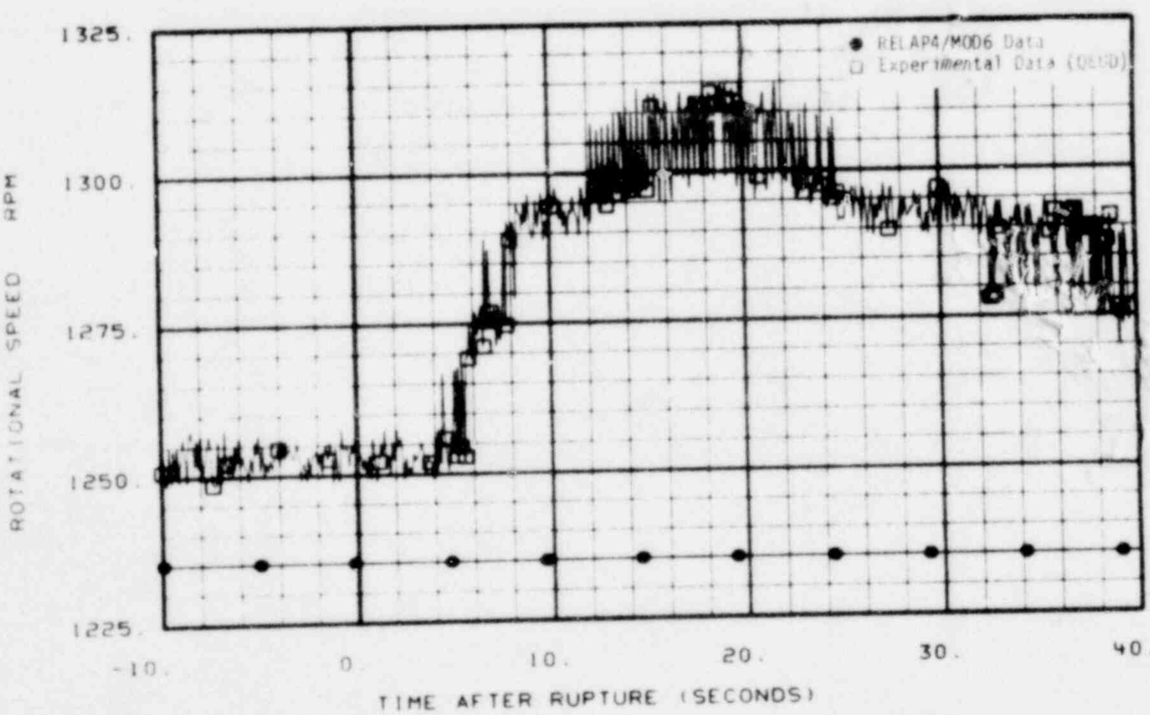

Fig. 48 Comparison of predicted and measured pump speed for Pump 1 (RPE-PC-1).

995 336

POOR ORIGINAL

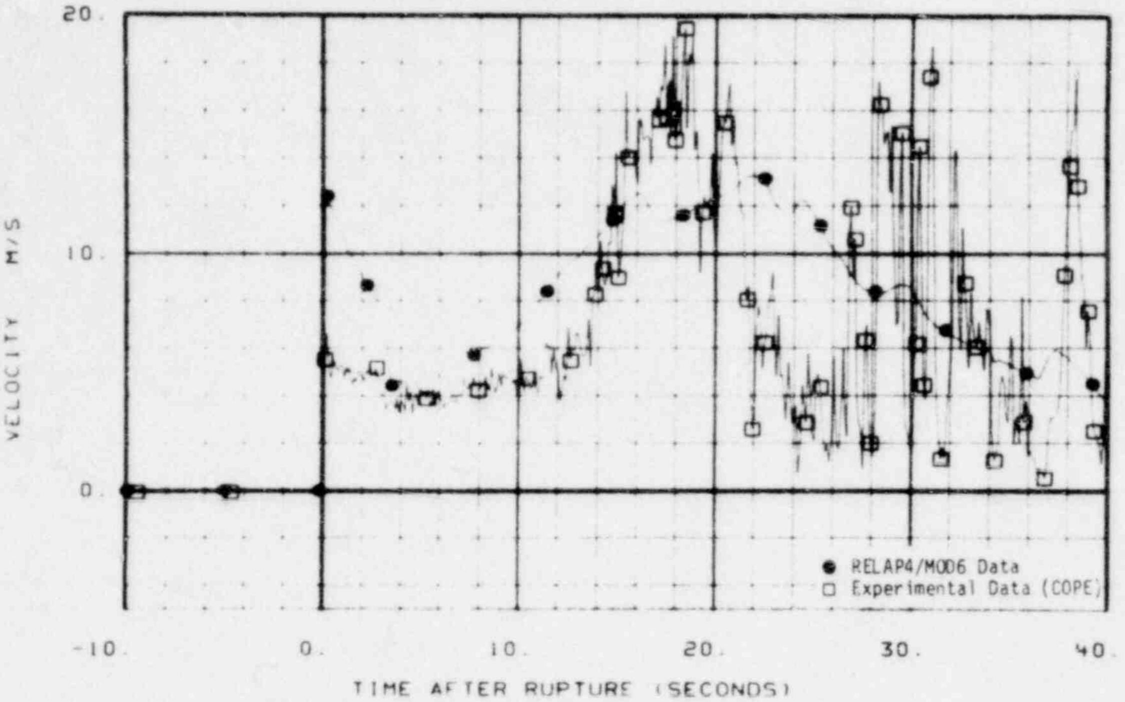

Fig. 49 Comparison of predicted and measured average velocity in broken loop cold leg (FE-BL-1).

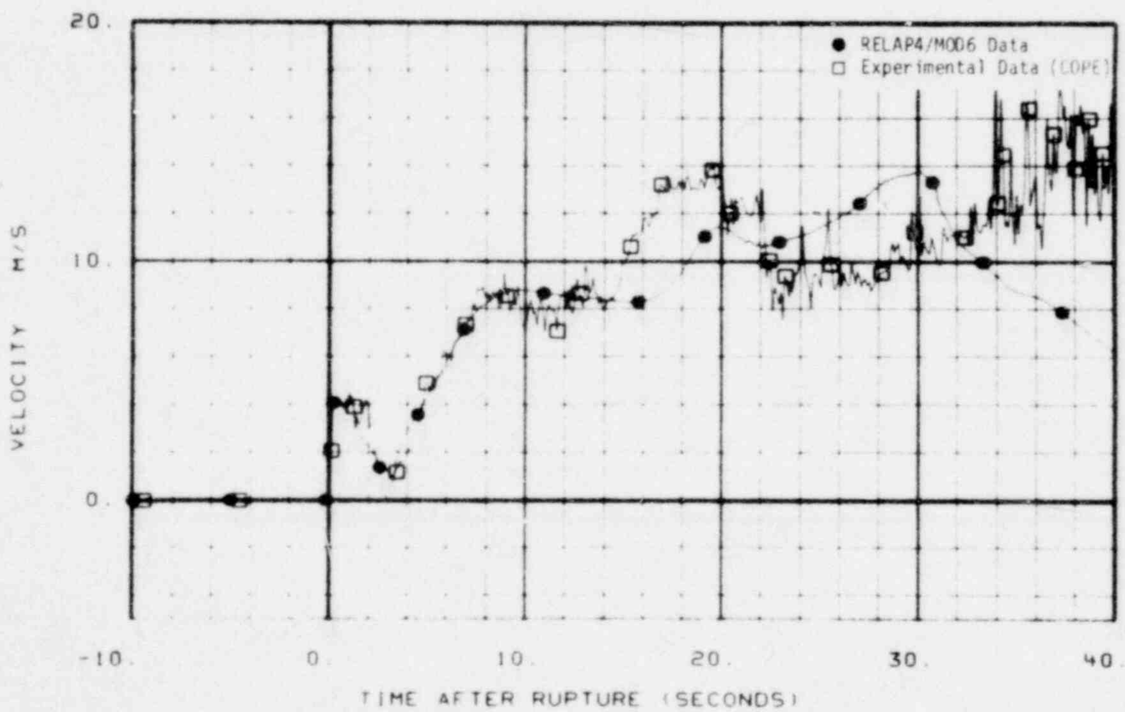

Fig. 50 Comparison of predicted and measured average velocity in broken loop hot leg (FE-BL-2).

995 337

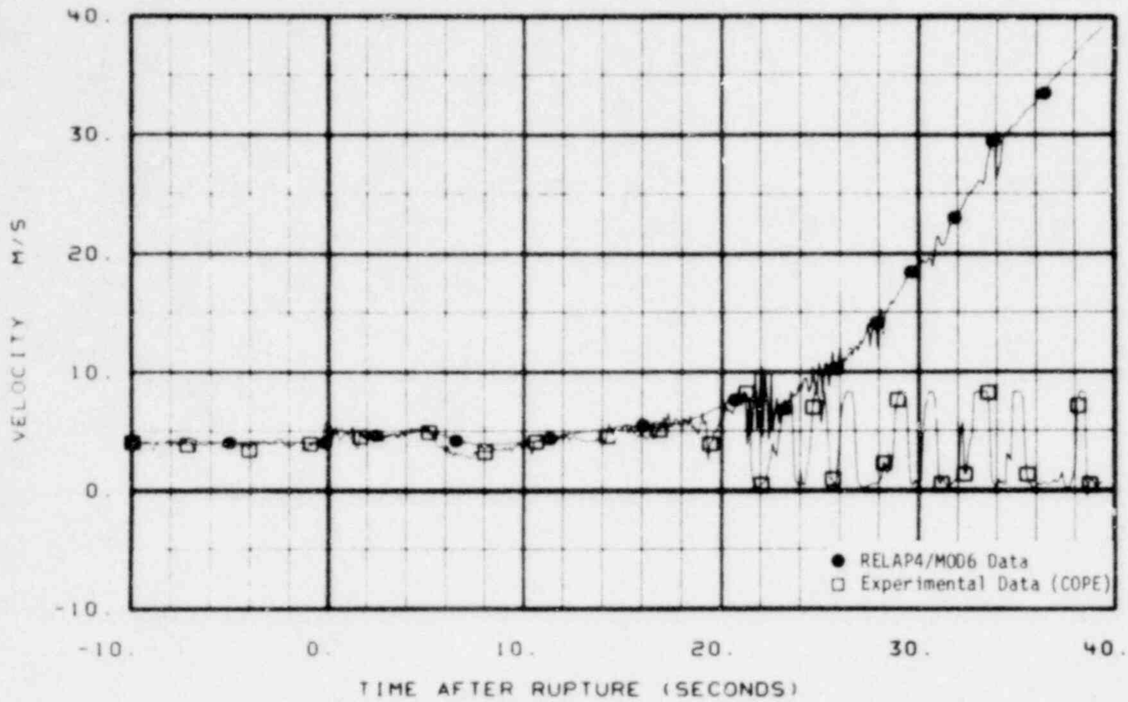

Fig. 51 Comparison of predicted and measured average velocity in intact loop cold leg (FE-PC-1).

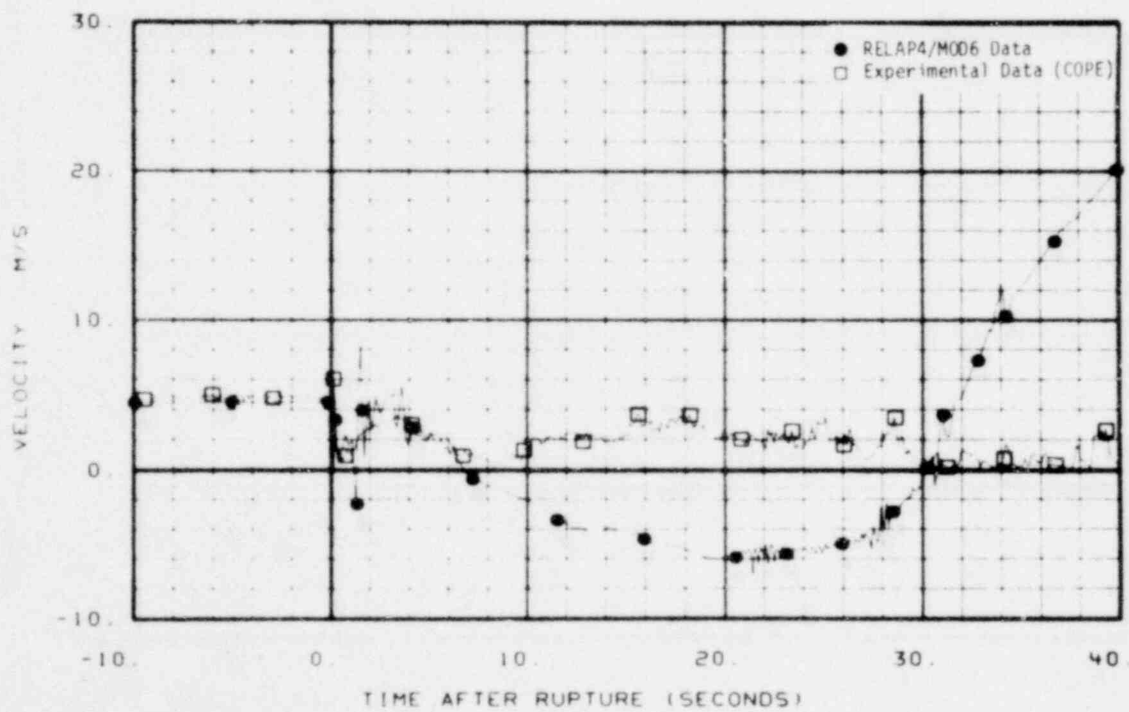

Fig. 52 Comparison of predicted and measured average velocity in intact loop hot leg (FE-PC-2).

995 338

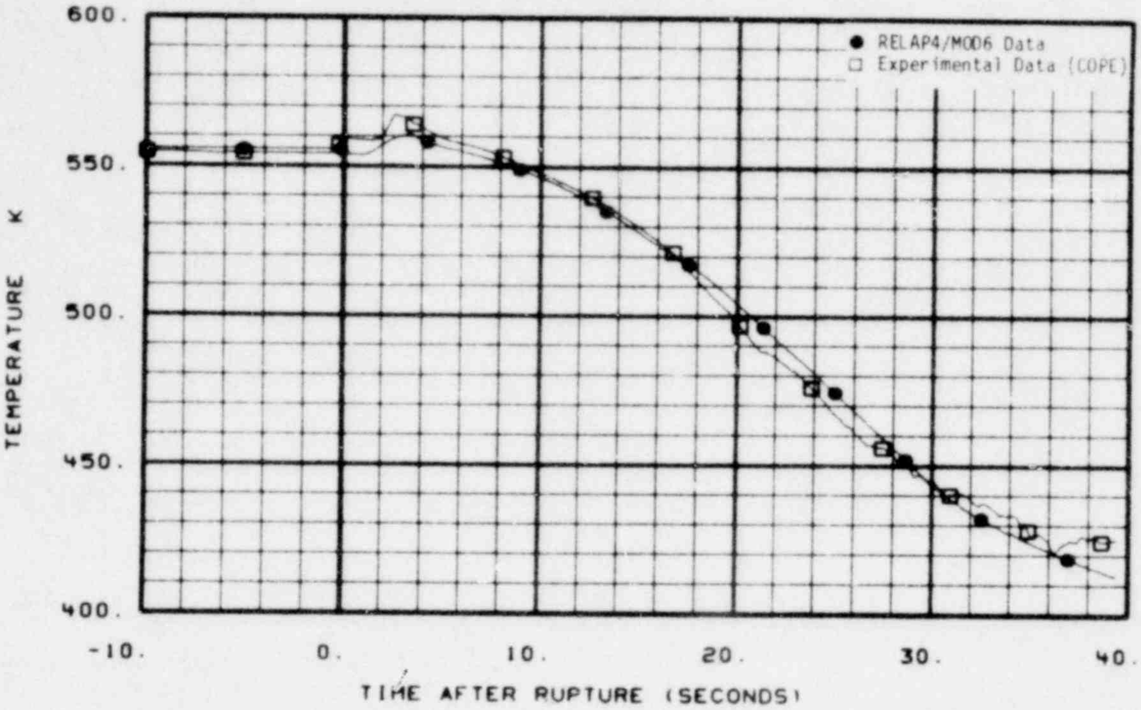

Fig. 53 Comparison of predicted and measured average coolant temperature in broken loop cold leg (TE-BL-1).

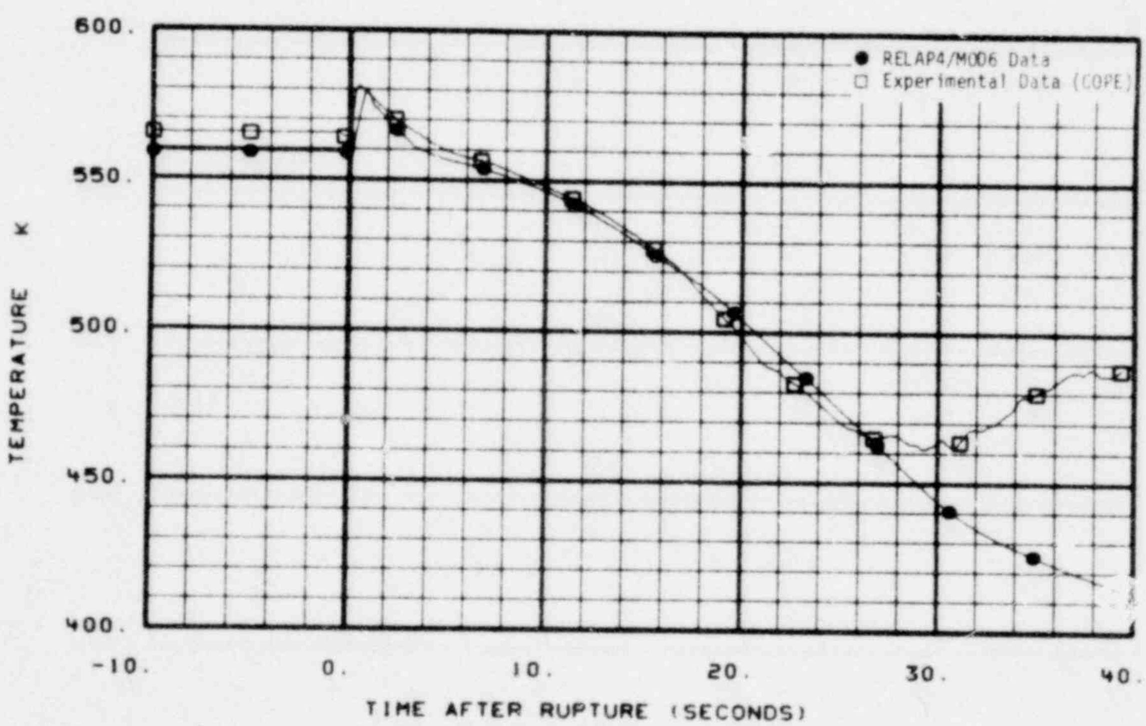

Fig. 54 Comparison of predicted and measured average coolant temperature in broken loop hot leg (TE-BL-2).

995 339

POOR ORIGINAL

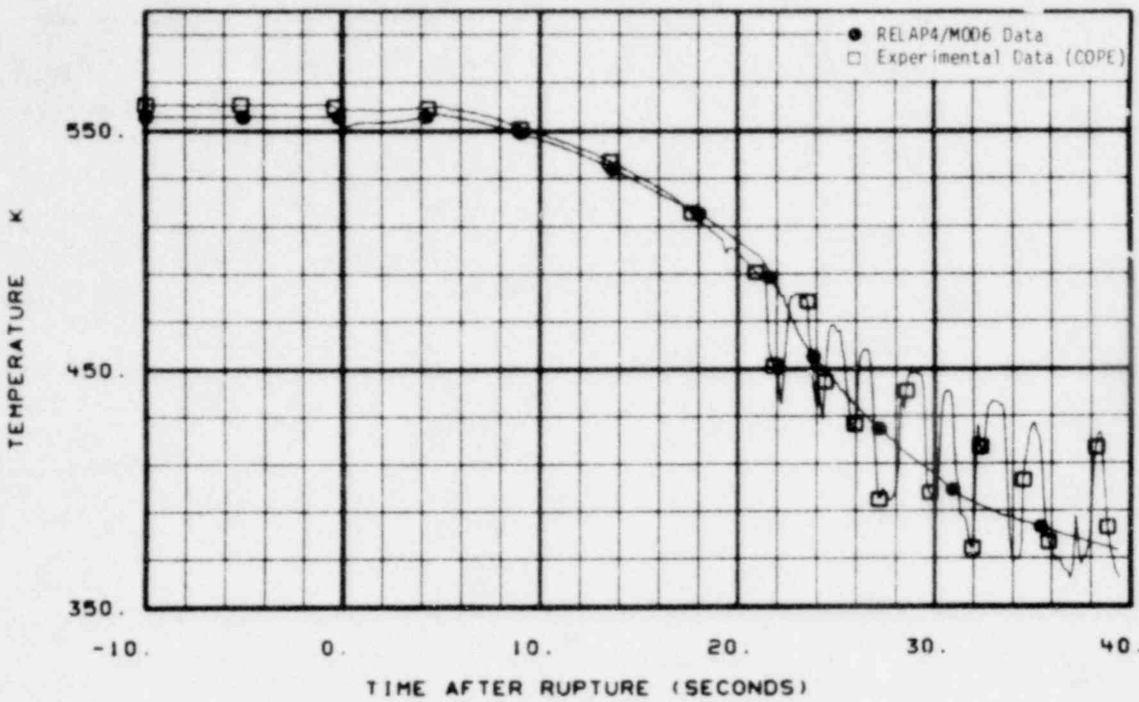

Fig. 55 Comparison of predicted and measured average coolant temperature in intact loop cold leg (TE-PC-1).

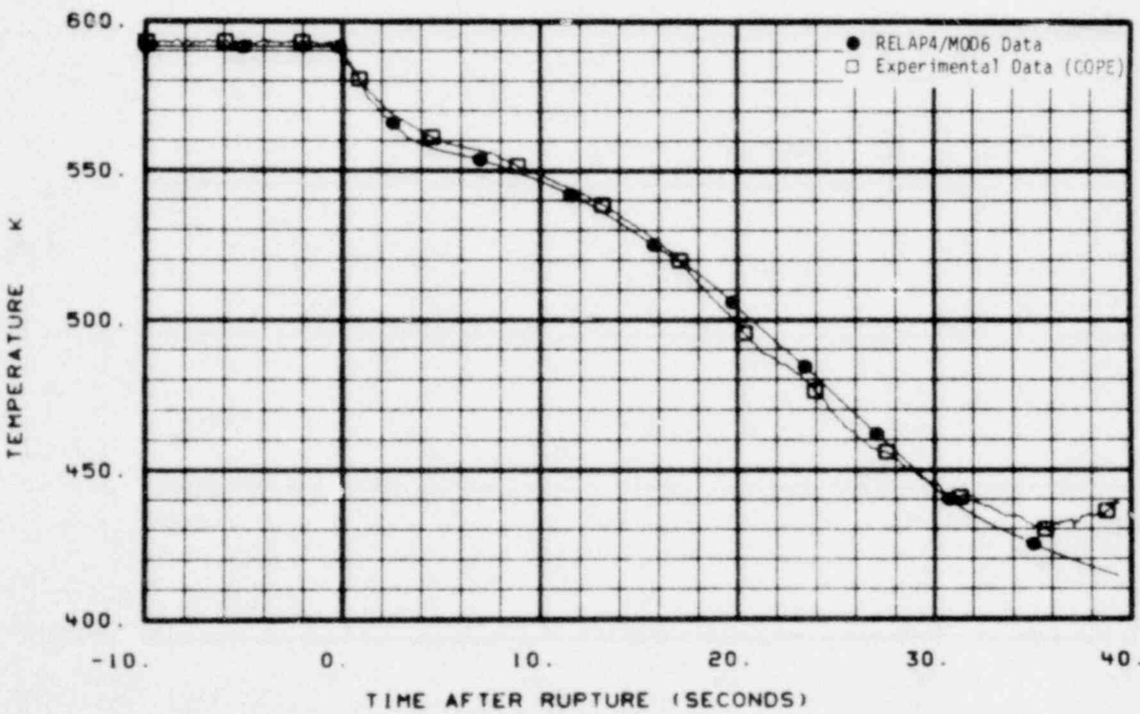

Fig. 56 Comparison of predicted and measured average coolant temperature in intact loop hot leg (TE-PC-2).

995 340

POOR ORIGINAL

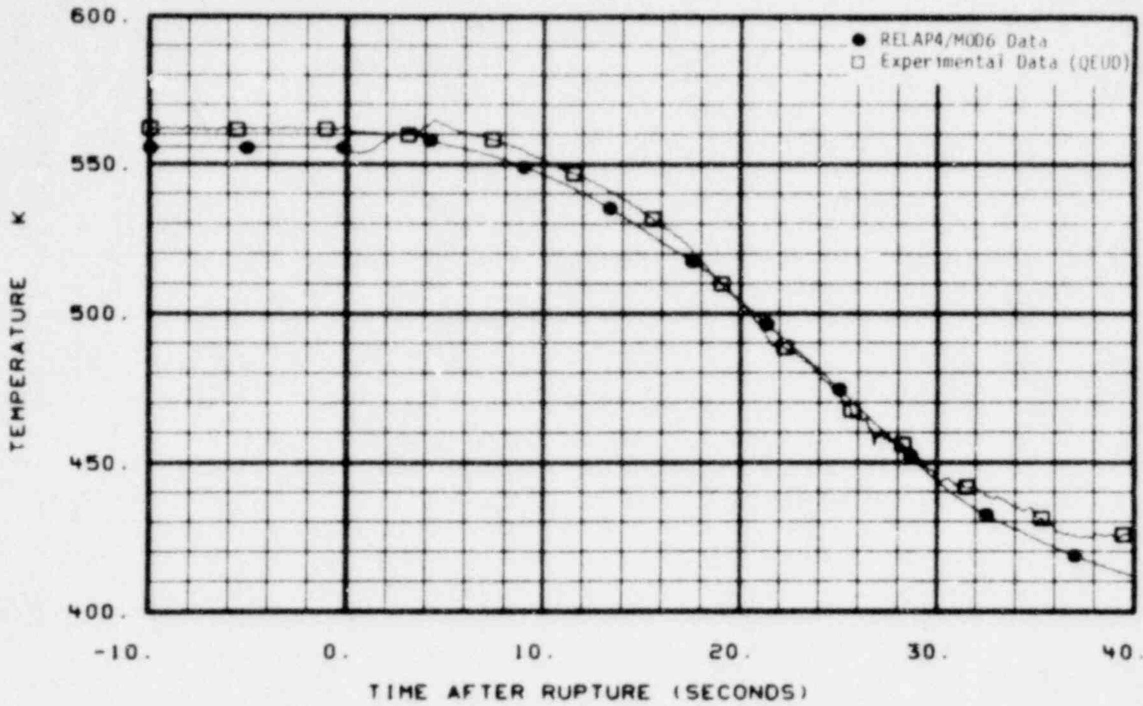

Fig. 57 Comparison of predicted and measured coolant temperature on instrument Stalk 1 (TE-1ST-1).

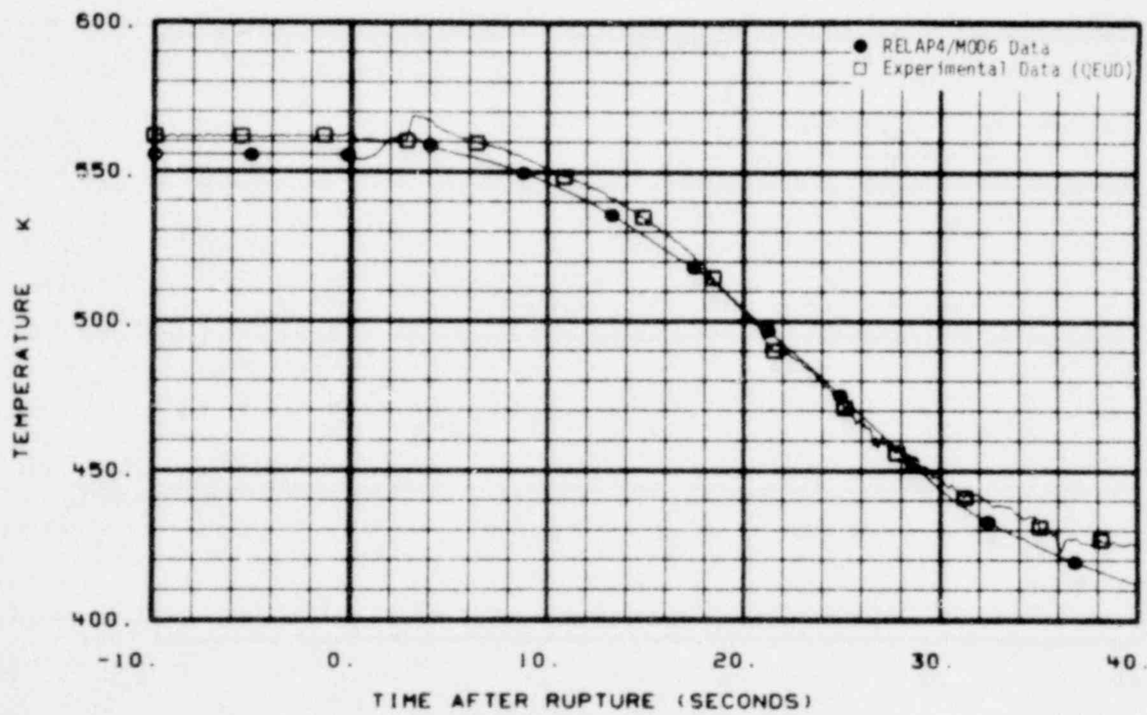

Fig. 58 Comparison of predicted and measured coolant temperature on instrument Stalk 1 (TE-1ST-2).

995 341

POOR ORIGINAL

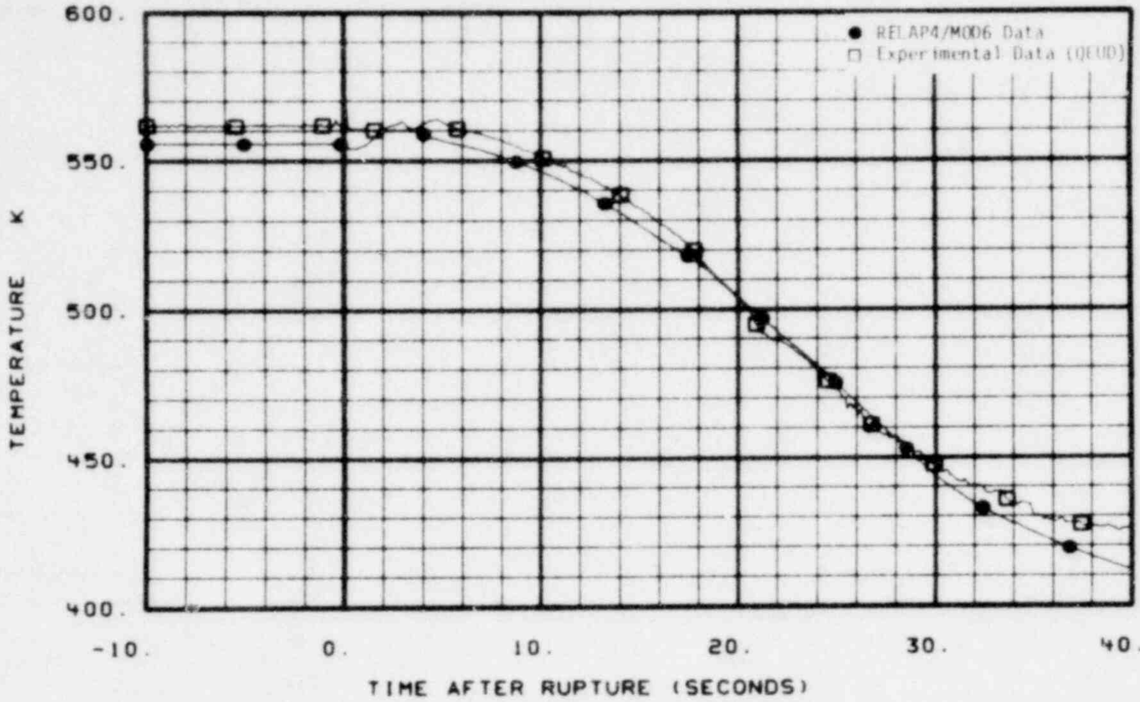

Fig. 59 Comparison of predicted and measured coolant temperature on instrument Stalk 1 (TE-1ST-3).

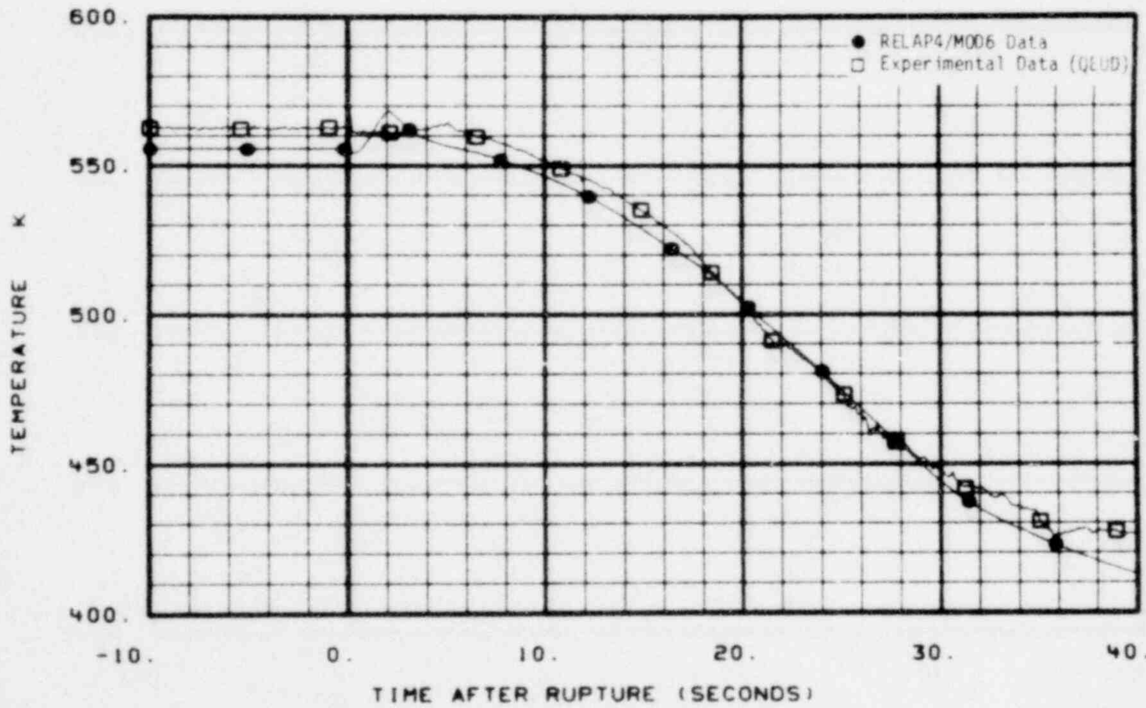

Fig. 60 Comparison of predicted and measured coolant temperature on instrument Stalk 1 (TE-1ST-4).

995 342

POOR ORIGINAL

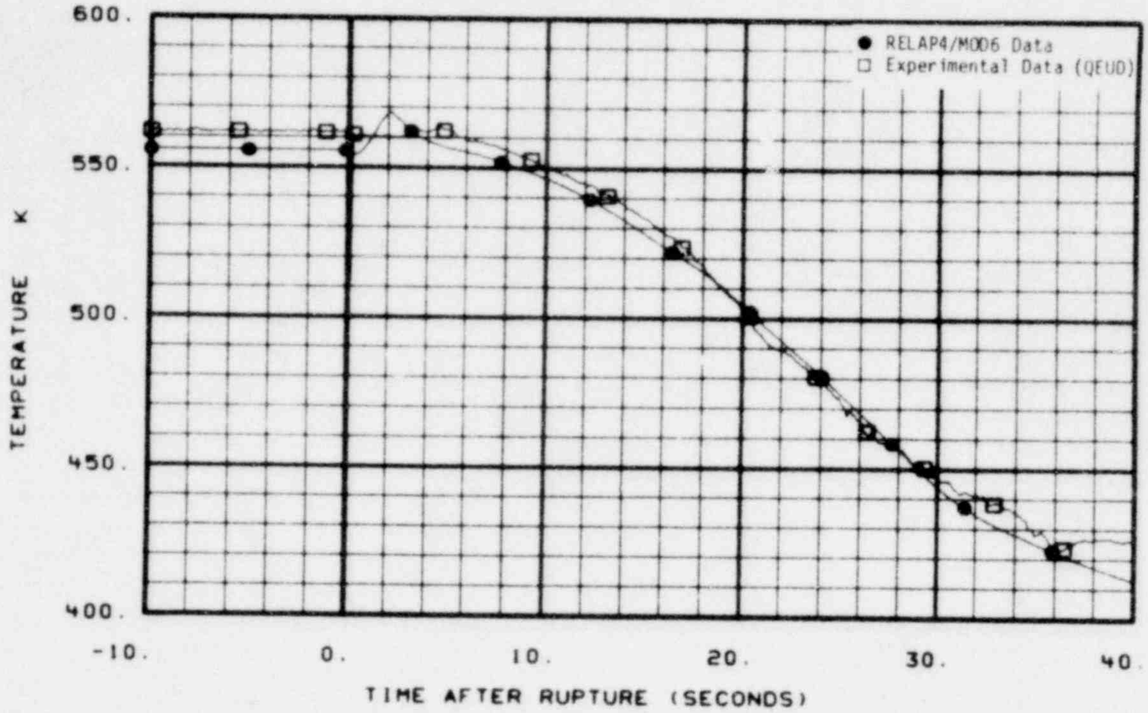

Fig. 61 Comparison of predicted and measured coolant temperature on instrument Stalk 1 (TE-1ST-5).

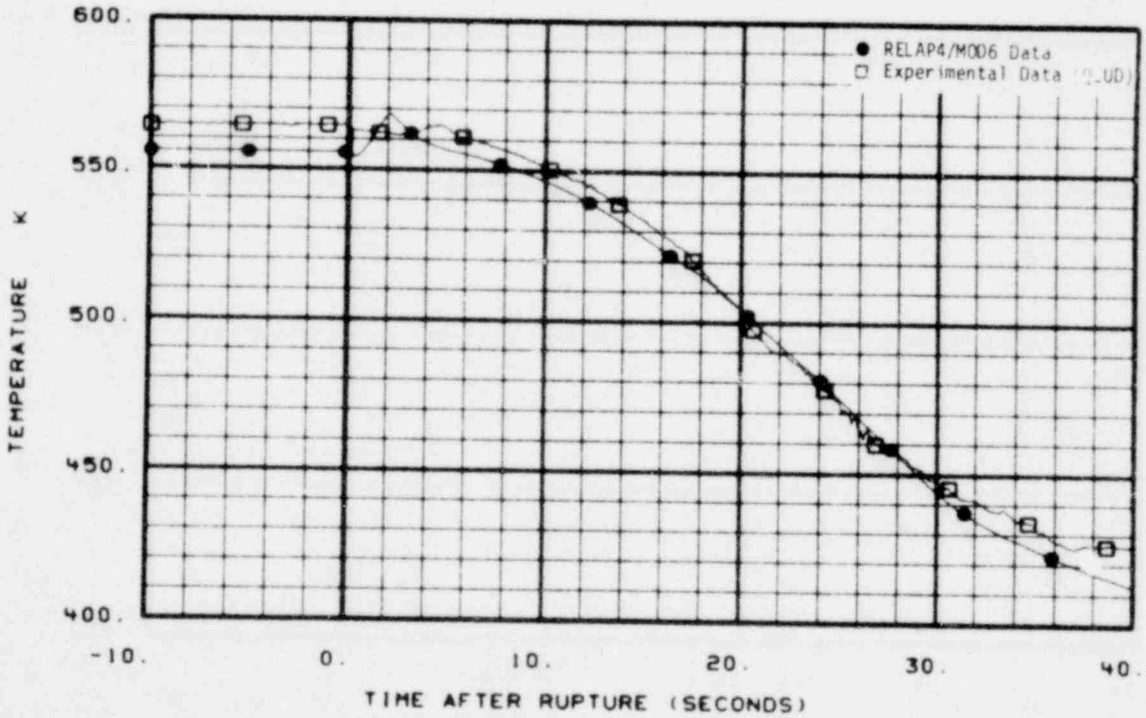

Fig. 62 Comparison of predicted and measured coolant temperature on instrument Stalk 1 (TE-1ST-6).

995 343

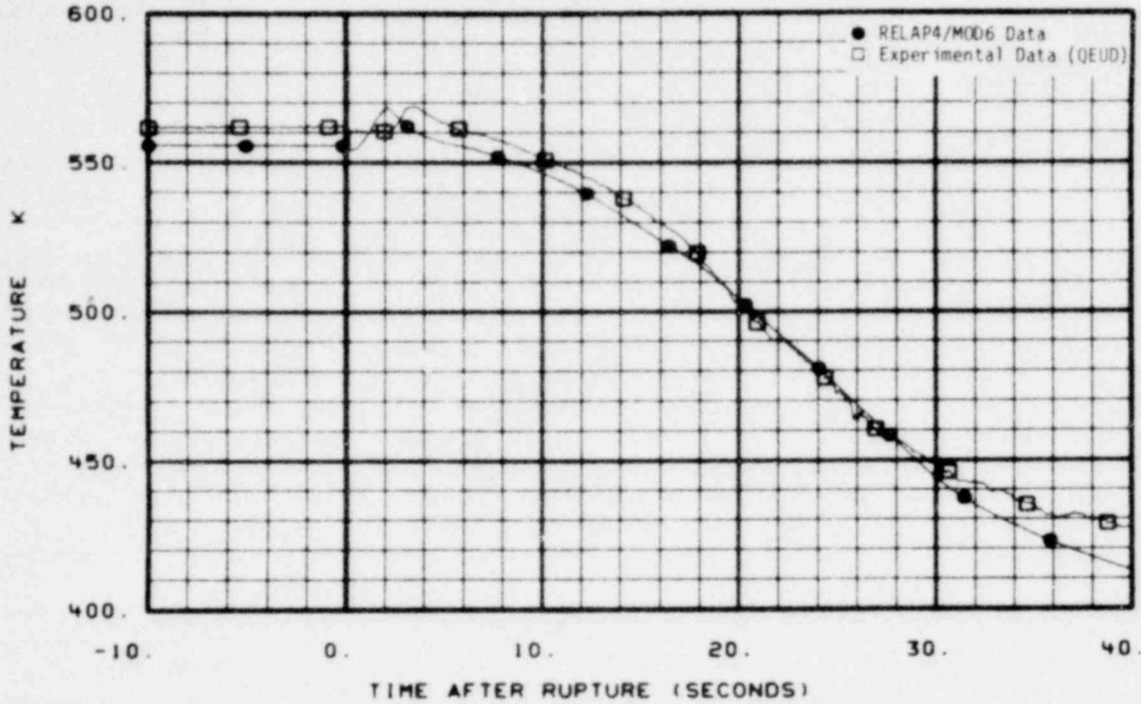

Fig. 63 Comparison of predicted and measured coolant temperature on instrument Stalk 1 (TE-1ST-8).

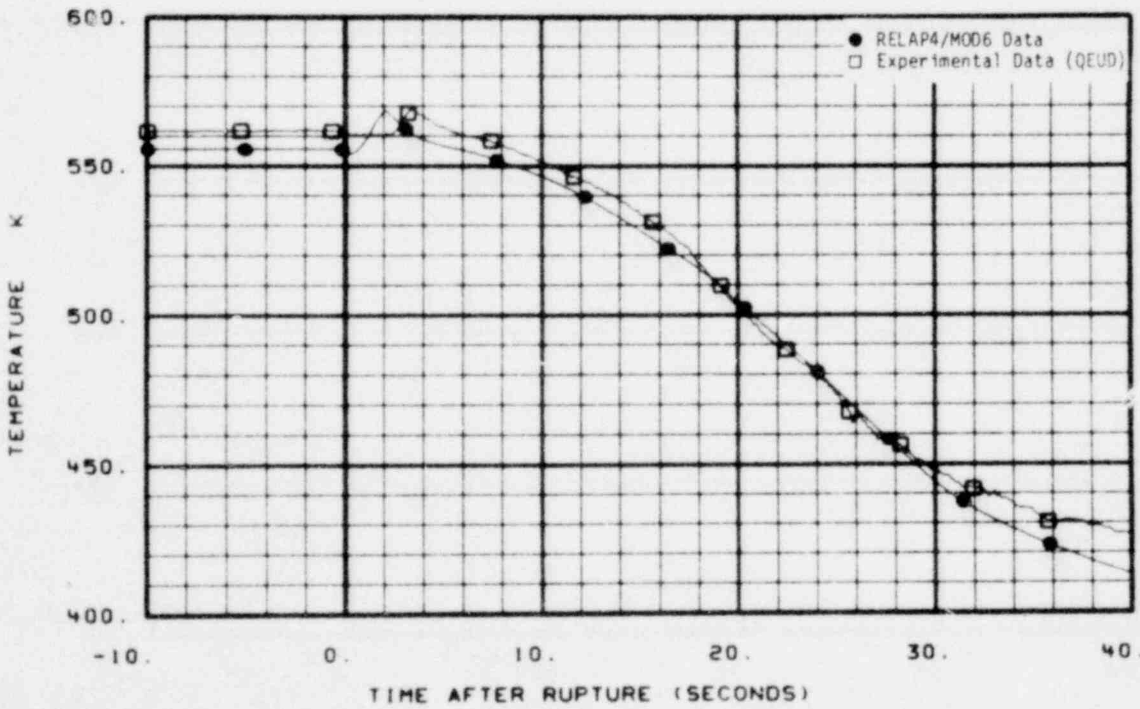

Fig 64 Comparison of predicted and measured coolant temperature on instrument Stalk 1 (TE-1ST-9).

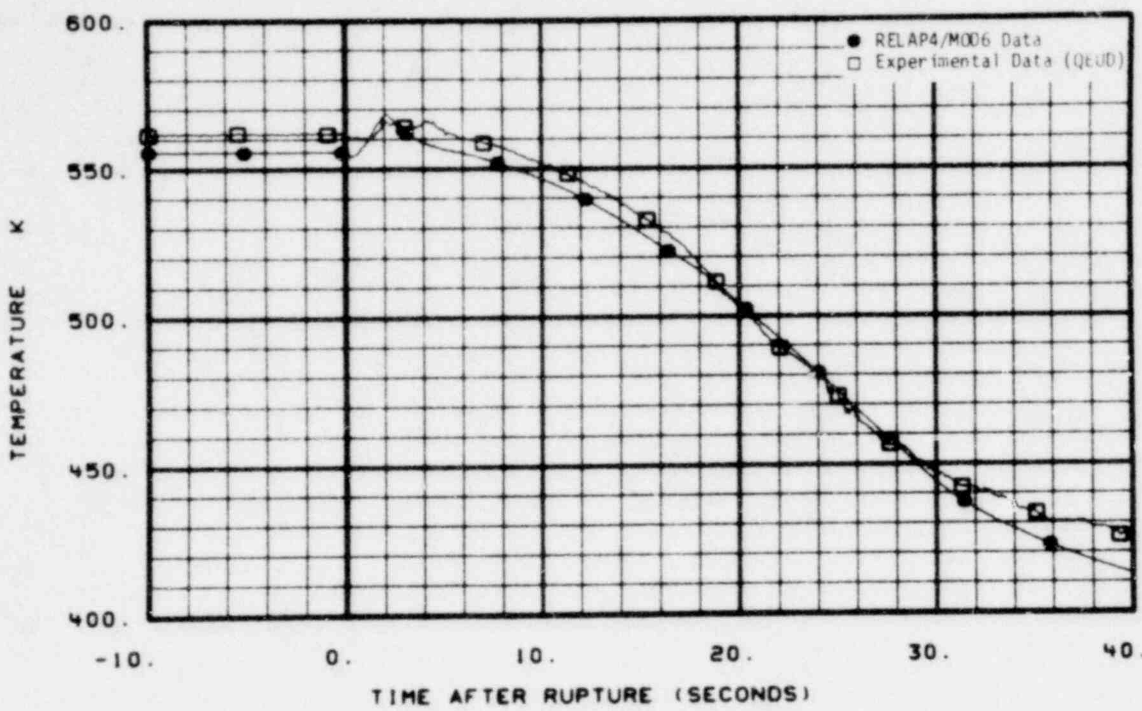

Fig. 65 Comparison of predicted and measured coolant temperature on instrument Stalk 1 (TE-1ST-11).

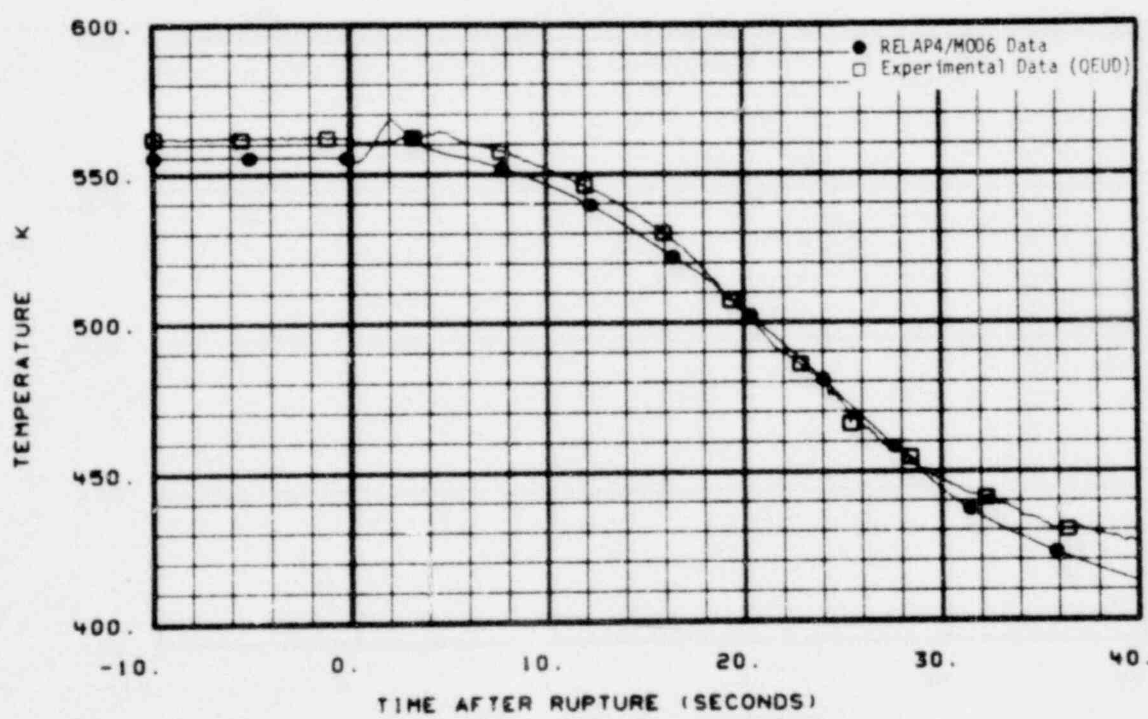

Fig. 66 Comparison of predicted and measured coolant temperature on instrument Stalk 1 (TE-1ST-12).

995 345

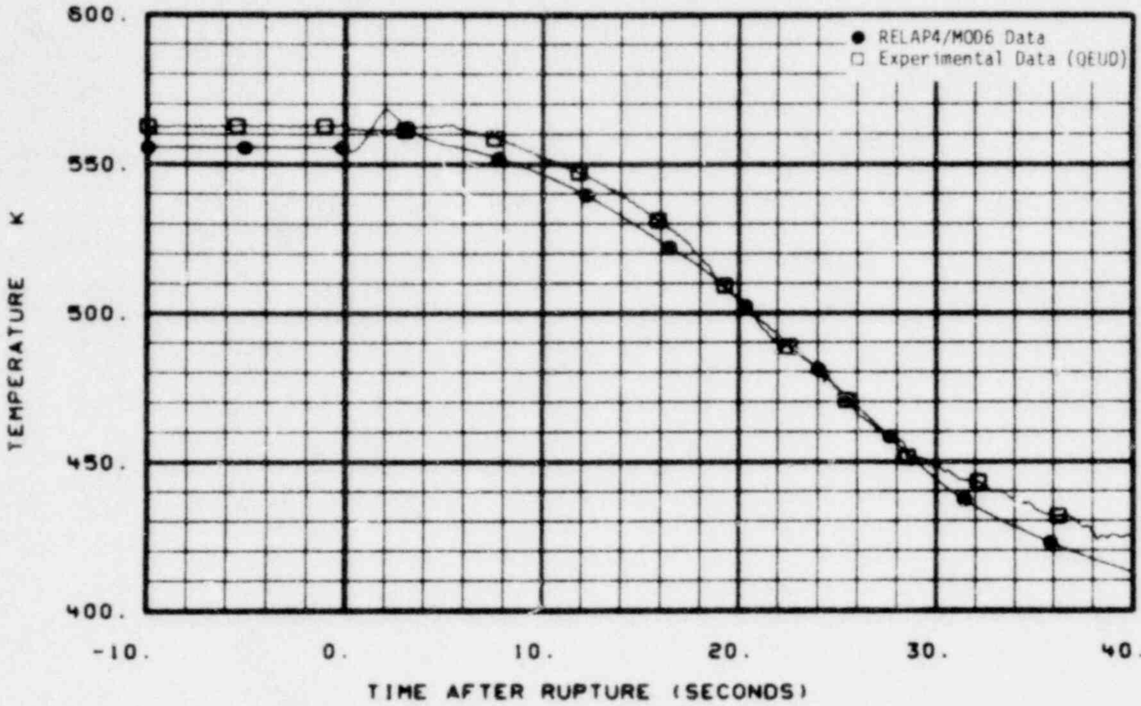

Fig. 67 Comparison of predicted and measured coolant temperature on instrument Stalk 1 (TE-1ST-13).

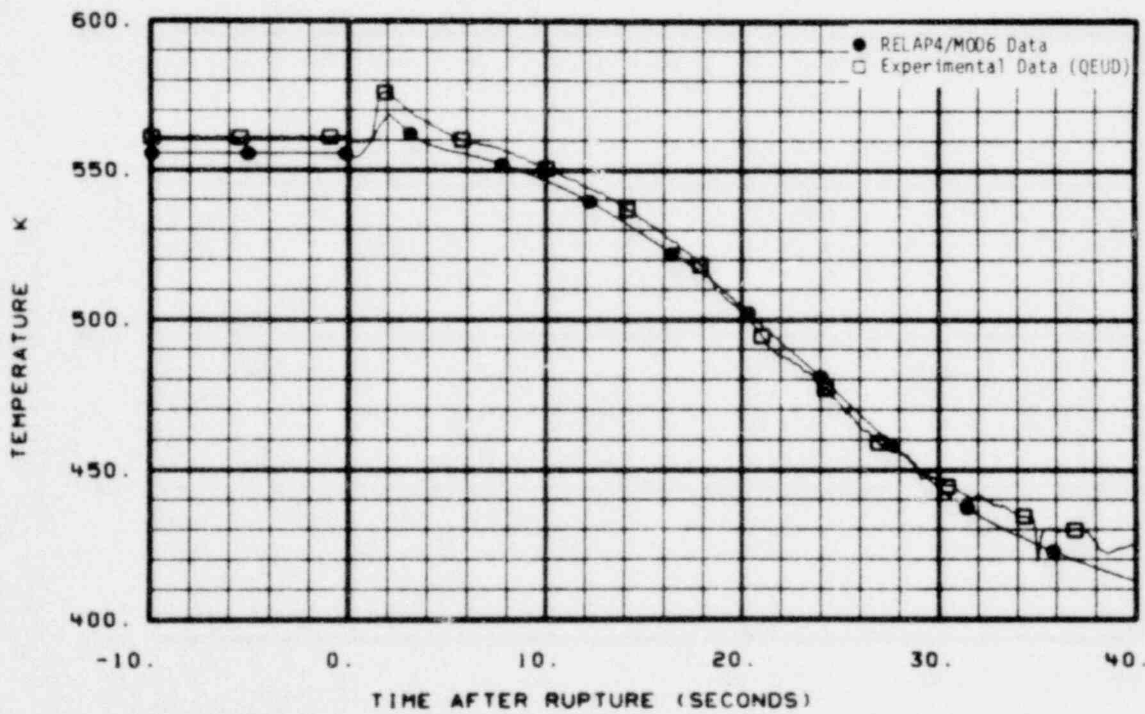

Fig. 68 Comparison of predicted and measured coolant temperature on instrument Stalk 1 (TE-1ST-14).

995 346

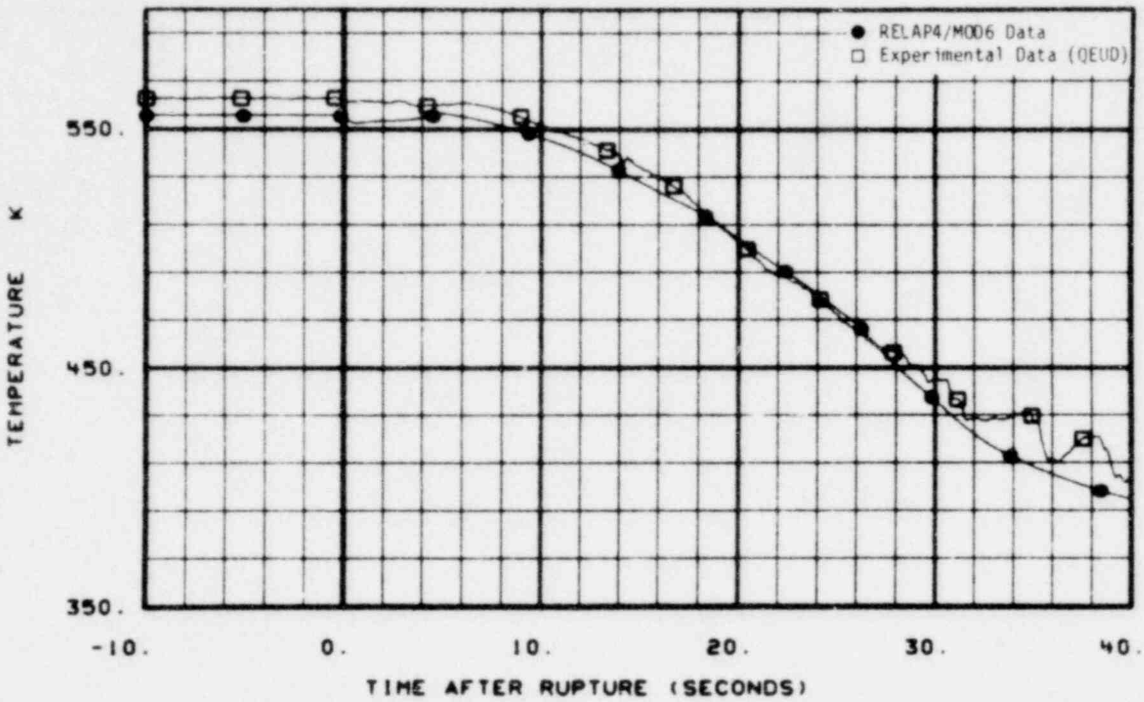

Fig. 69 Comparison of predicted and measured coolant temperature on instrument Stalk 2 (TE-2ST-1).

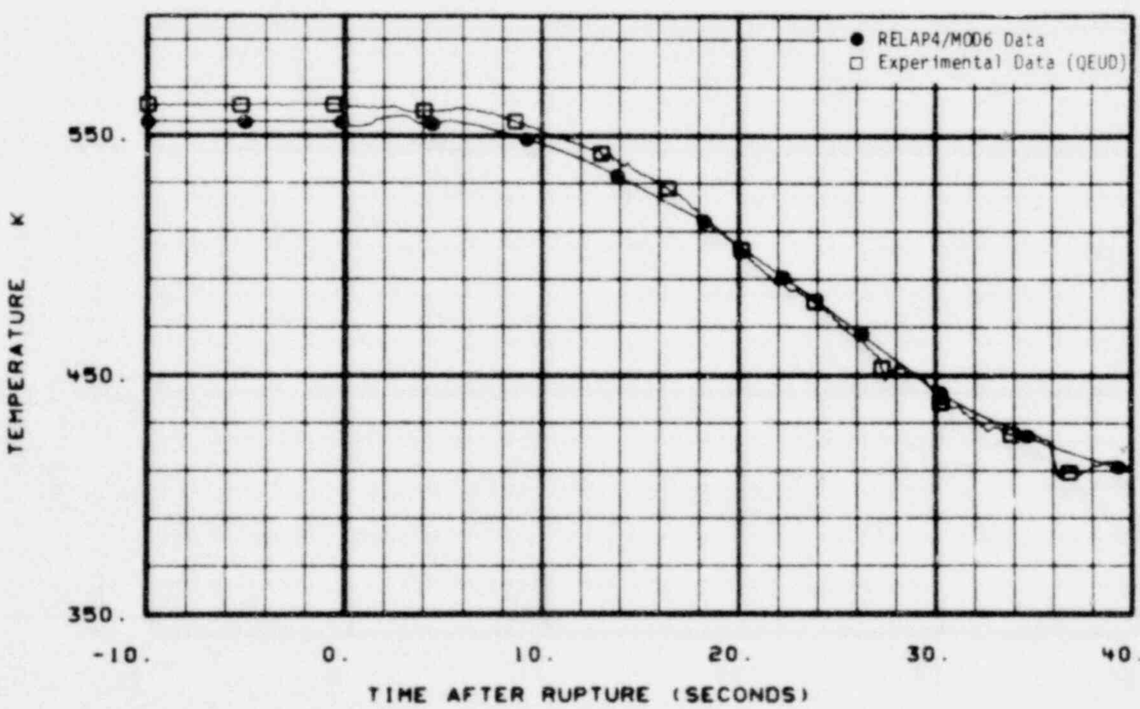

Fig. 70 Comparison of predicted and measured coolant temperature on instrument Stalk 2 (TE-2ST-2).

995 347

POOR ORIGINAL

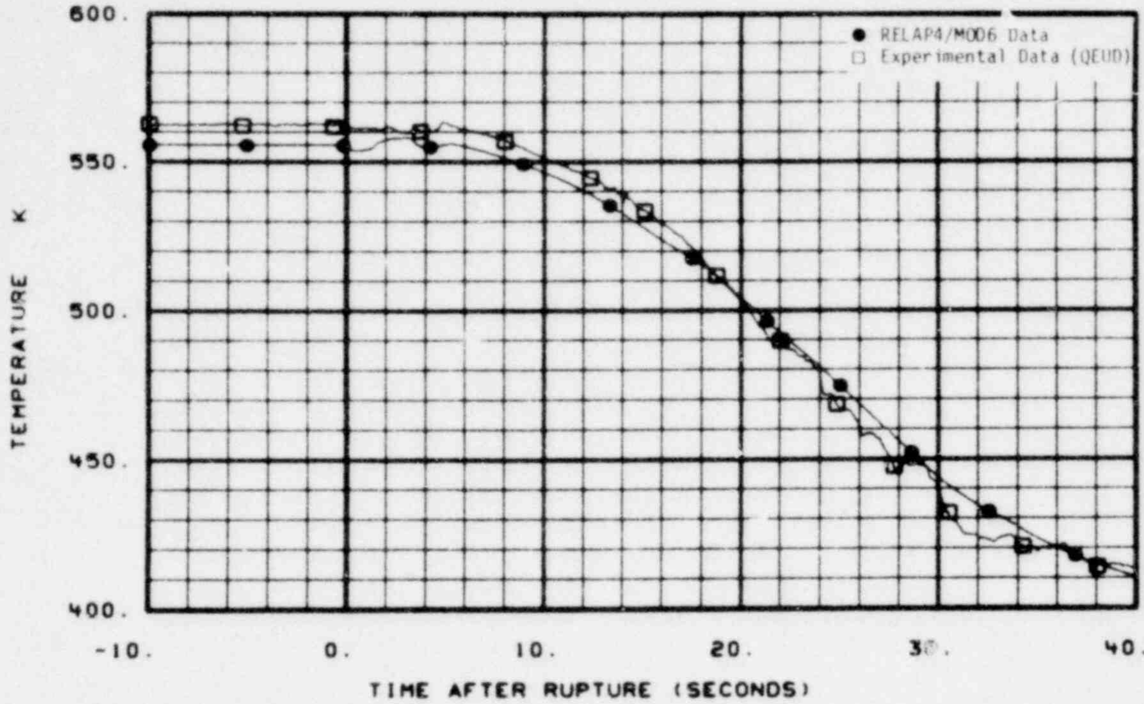

Fig. 71 Comparison of predicted and measured coolant temperature on instrument Stalk 2 (TE-2ST-3).

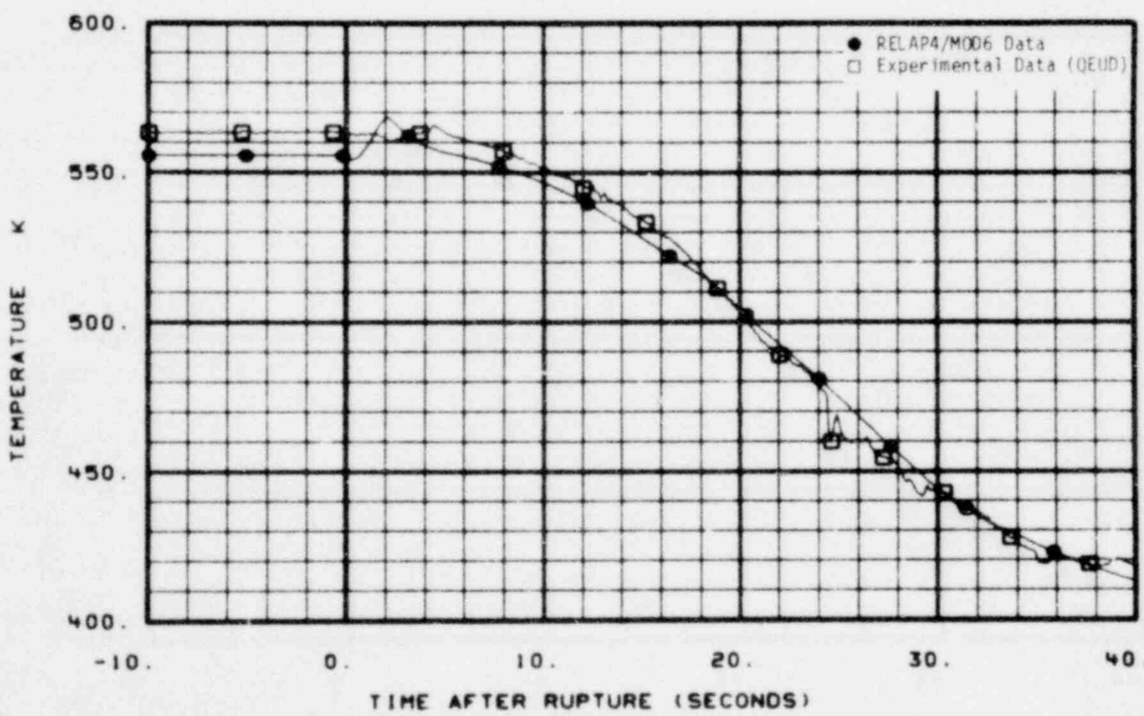

Fig. 72 Comparison of predicted and measured coolant temperature on instrument Stalk 2 (TE-2ST-5).

995 348

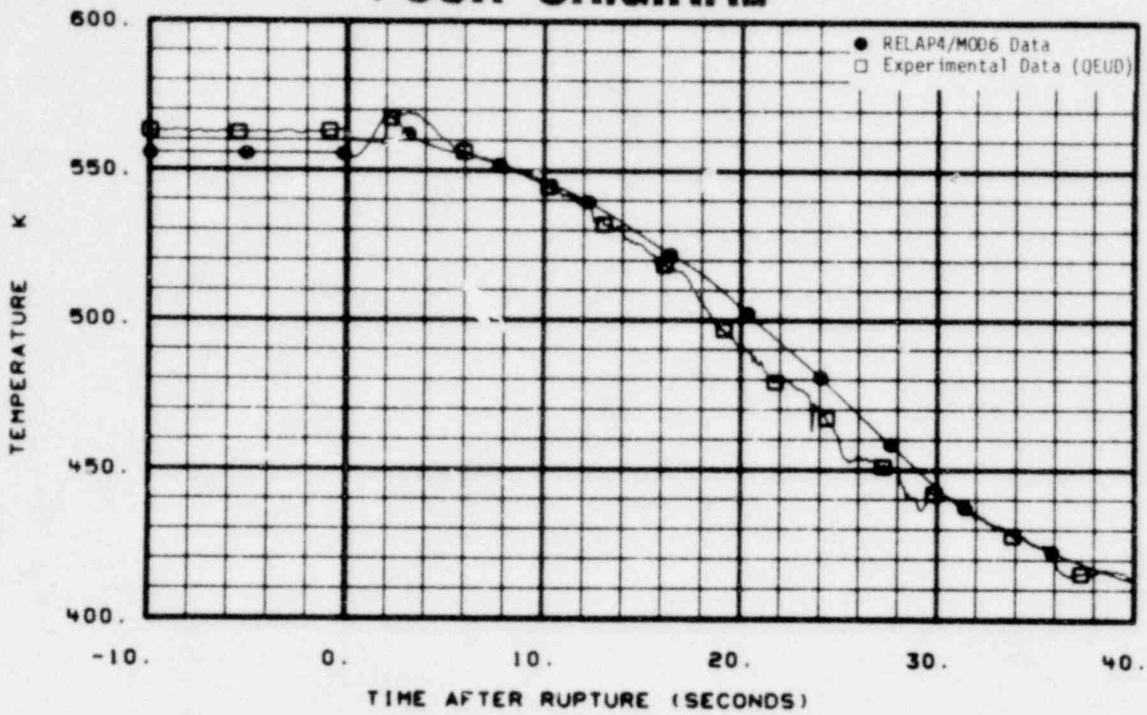

Fig. 73 Comparison of predicted and measured coolant temperature on instrument Stalk 2 (TE-2ST-7).

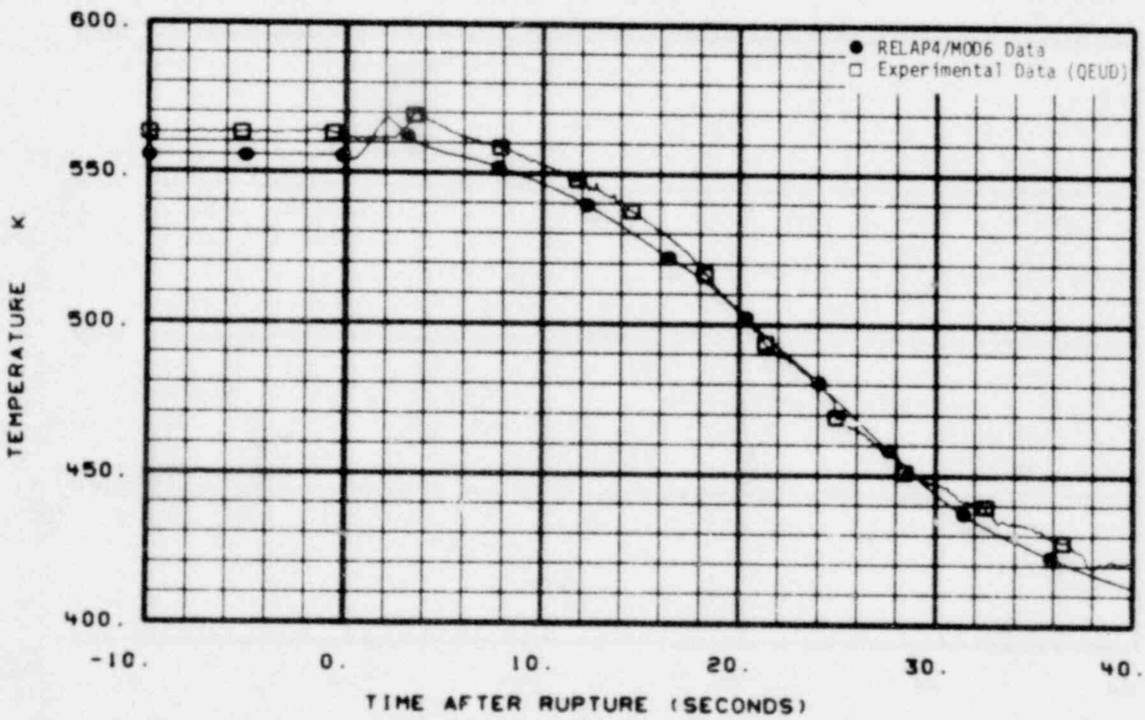

Fig. 74 Comparison of predicted and measured coolant temperature on instrument Stalk 2 (TE-2ST-9).

995 349

POOR ORIGINAL

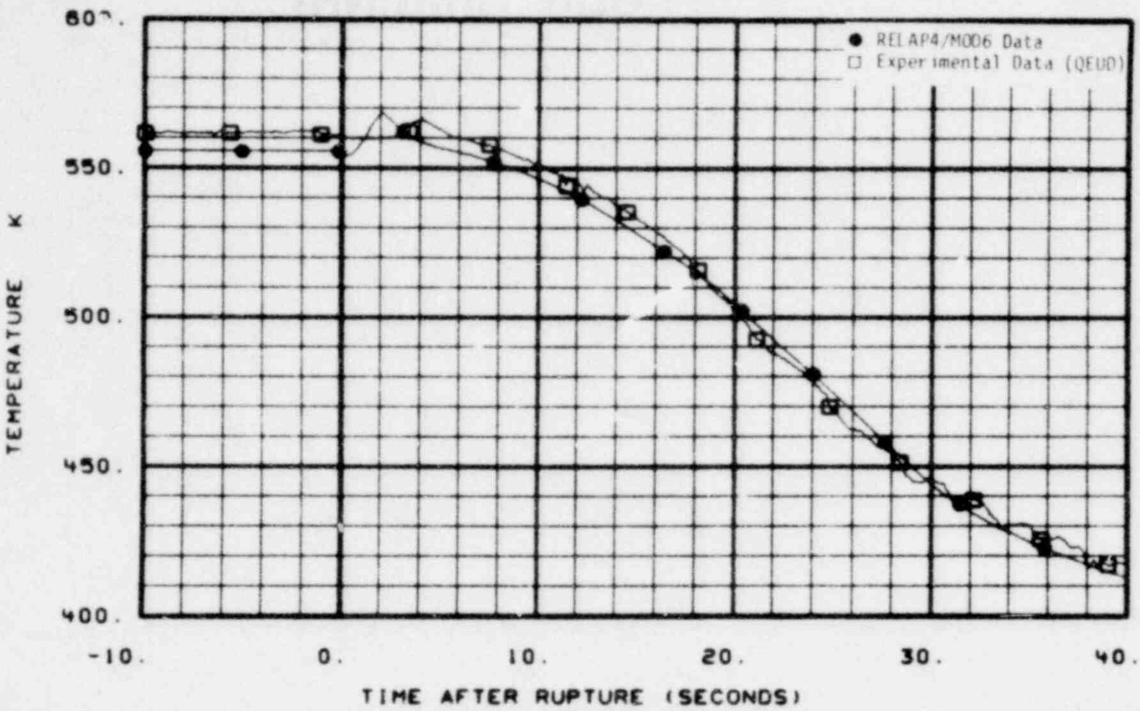

Fig. 75 Comparison of predicted and measured coolant temperature on instrument Stalk 2 (TE-2ST-10).

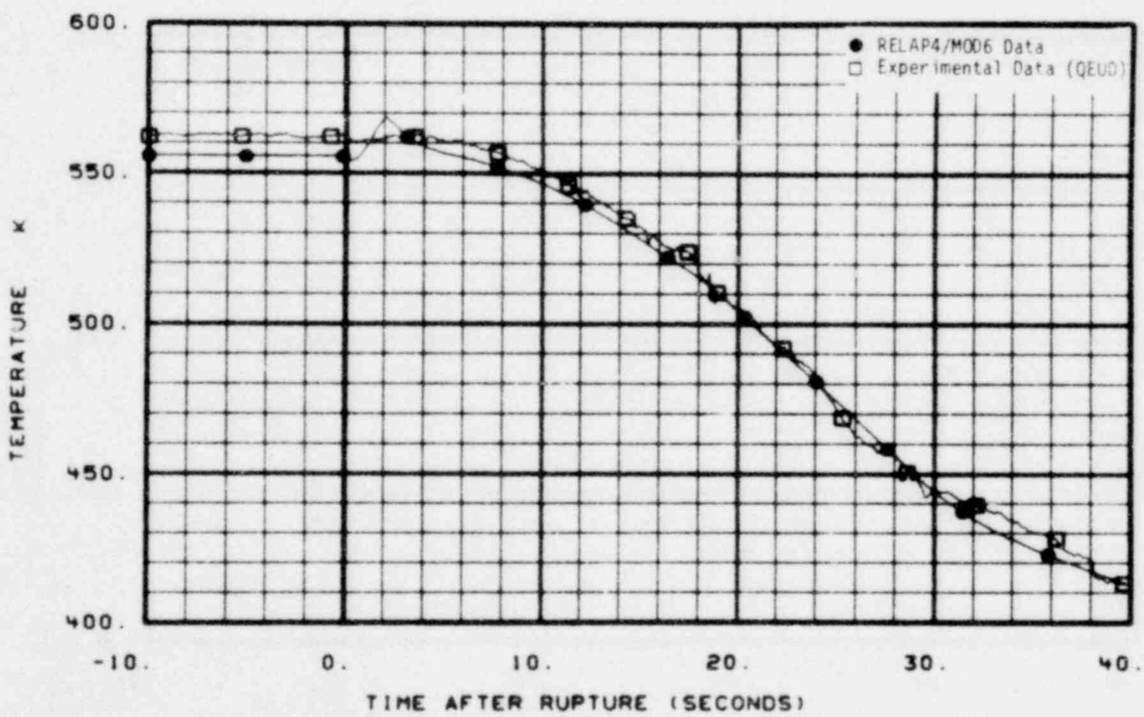

Fig. 76 Comparison of predicted and measured coolant temperature on instrument Stalk 2 (TE-2ST-13).

995 350

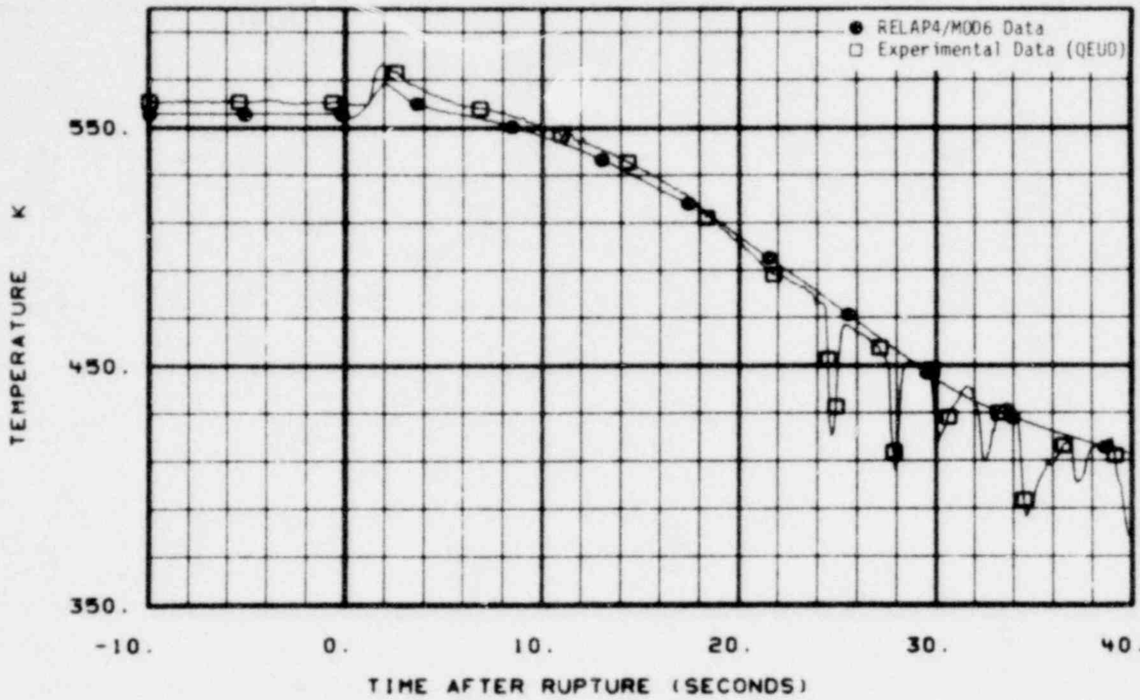

Fig. 77 Comparison of predicted and measured coolant temperature on instrument Stalk 2 (TE-2ST-14).

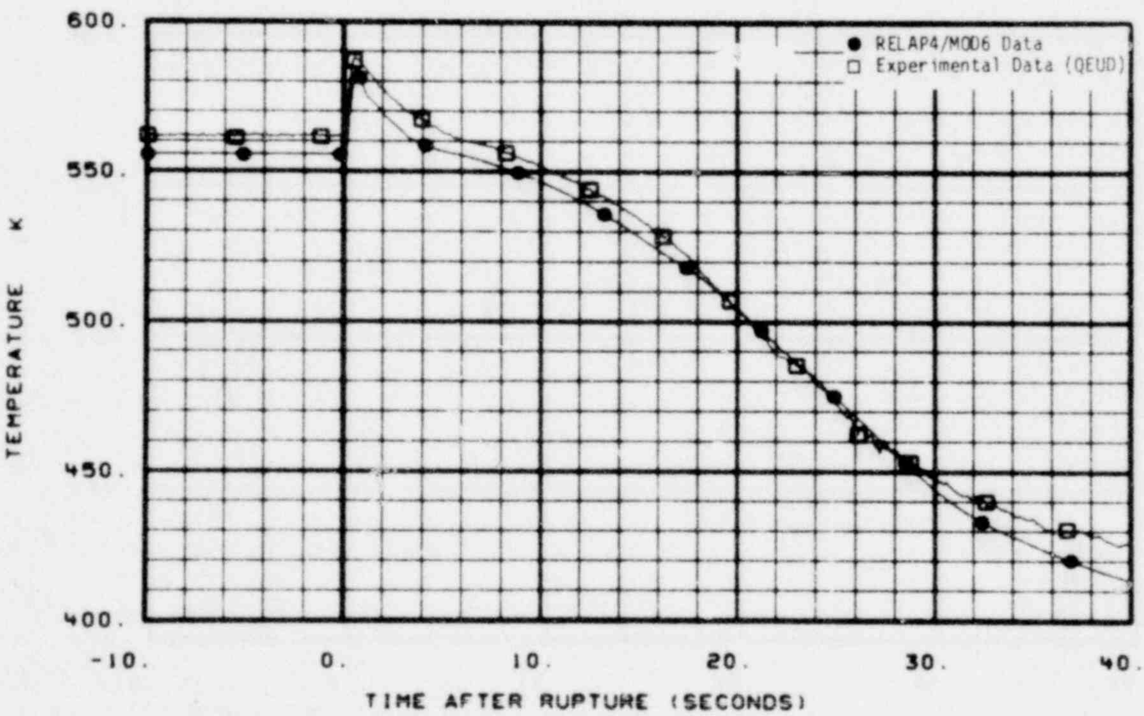

Fig. 78 Comparison of predicted and measured coolant temperature in lower end box (TE-1LP-1).

995 351

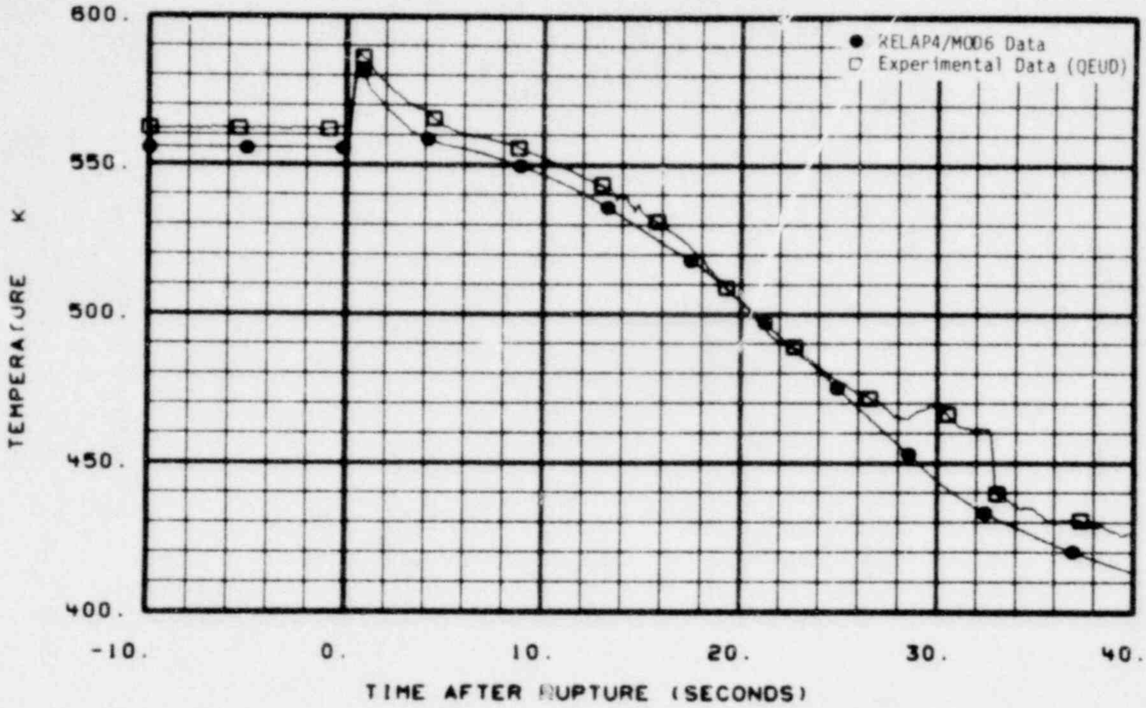

Fig. 79 Comparison of predicted and measured coolant temperature in lower end box (TE-2LP-1).

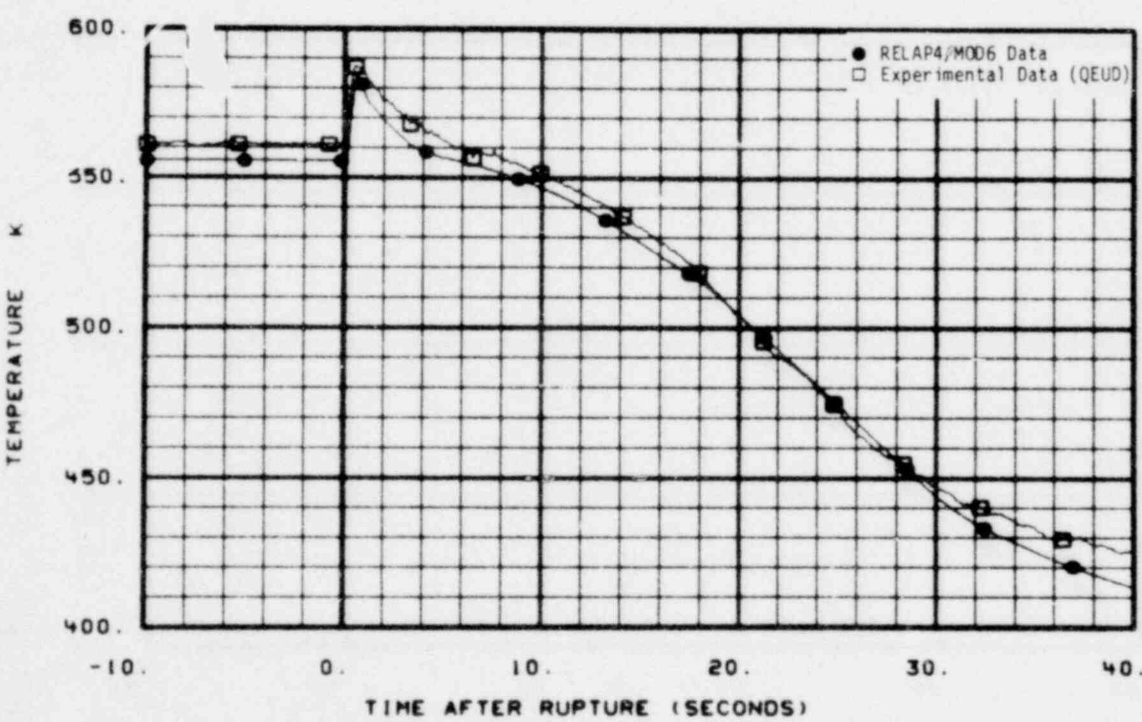

Fig. 80 Comparison of predicted and measured coolant temperature in lower end box (TE-3LP-1).

995 352

POOR ORIGINAL

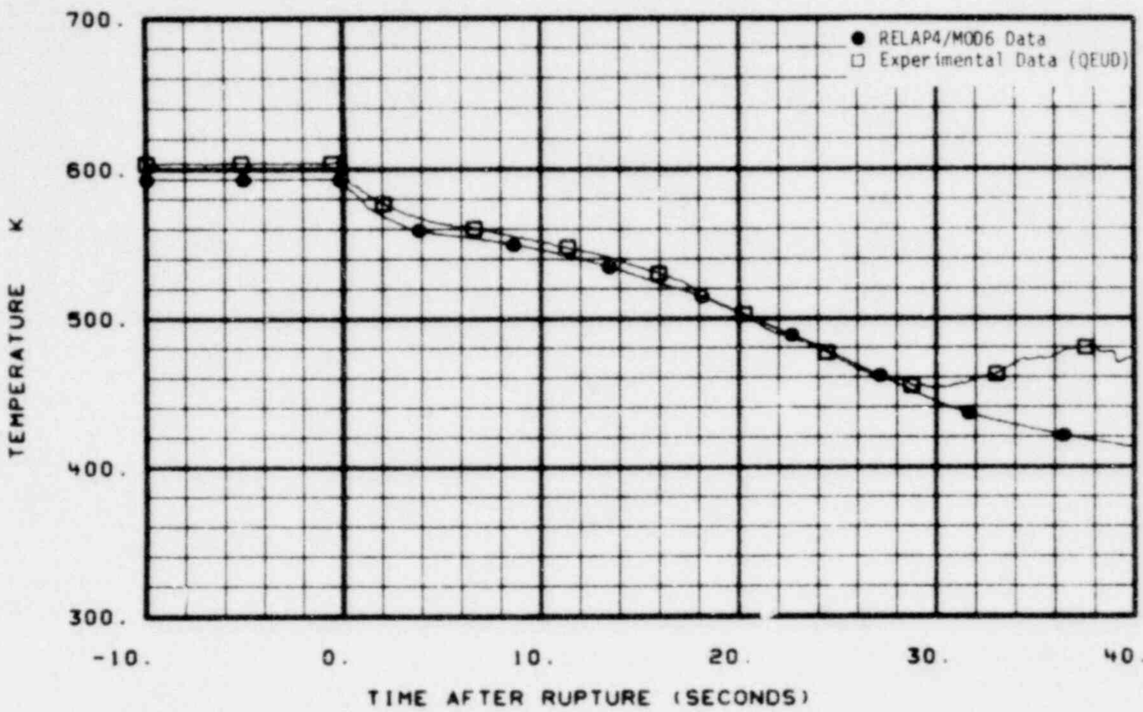

Fig. 81 Comparison of predicted and measured coolant temperature in upper end box (TE-1UP-1).

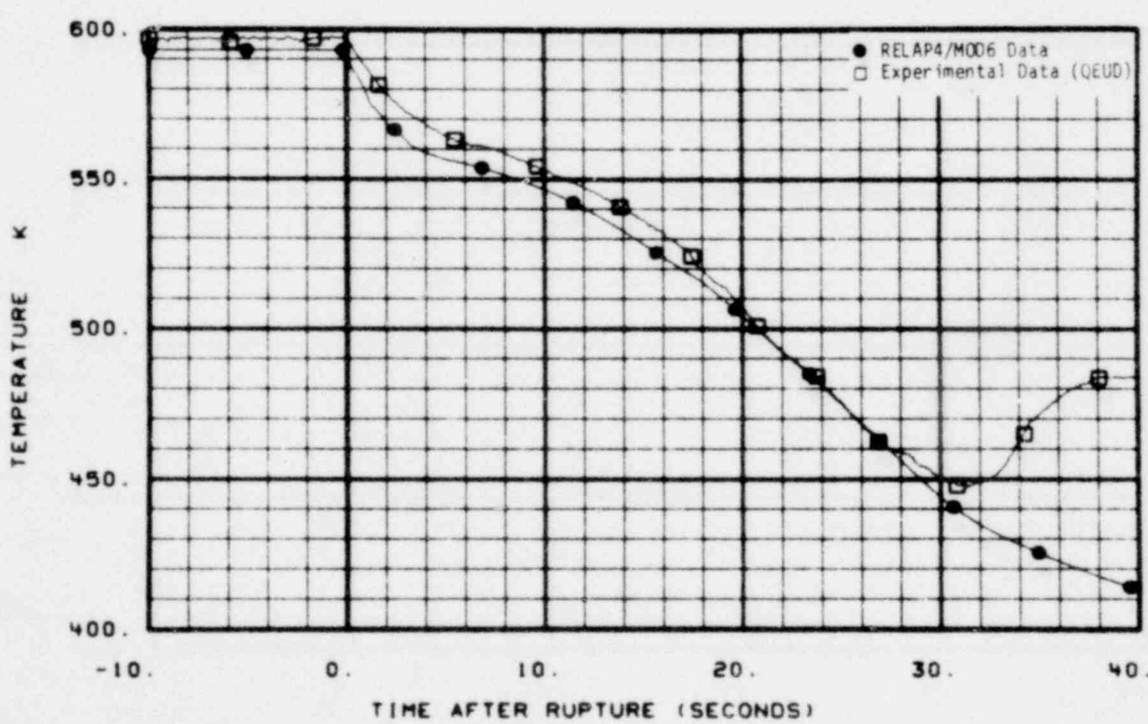

Fig. 82 Comparison of predicted and measured coolant temperature on drag disc-turbine transducer FE-1UP-1 (TE-1UP-5).

995 353

POOR ORIGINAL

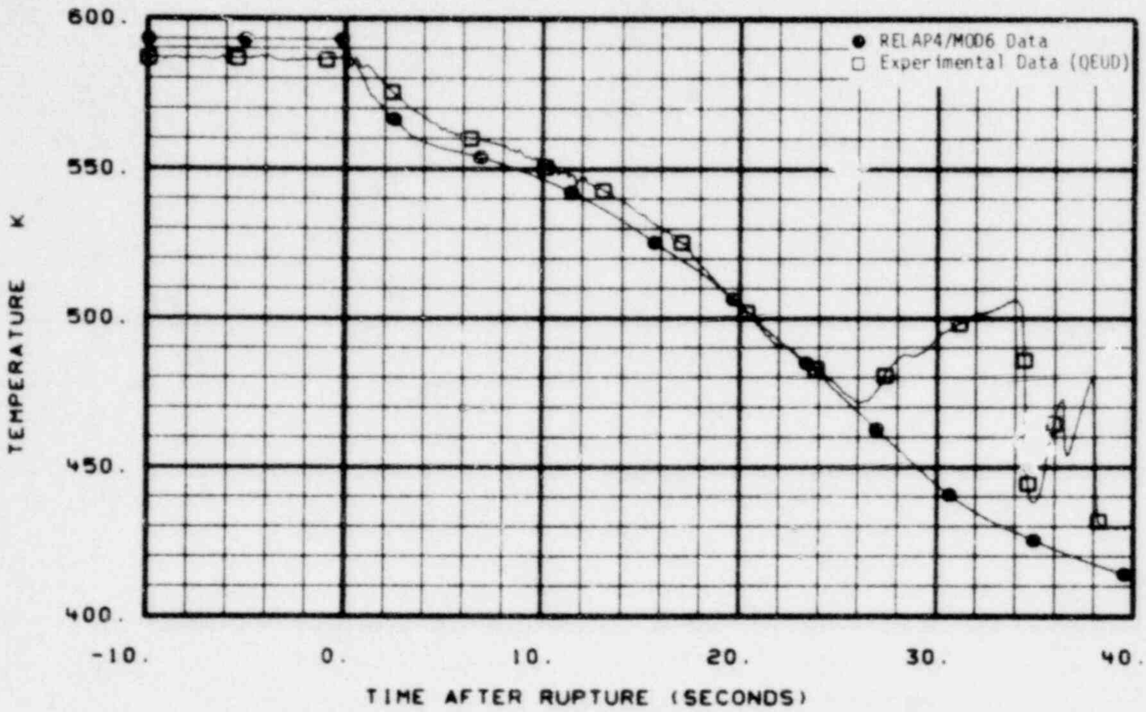

Fig. 83 Comparison of predicted and measured coolant temperature in upper end box (TE-2UP-1).

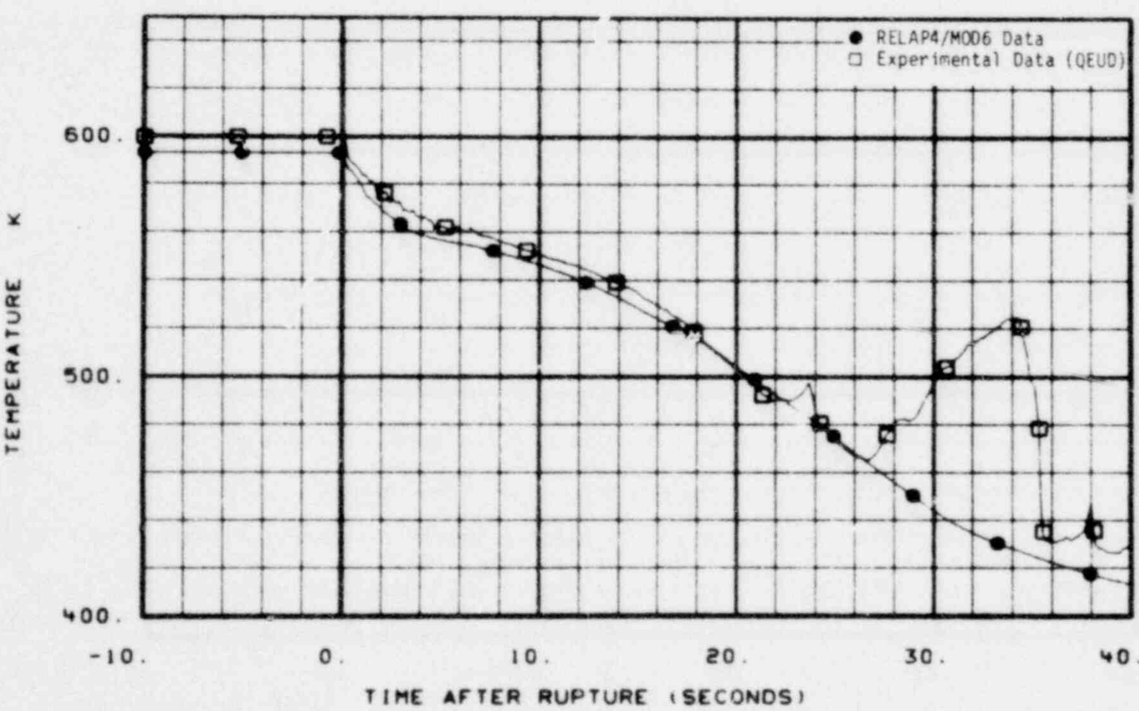

Fig. 84 Comparison of predicted and measured coolant temperature in upper end box (TE-3UP-1).

995 354

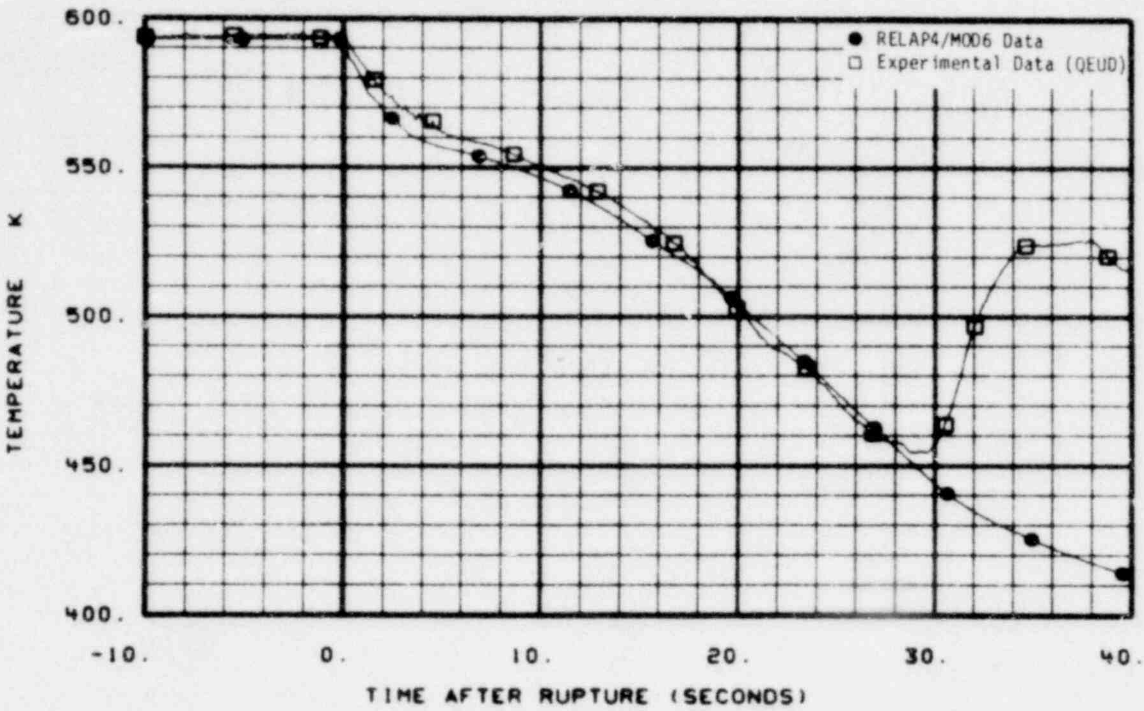

Fig. 85 Comparison of predicted and measured coolant temperature on drag disc-turbine transducer FE-3UP-1 (TE-3UP-5).

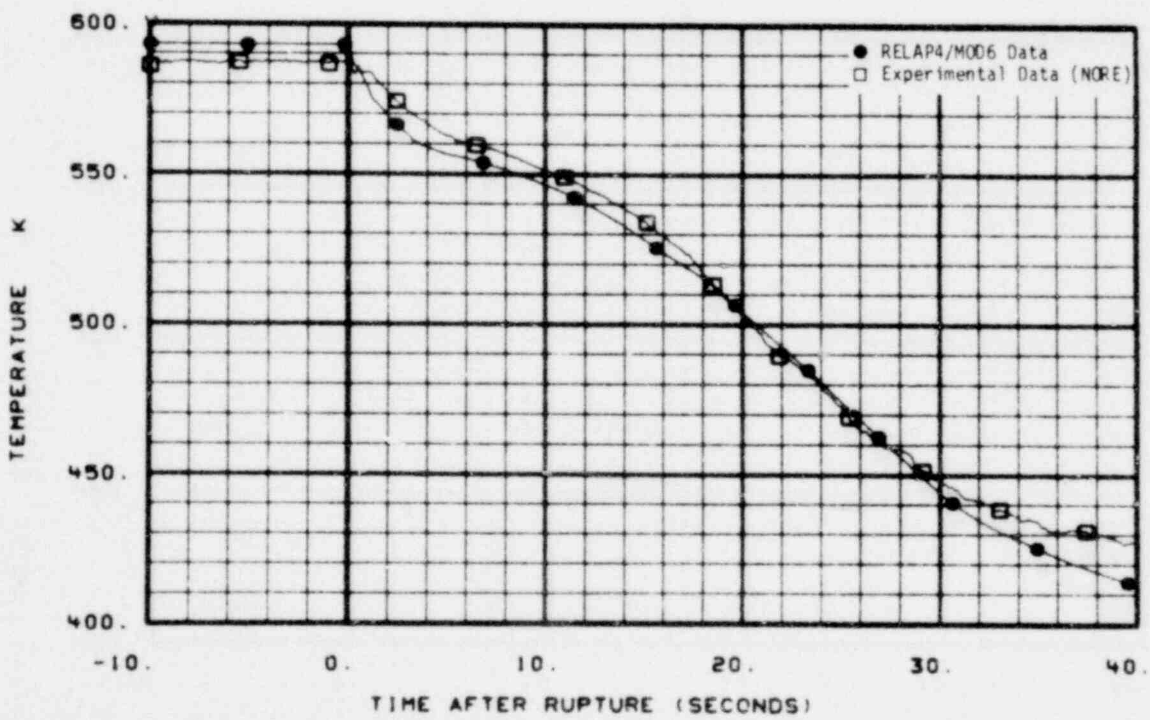

Fig. 86 Comparison of predicted and measured coolant temperature in upper end box (TE-4UP-1).

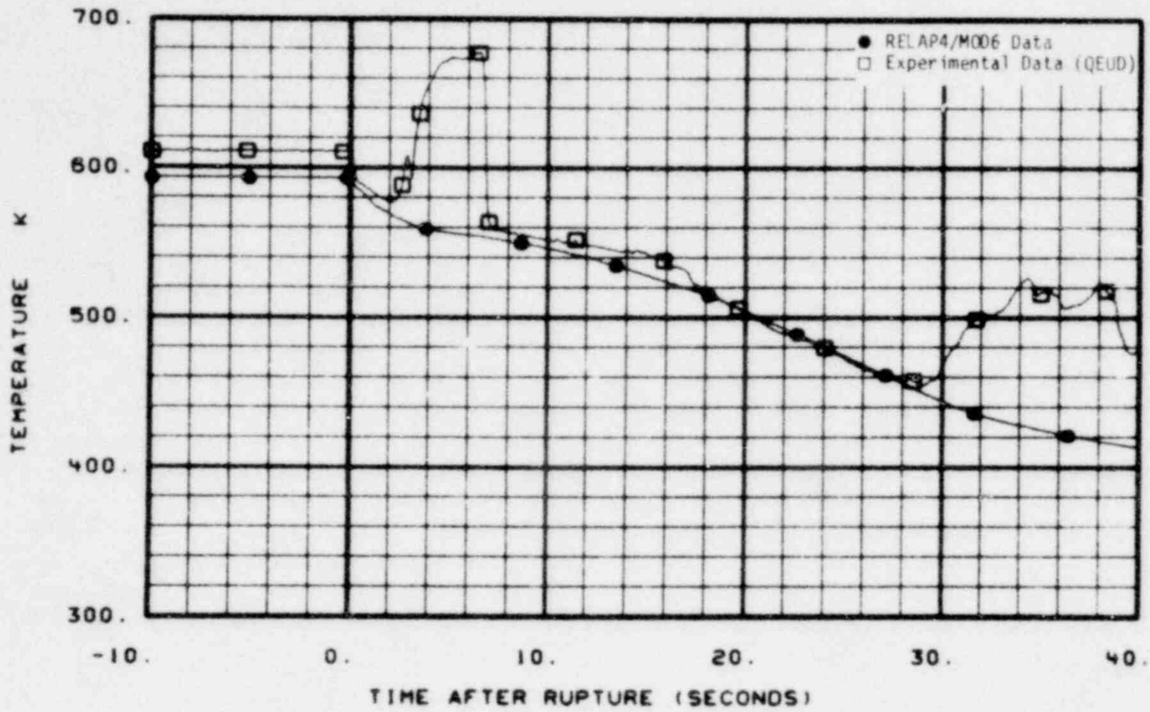

Fig. 87 Comparison of predicted and measured coolant temperature in upper end box (TE-5UP-1).

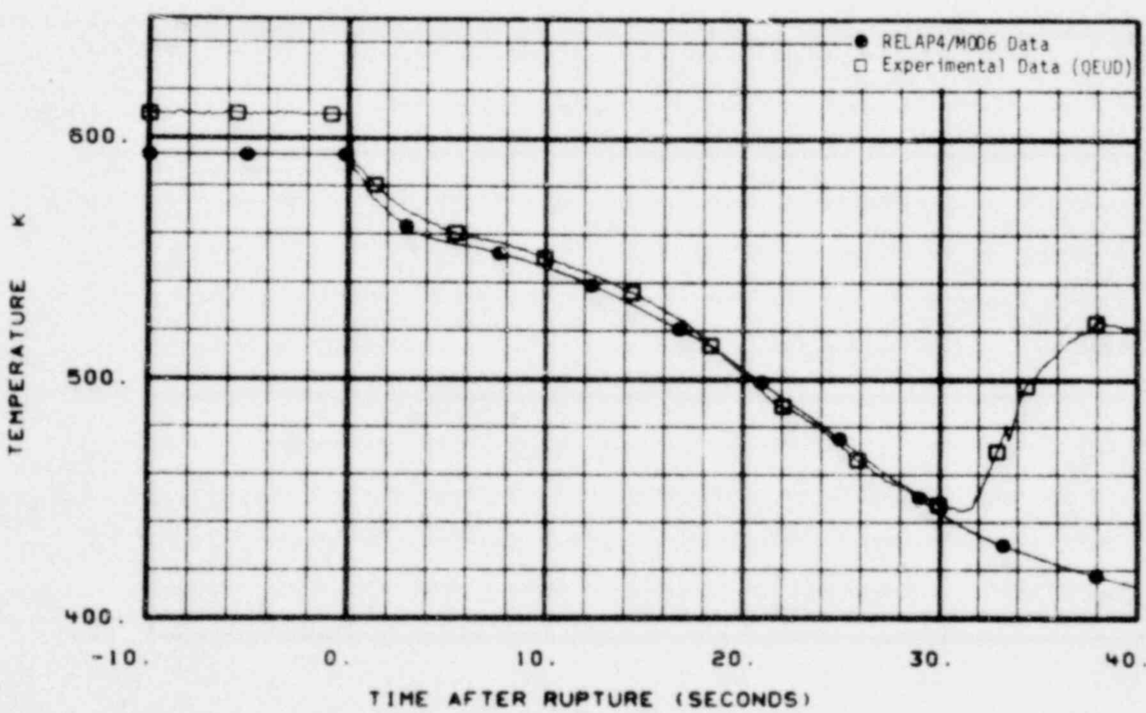

Fig. 88 Comparison of predicted and measured coolant temperature on drag disc-turbine transducer FE-5UP-1 (TE-5UP-9).

995 356

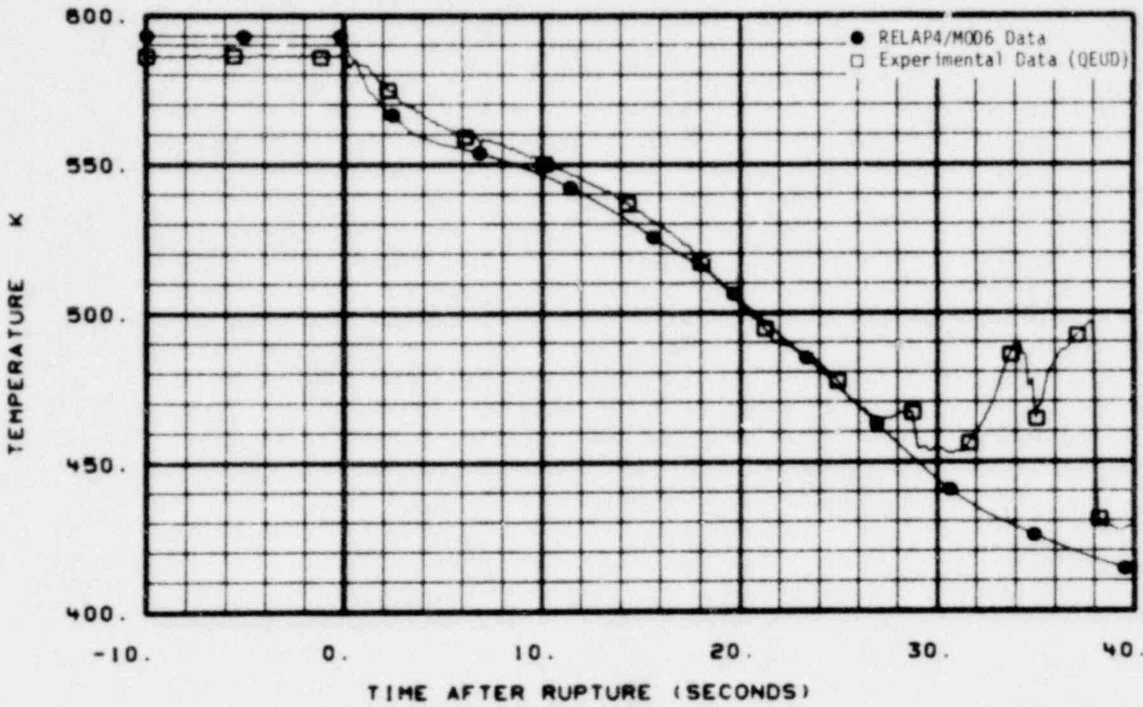

Fig. 89 Comparison of predicted and measured coolant temperature in upper end box (TE-6UP-1).

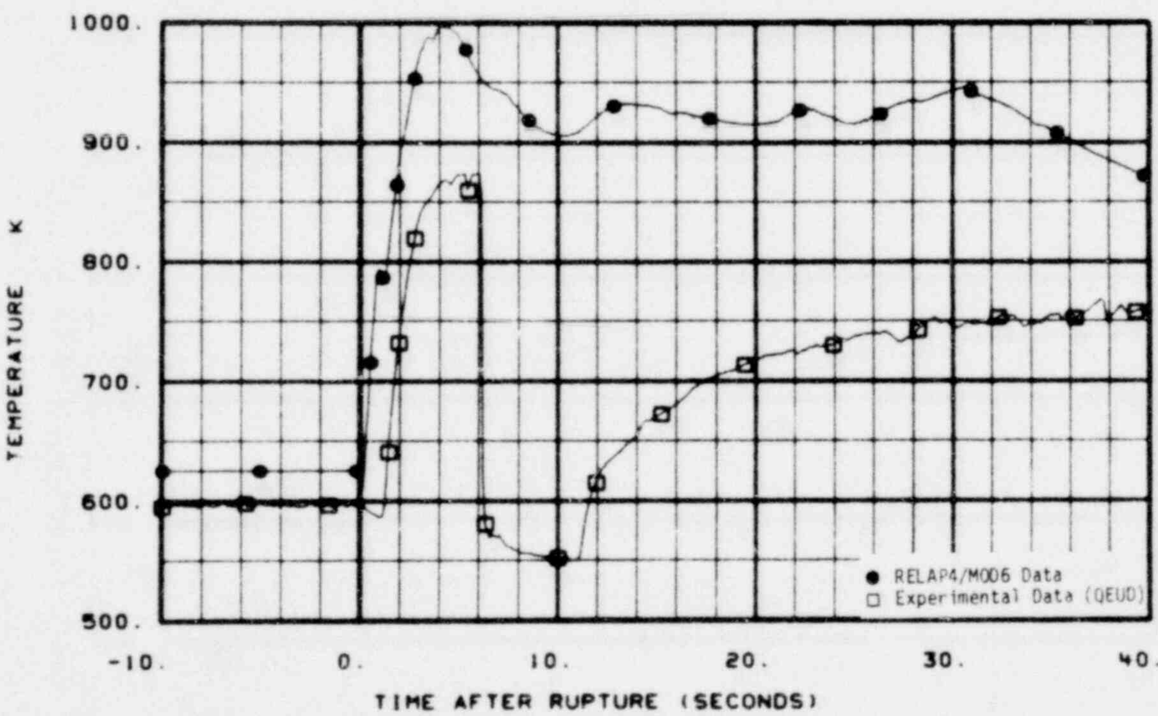

Fig. 90 Comparison of predicted and measured cladding temperature in fuel Assembly 5 (TE-5F4-15).

995 357

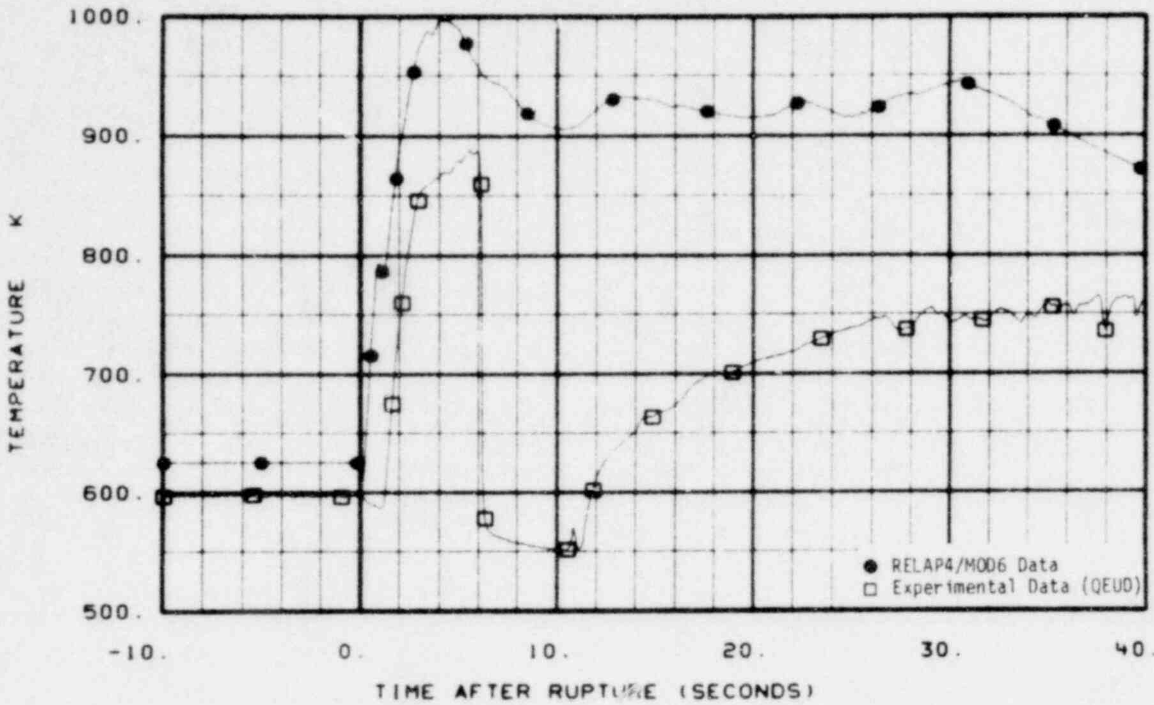

Fig. 91 Comparison of predicted and measured cladding temperature in fuel Assembly 5 (TE-5J4-15).

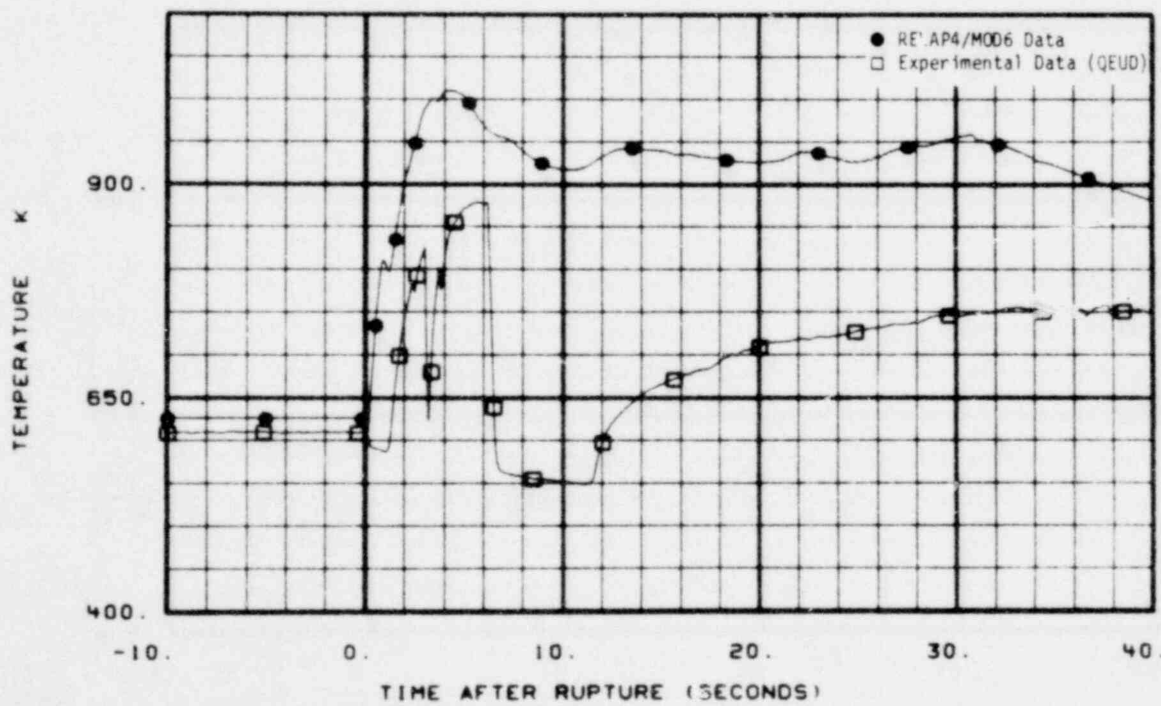

Fig. 92 Comparison of predicted and measured cladding temperature in fuel Assembly 5 (TE-5F4-21).

995 358

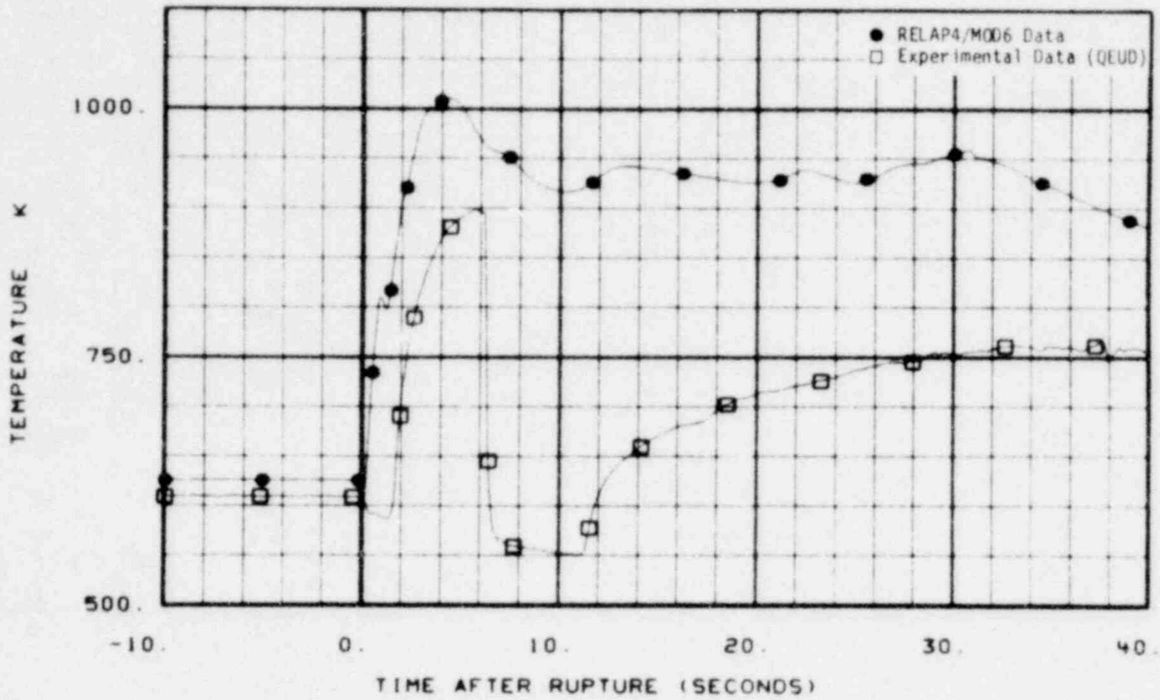

Fig. 93 Comparison of predicted and measured cladding temperature in fuel Assembly 5 (TE-5J4-21).

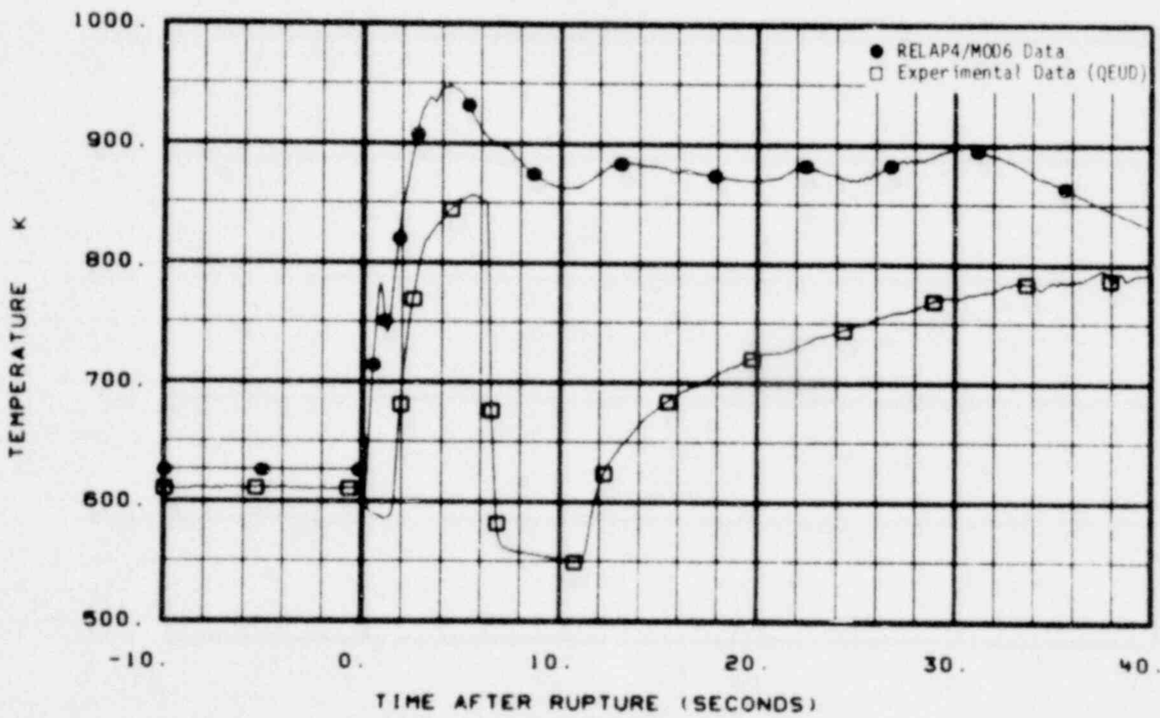

Fig 94 Comparison of predicted and measured cladding temperature in fuel Assembly 5 (TE-5F4-26).

995 359

POOR ORIGINAL

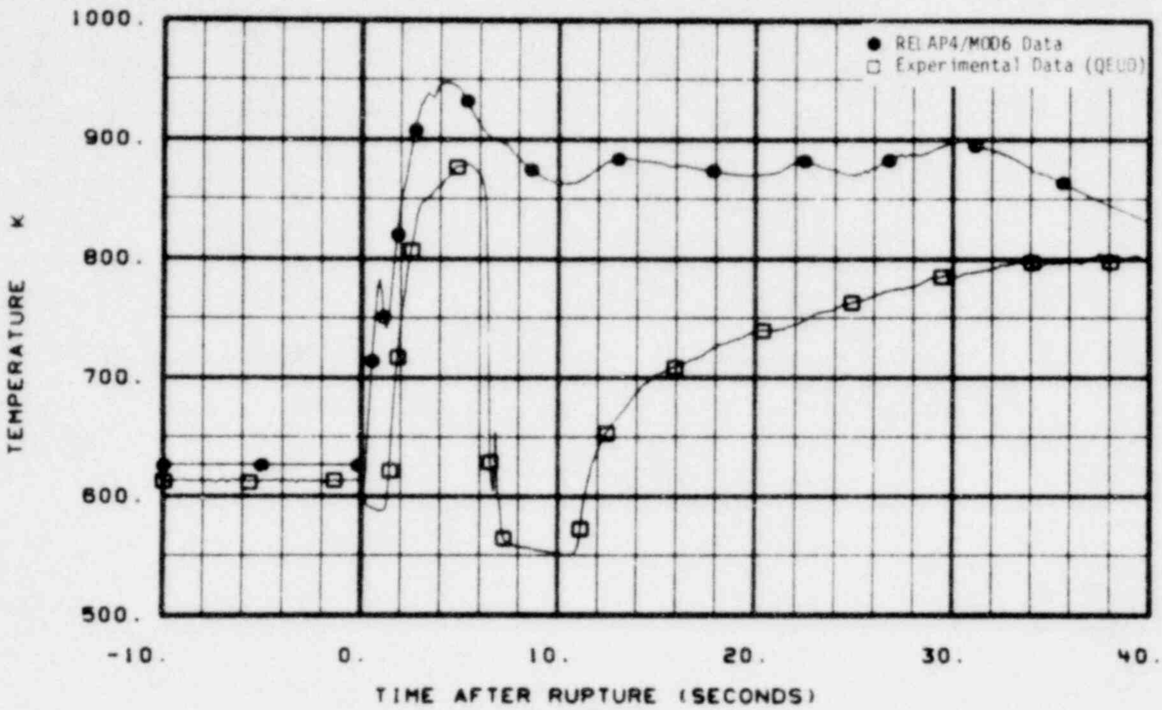

Fig. 95 Comparison of predicted and measured cladding temperature in fuel Assembly 5 (TE-5J4-26).

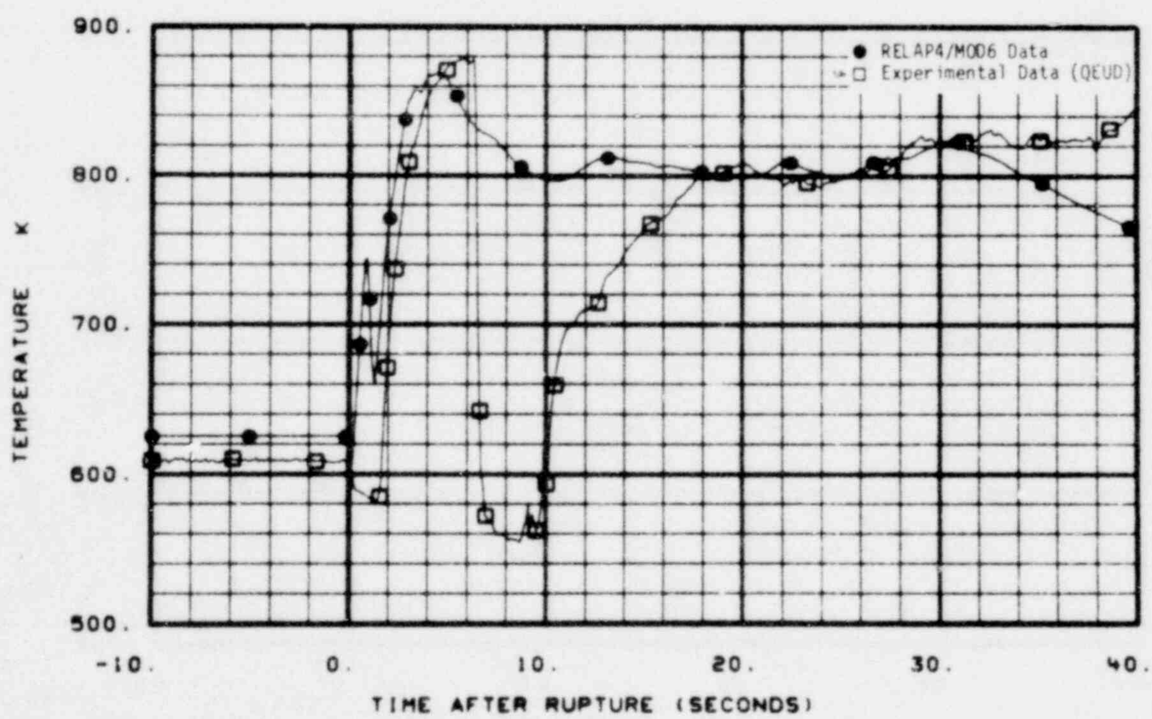

Fig. 96 Comparison of predicted and measured cladding temperature in fuel Assembly 5 (TE-5D6-30).

995 360

IMAGE EVALUATION
TEST TARGET (MT-3)

6″

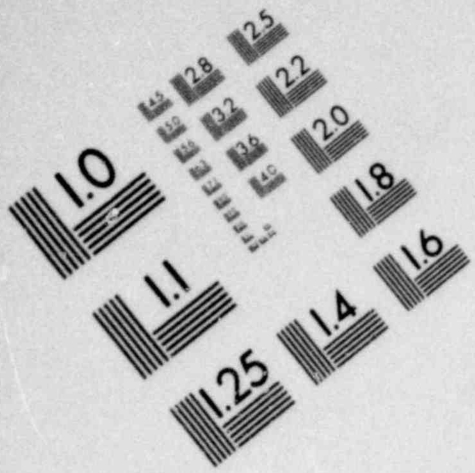

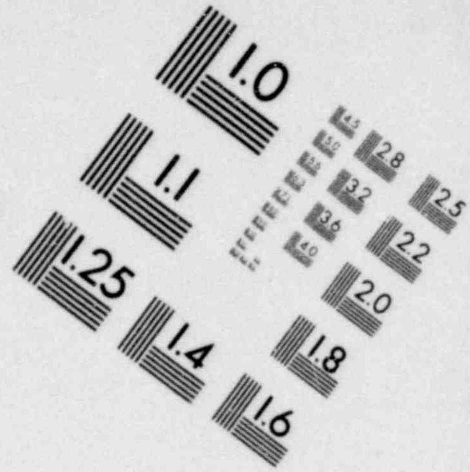

IMAGE EVALUATION
TEST TARGET (MT-3)

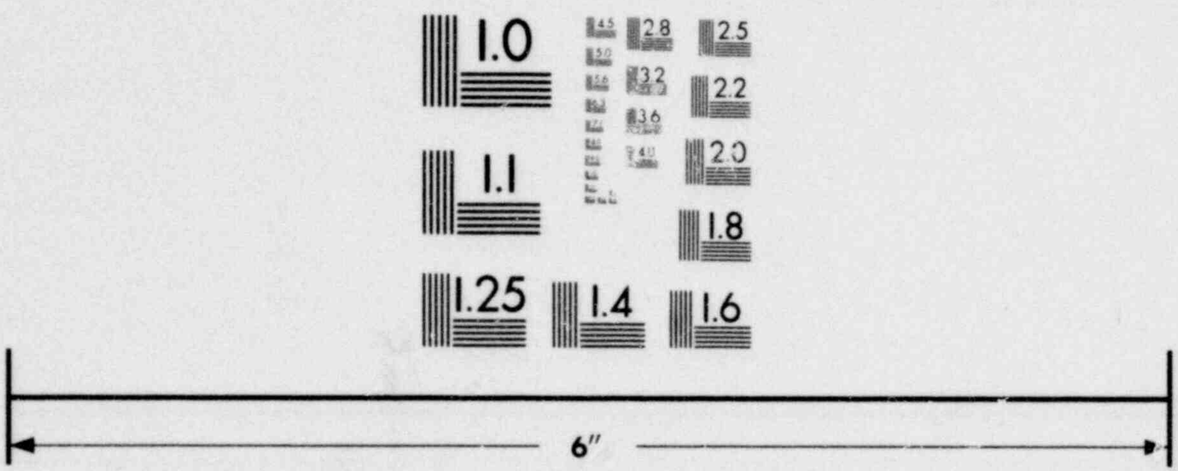

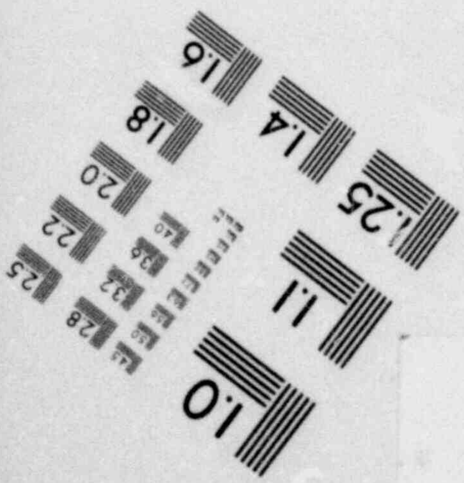

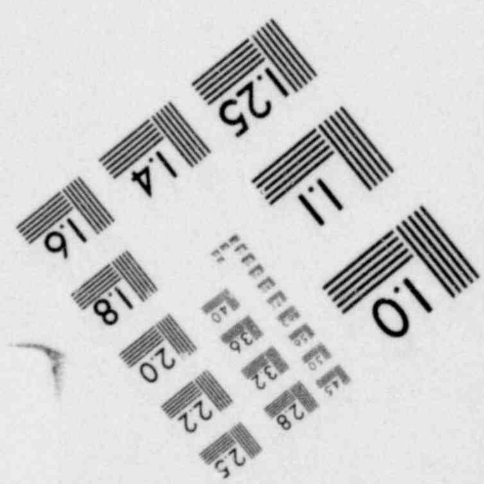

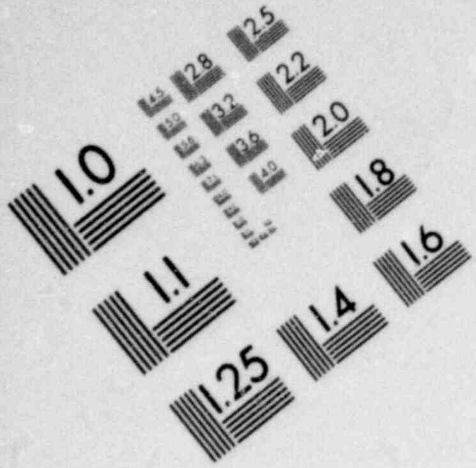

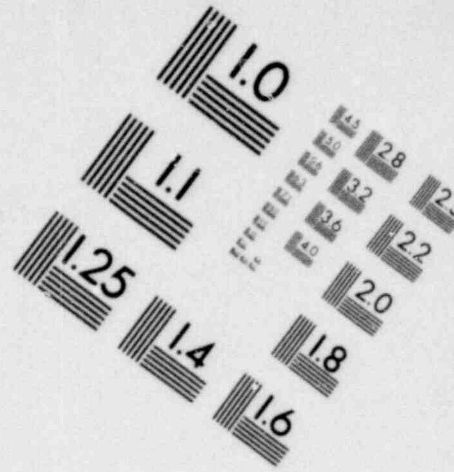

IMAGE EVALUATION TEST TARGET (MT-3)

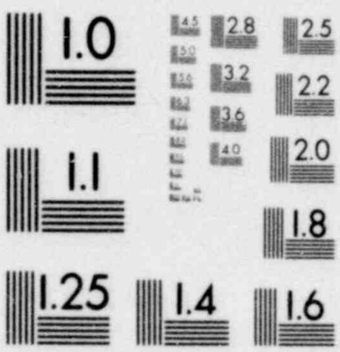

6″

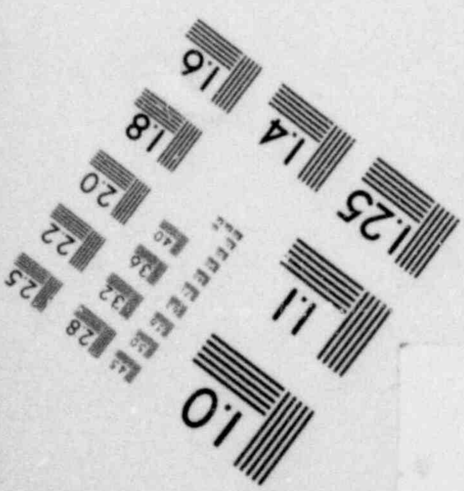

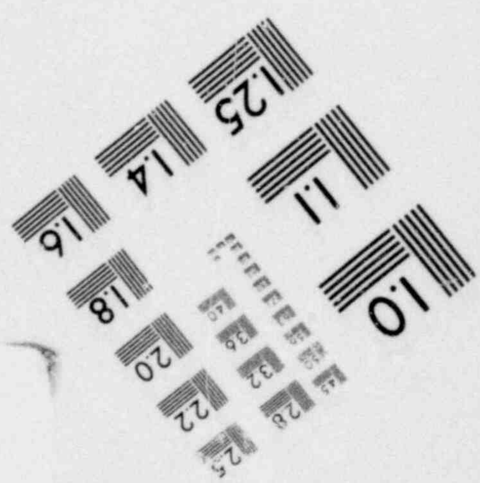

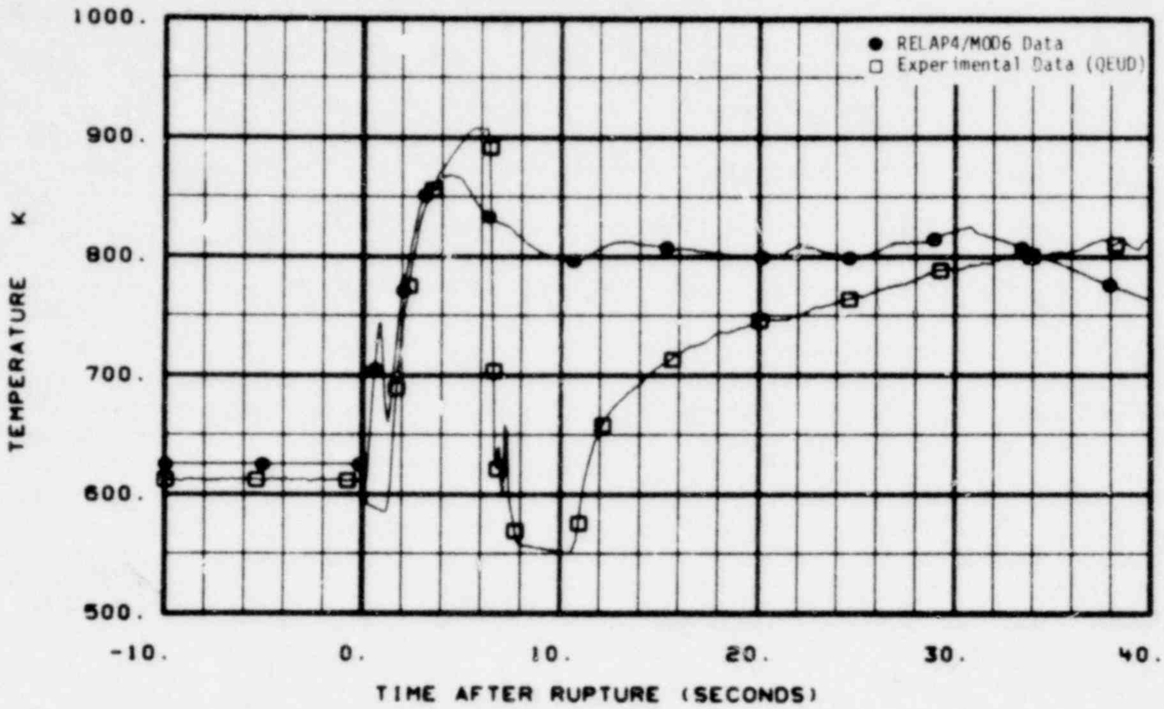

Fig. 97 Comparison of predicted and measured cladding temperature in fuel Assembly 5 (TE-5F4-30).

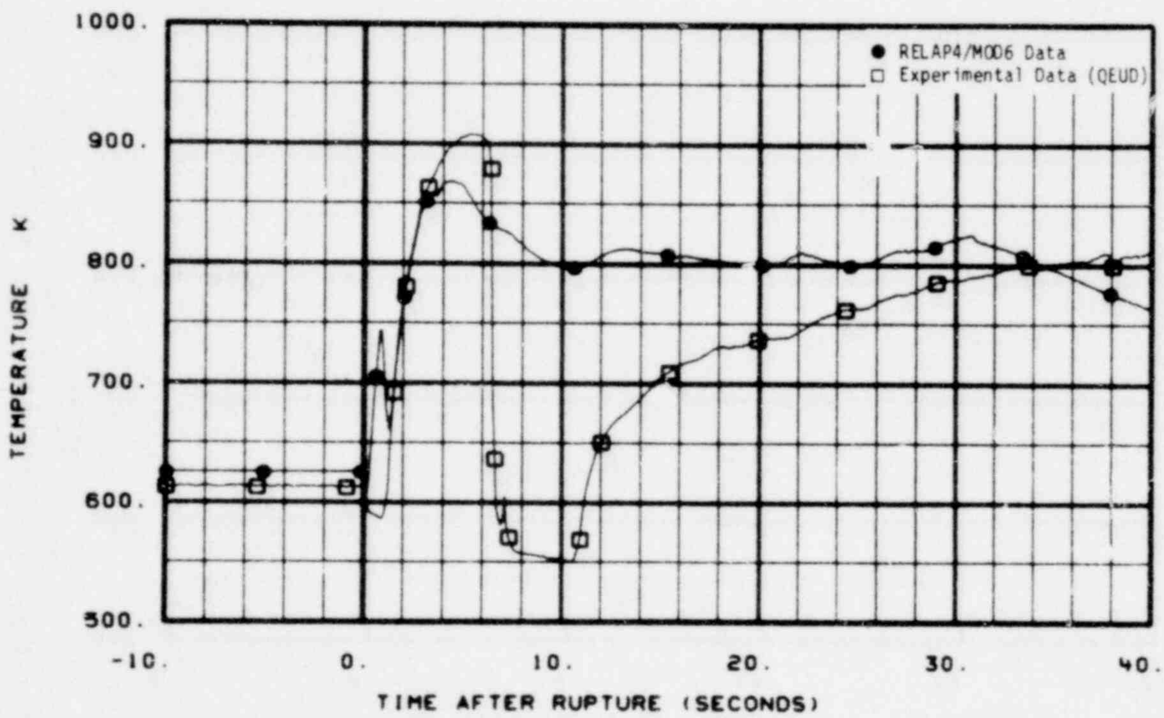

Fig. 98 Comparison of predicted and measured cladding temperature in fuel Assembly 5 (TE-5J4-30).

996 001

POOR ORIGINAL

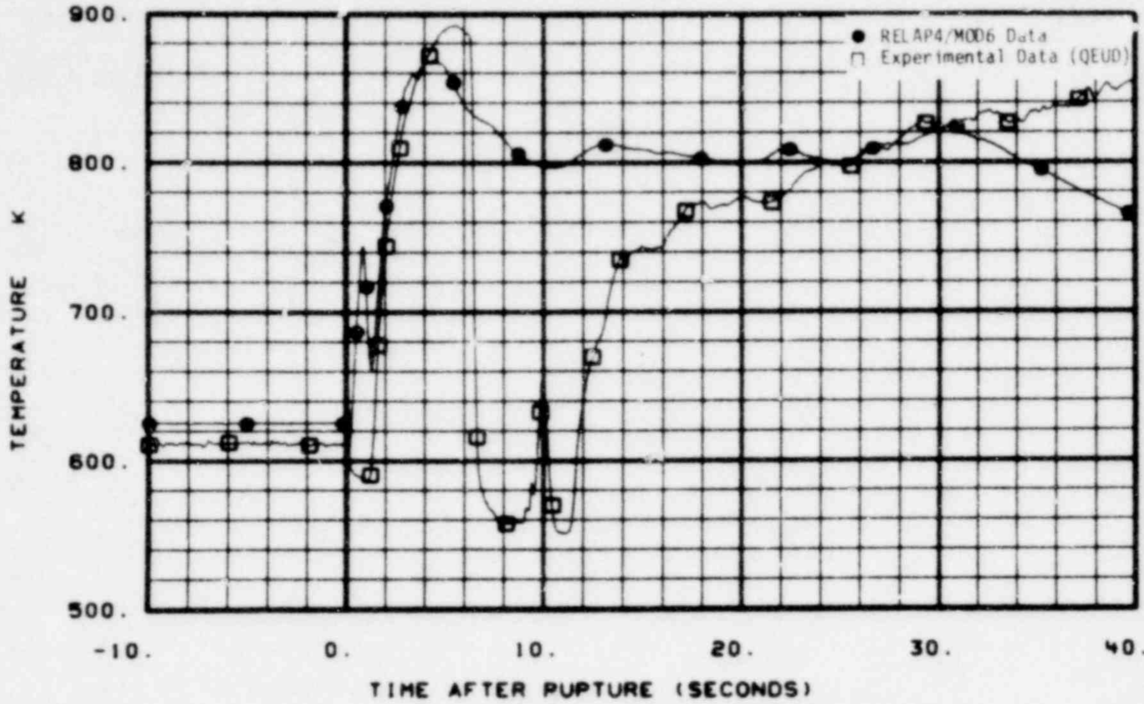

Fig. 99 Comparison of predicted and measured cladding temperature in fuel Assembly 5 (TE-5L6-30).

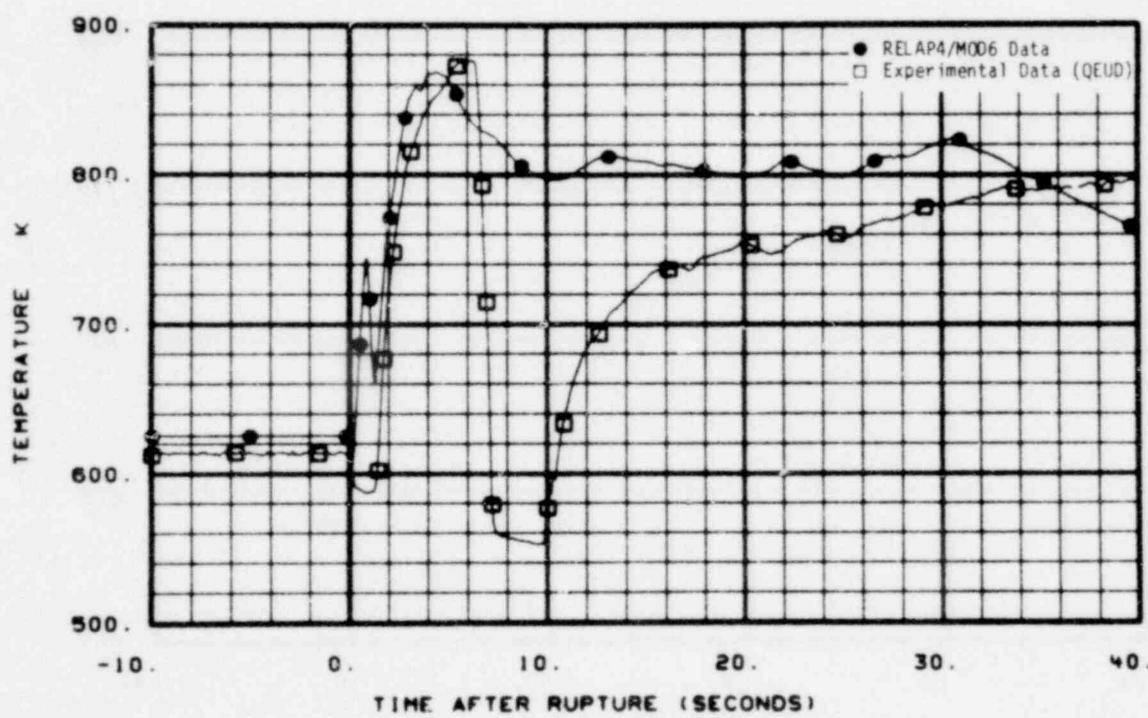

Fig. 100 Comparison of predicted and measured cladding temperature in fuel Assembly 5 (TE-5D6-32).

996 002

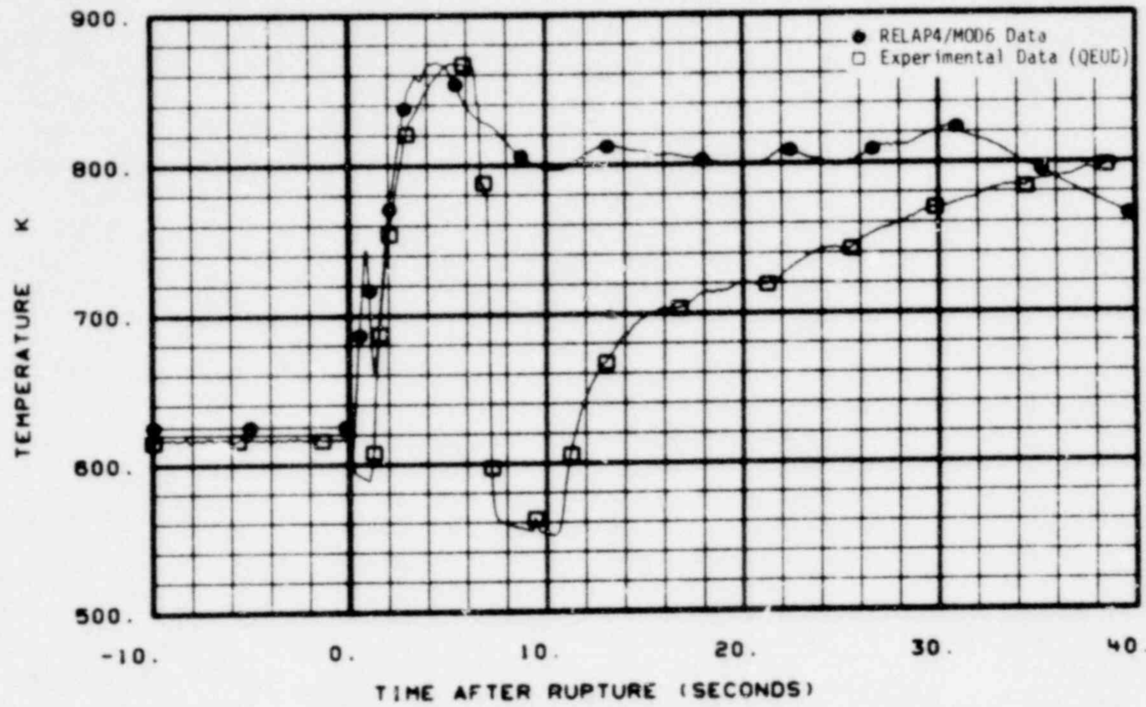

Fig. 101 Comparison of predicted and measured cladding temperature in fuel Assembly 5 (TE-5L6-32).

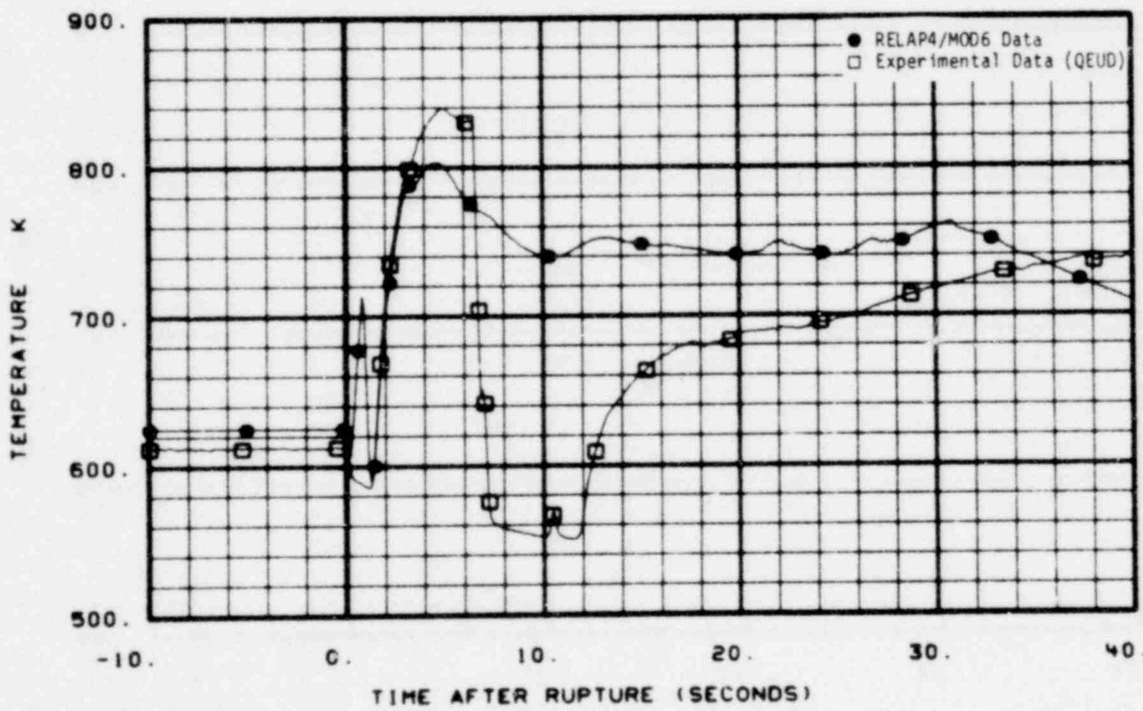

Fig. 102 Comparison of predicted and measured cladding temperature in fuel Assembly 5 (TE-5D6-37).

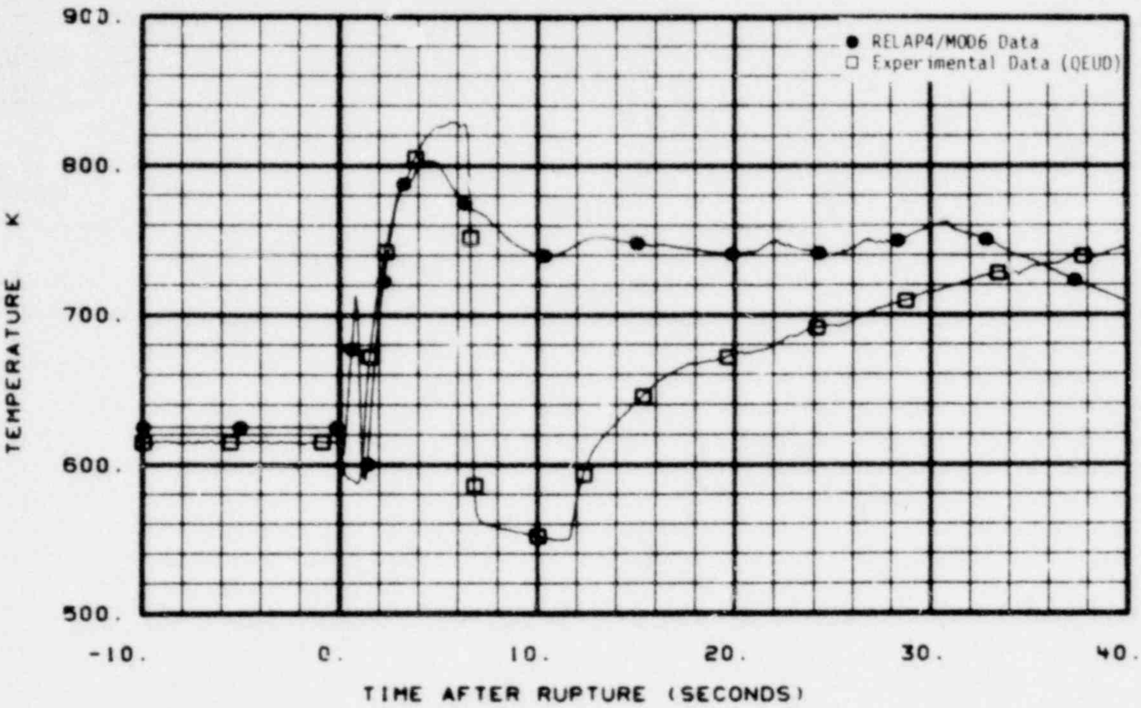

Fig. 103 Comparison of predicted and measured cladding temperature in fuel Assembly 5 (TE-5L6-37).

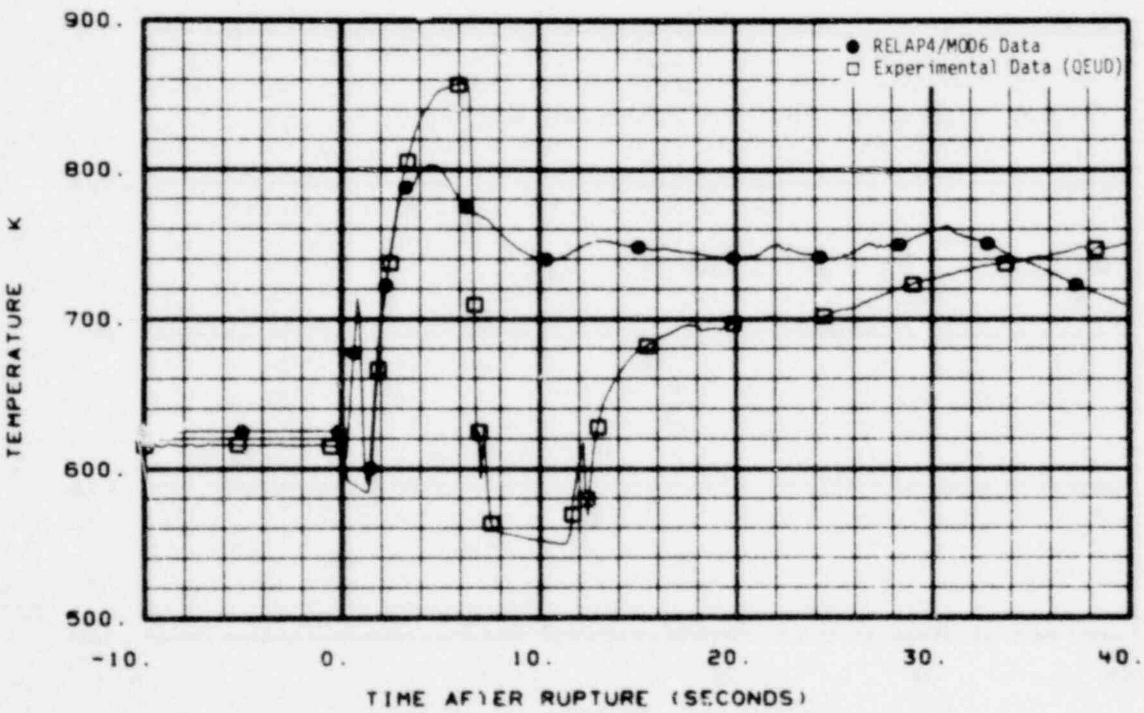

Fig. 104 Comparison of predicted and measured cladding temperature in fuel Assembly 5 (TE-5D6-39).

996 004

POOR ORIGINAL

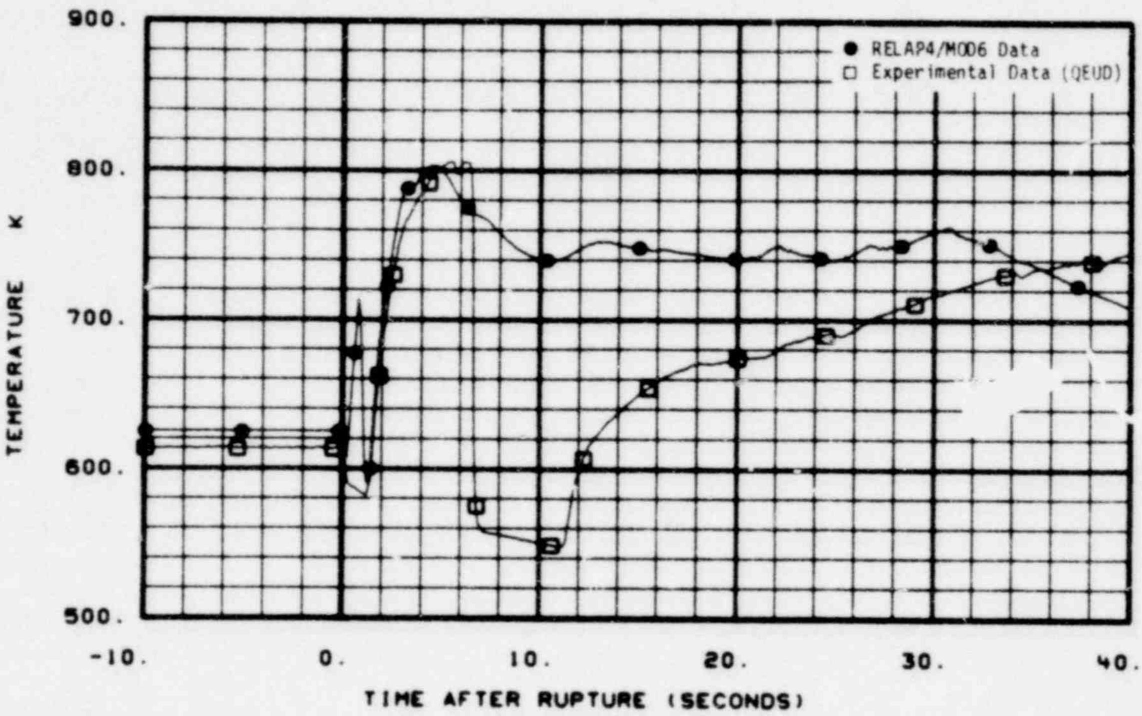

Fig. 105 Comparison of predicted and measured cladding temperature in fuel Assembly 5 (TE-5L6-39).

996 005

3. CONCLUSIONS AND RECOMMENDATIONS

The overall agreement between the experiment predictions and the experimental data is good, except for the fuel rod cladding thermal response and the performance of the steam generator secondary side.

It is recommended that future LOCE L2-3 posttest analysis activities be centered on gaining a better understanding of modeling rewet phenomena with the RELAP4/MOD6 heat transfer surface. In addition, better modeling of the performance of the steam generator secondary side is needed before modeling small break LOCEs.

4. REFERENCES

1. P. G. Prassinos, B. M. Galusha, D. G. Engelman, Experiment Data Report for LOFT Power Ascension Experiment L2-3, NUREG-CR-0792, TREE-1326 (July 1979).

2. E. J. Kee and W. H. Grush, Best Estimate Prediction for LOFT Nuclear Experiment L2-3, EP-L2-3 (April 1979).

3. D. L. Reeder, LOFT System and Test Description (5.5-ft Nuclear Core 1 LOCEs), NUREG/CR-0247, TREE-1208 (July 1978).

4. P. A. Harris, T. K. Samuels, H. J. Welland, "Power Ascension Test Series L2," LOFT Experiment Operating Specification, Volume 2, NE L2 Series, Revision 2 (July 1978).

5. EG&G Idaho, Inc., RELAP4/MOD6 -- A Computer Program for Transient Thermal-Hydraulic Analysis of Nuclear Reactors and Related Systems -- User's Manual, CDAP-TR-003 (January 1978).

996 006

APPENDIX A

EXPERIMENTAL MEASUREMENT LOCATIONS IN THE LOFT SYSTEM

BLANK

996 003

APPENDIX A

EXPERIMENTAL MEASUREMENT LOCATIONS IN THE LOFT SYSTEM

Figure A-1 shows the intact loop and external reactor vessel instrumentation. Figure A-2 shows the broken loop instrumentation, Figures A-3 and A-4 show the internal reactor vessel instrumentation. Figure A-5 shows a core map. The core thermocouple identification number can be used with this map to locate a transducer in the core. The identification number is broken down as follows

Transducer location (inches from bottom of core)
Fuel assembly row
Fuel assembly column
Fuel assembly number
Transducer type

TE-3B11-23

BLANK

996 010

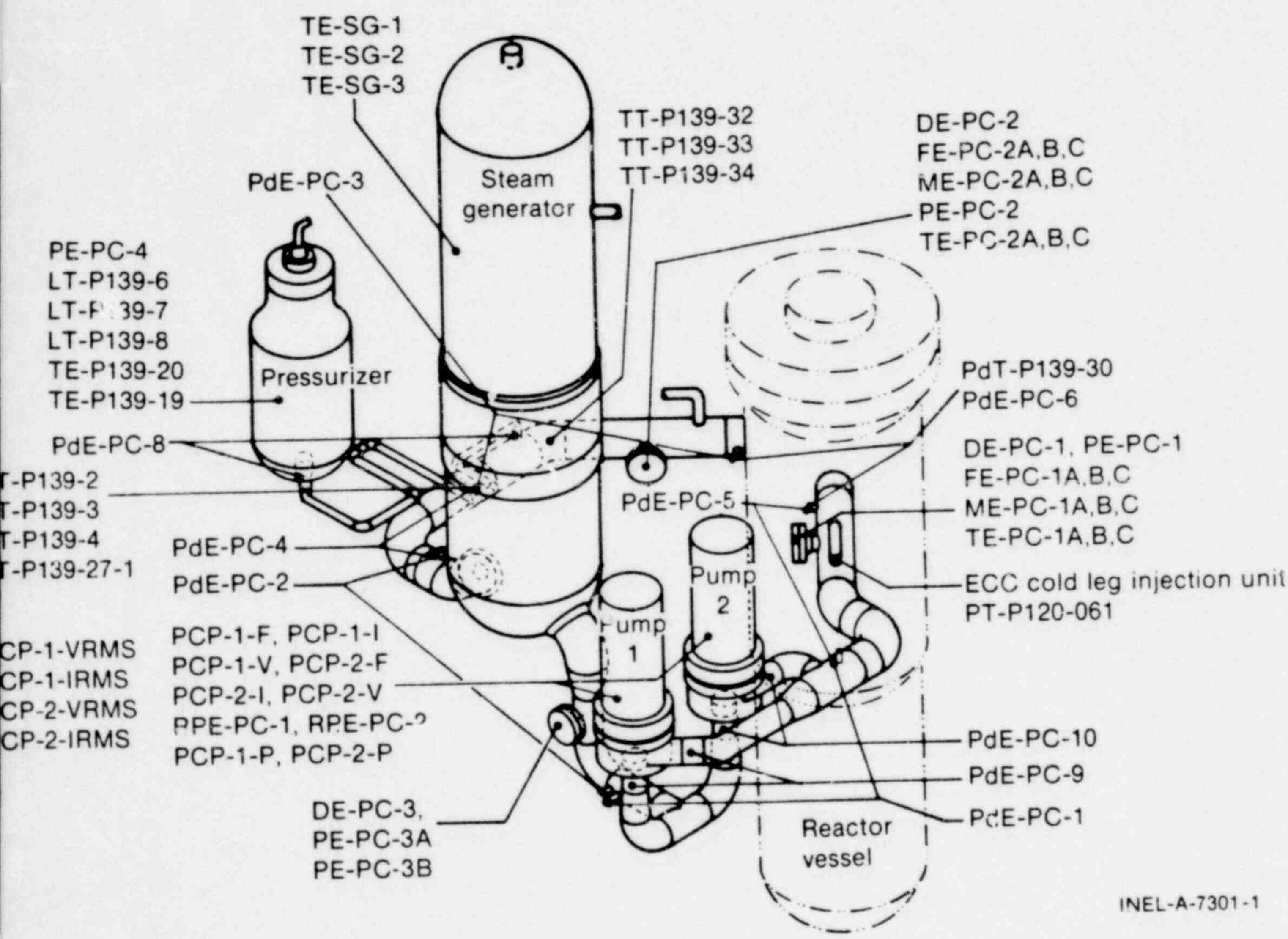

Fig. A-1 Intact loop measurement locations.

996 011

BLANK

996 012

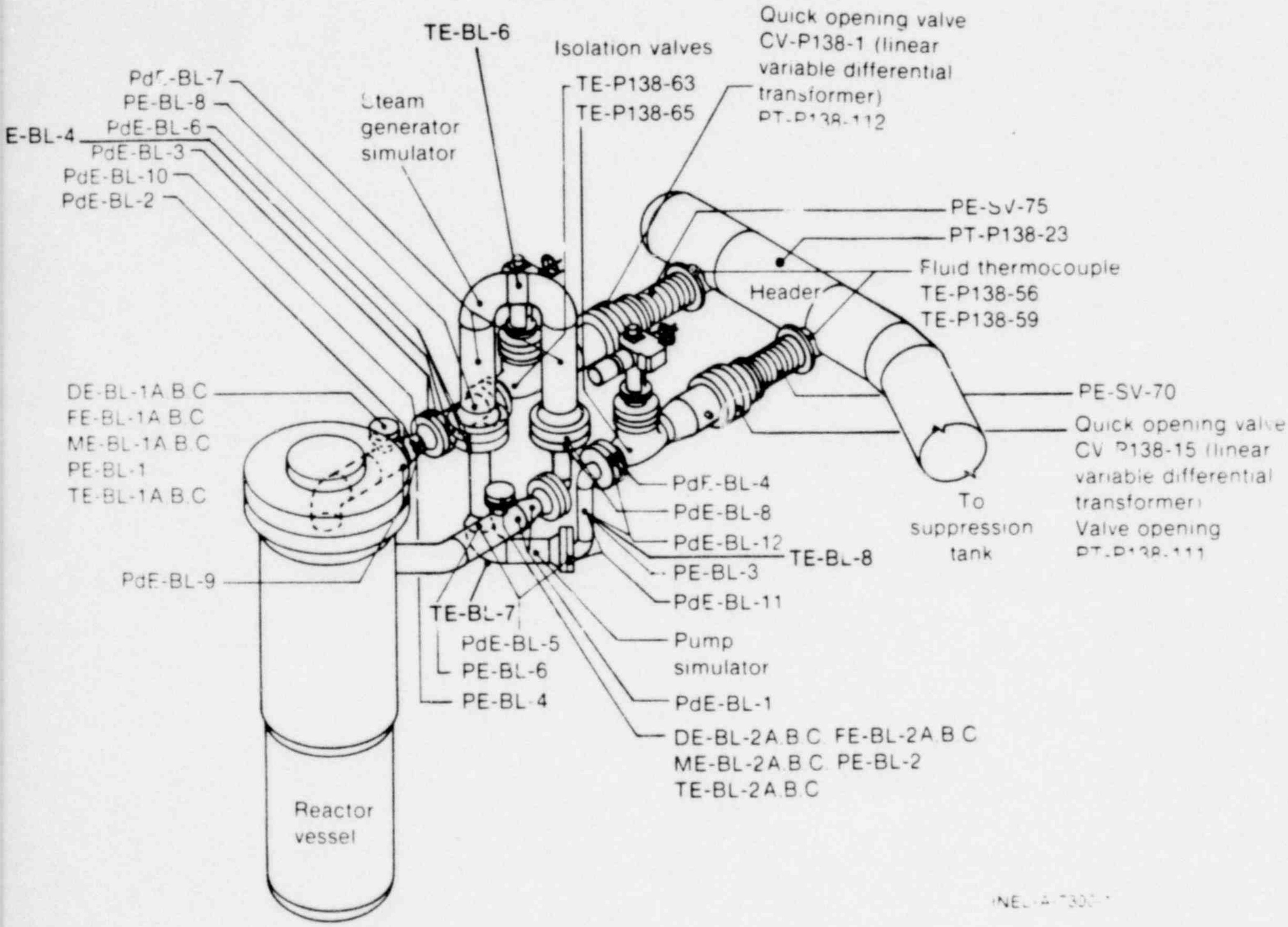

Fig. A-2 Broken loop measurement locations.

996 013

BLANK

POOR ORIGINAL

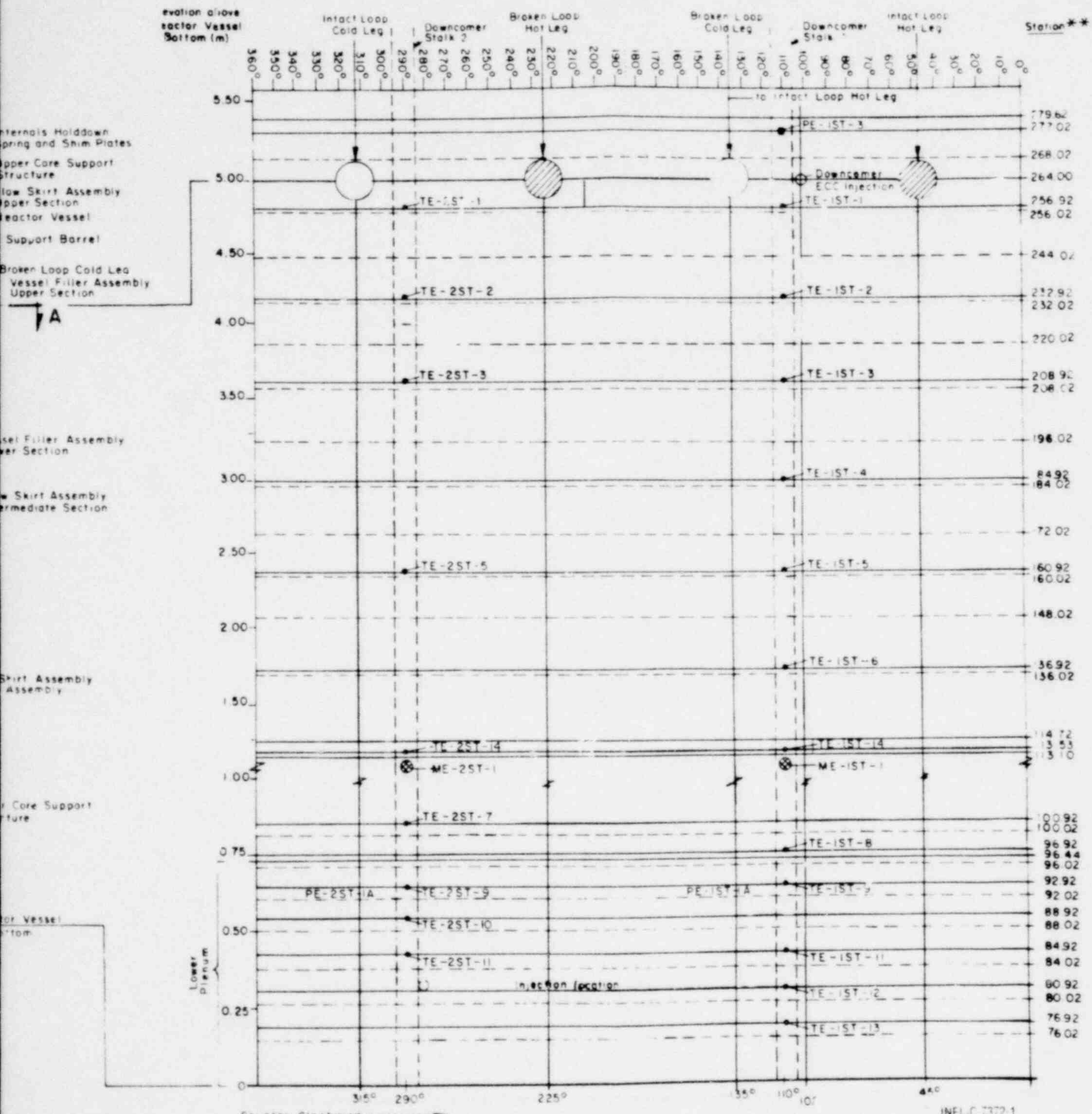

tor vessel measurement locations.

996 015

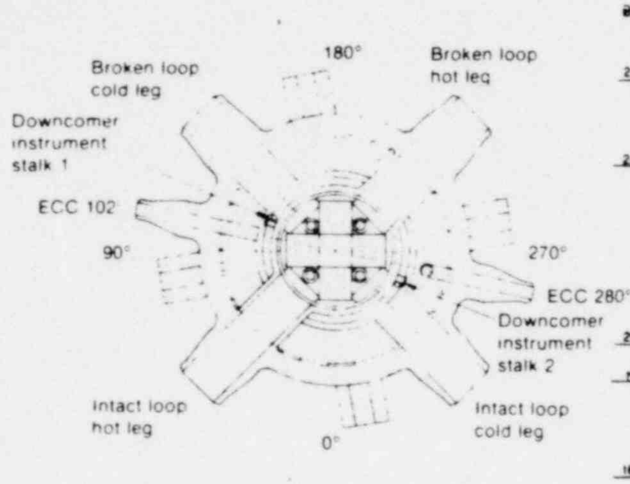

Section A-A

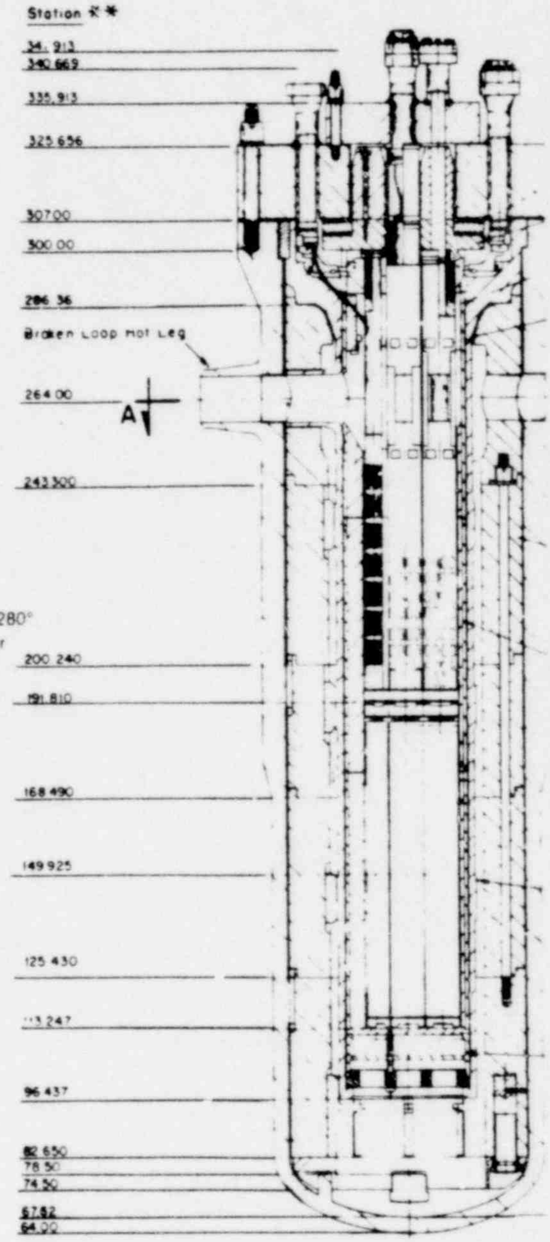

● Thermocouple

■ Pressure

⊗ Drag Discs

** Station numbers are a dimensionless measure of relative elevation within the reactor vessel. They are assigned in increments of 2.54 centimeters with station 300.00 defined at the core barrel support ledge inside the reactor vessel flange.

Fig. A-3 F

996 016

BLANK

996 017

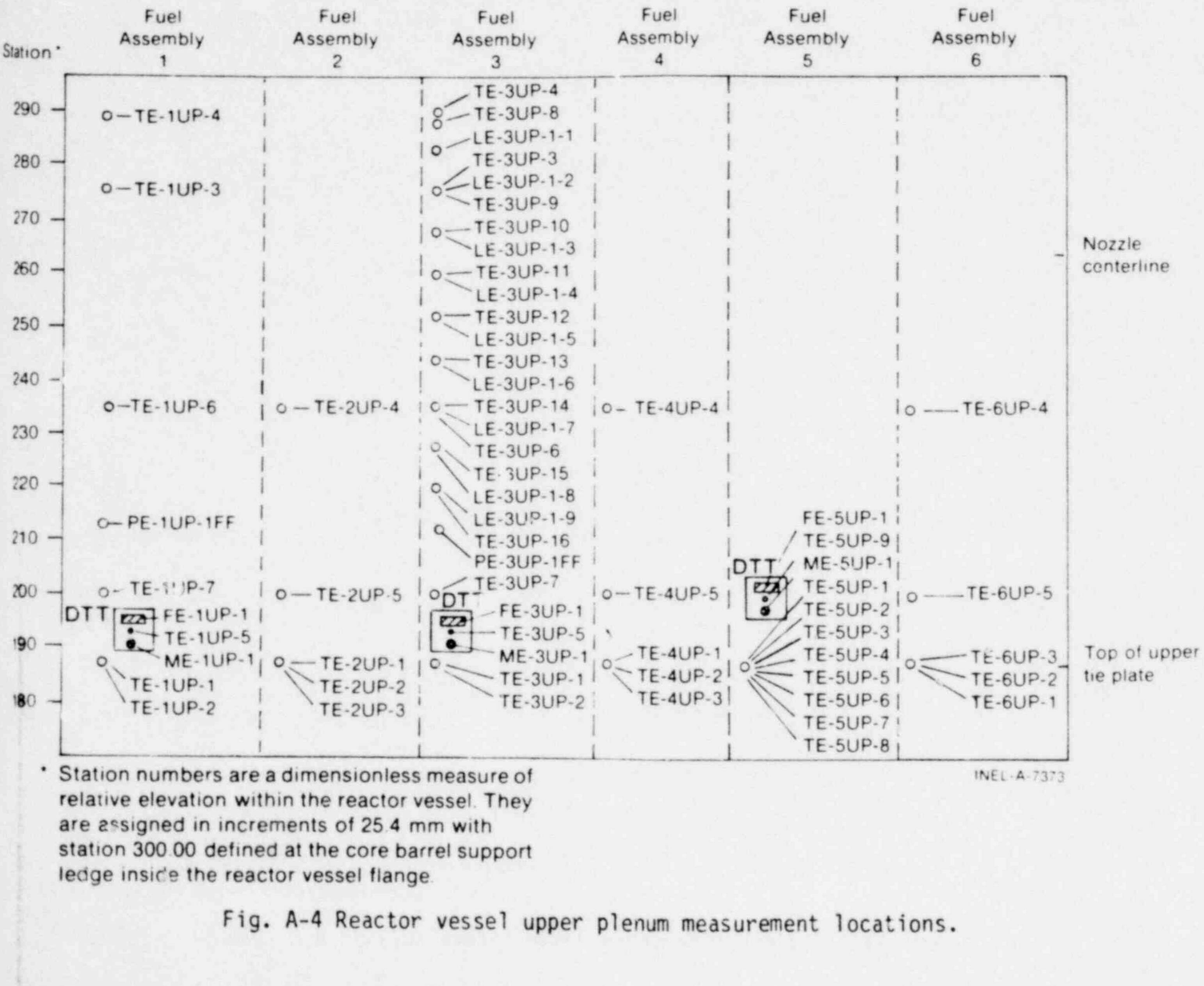

* Station numbers are a dimensionless measure of relative elevation within the reactor vessel. They are assigned in increments of 25.4 mm with station 300.00 defined at the core barrel support ledge inside the reactor vessel flange.

Fig. A-4 Reactor vessel upper plenum measurement locations.

BLANK

996 019

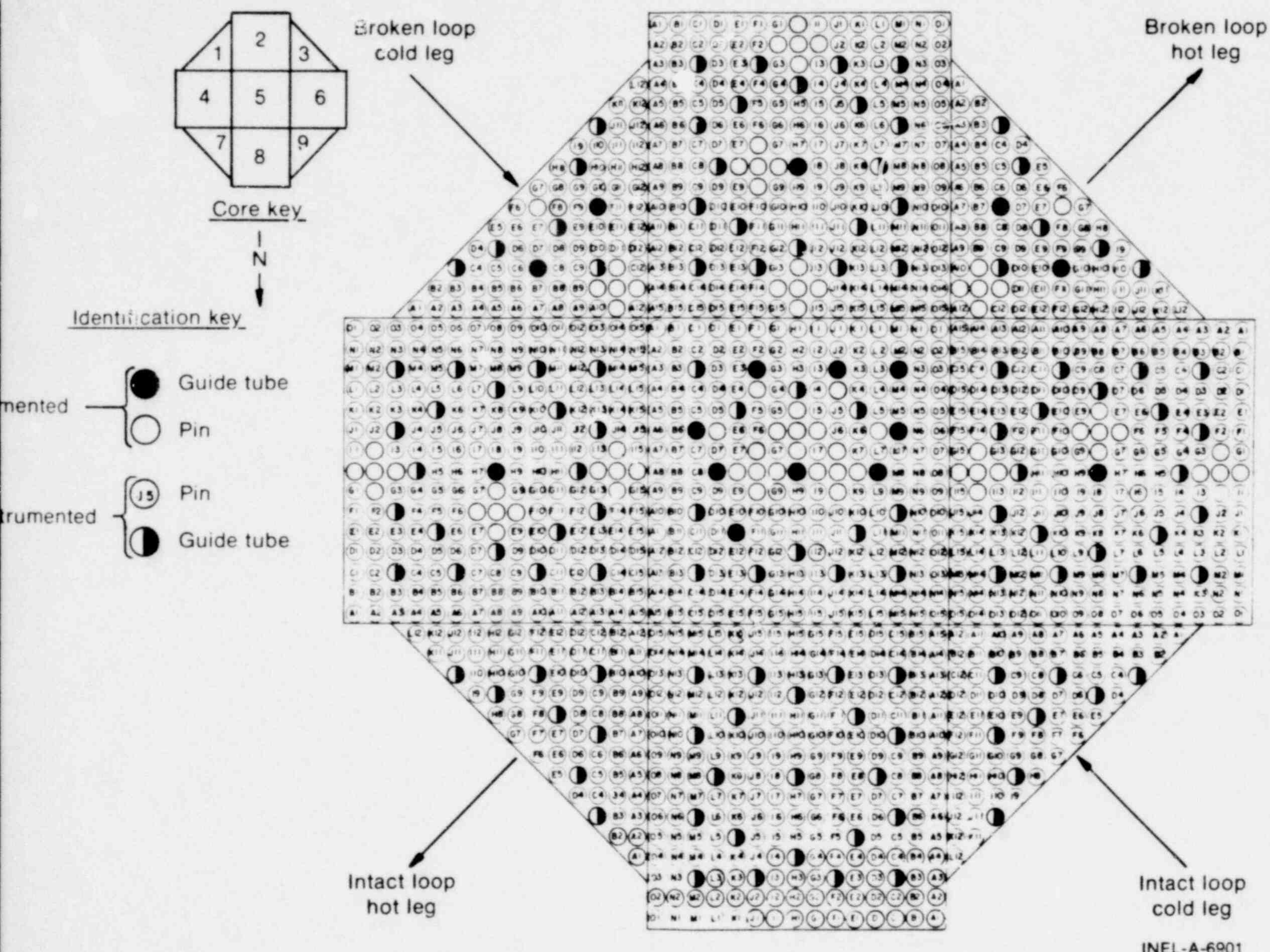

Fig. A-5 Core map showing fuel rod position designations.

996 020